Lecture notes 2021-2022
Numerical Simulations
Master 2 "Physics of complex systems"

Pascal Viot
Email : pascal.viot@sorbonne-universite.fr

August 14, 2021

These lecture notes provide an introduction to the methods of numerical simulation in classical statistical physics.

Based on simple models, we start in a first part on the basics of the Monte Carlo method and of the Molecular Dynamics. A second part is devoted to the introduction of the basic microscopic quantities available in simulation methods, and to the description of the methods allowing for studying the phase transitions. In a third part, we consider the study of out-of-equilibrium systems as well as the characterization of the dynamics: in particular, aging phenomena are presented.

1

Monte Carlo and Molecular Dynamics: basic methods

1.1 Introduction

Numerical simulations are effficient tools for investigating complex systems. Thanks to the increasing power of computers, there are able to provide various physical quantities which can be compared to experimental results and to theoretical predictions. For the sake of simplicity, they can be divided in two classes of methods: Monte Carlo simulations is based on Markovian dynamics, even if dynamics is not necessarily physical. Conversely, Molecular dynamics is based on ordinary differential equations (typically Newton equations for Hamiltonian systems) or stochastic differential equations for Brownian motion. In these two cases, one expects to obtain a physical kinetic description of the system, even if the model is generally a coarse-grained representation of the system.

1.2 Generating non uniform random numbers

1.2.1 Introduction

We propose here a brief recap on random numbers generators. Many decades ago, uniform random generators were of low quality. It was due to the limited representation of integers in computers. Indeed, two kinds of algorithms are at the origin of random number generators. The first one is based on a linear congruence relation

$$x_{n+1} = (ax_n + c) \, mod \, m \tag{1.1}$$

where all variables are integers. This relation generates a sequence of pseudo-random integer numbers between 0 and $m-1$. m corresponds to the generator period. Historically, the periods of these generators go from 2^{29} (randu IBM) to 2^{48} (ranf).

The generalization of this king of the algorithm consists in using a set of coupled congruence relations. A classical random generator, generally available in many libraries the Matsumoto and Nishimura, known by the name MT19937 (Mersenne Twister generator). Its period is 10^{6000}! It uses 624 words and it is equidistributed in 623 dimensions!. The second kind of random generator is based on The second class of random number generators is based on the register shift through the logical operation "exclusive or". An example is provided by the Kirkpatrick and Stoll generator.

$$x_n = x_{n-103} \bigoplus x_{n-250} \tag{1.2}$$

Its period is large, 2^{250}, but it needs to store 250 words.

By using a "classical" random generator, it is possible by converting the integer numbers in real numbers to obtain a "good" generator of uniform random numbers.

However, there exists some physical situations where it is necessary to generate non uniform random numbers, namely random numbers defined by a probability distribution $f(x)$ on an interval I, such that $\int_I dx f(x) = 1$ (condition of probability normalization). We here introduce several methods which generate random numbers with a specific probability distribution.

1.2.2 Inverse transformation

If $f(x)$ denotes the probability distribution on the interval I, one defines the cumulative distribution F as

$$F(x) = \int^x f(t)dt \tag{1.3}$$

If there exists an inverse function F^{-1}, then $u = F^{-1}(x)$ define a cumulative distribution for random numbers with a uniform distribution on the interval $[0, 1]$.

For instance, if one has a exponential distribution probability with a average λ, usually denoted $\mathcal{E}(\lambda)$, one has

$$\begin{aligned} F(x) &= \int_0^x dt\lambda e^{-\lambda t} \\ &= 1 - e^{-\lambda x} \end{aligned} \tag{1.4}$$

Therefore, inverting the relation $u = F(x)$, one obtains

$$x = -\frac{\ln(1-u)}{\lambda} \tag{1.5}$$

Considering the cumulative distribution $F(x) = 1 - x$, one immediately obtains that u is a uniform random variable defined on the unit interval, and $1 - u$ is also a uniform random variable uniform defined on the same interval. Therefore, Equ. (1.5) can be reexpressed as

$$x = -\frac{\ln(u)}{\lambda} \tag{1.6}$$

1.2.3 Box-Muller method

The Gaussian distribution is frequently used in simulations Unfortunately, the cumulative distribution is an error function. for a Gaussian distribution of unit variance centered on zero, denoted by $\mathcal{N}(0, 1)$ ($\mathcal{N}$ corresponds to a normal distribution), one has

$$F(x) = \frac{1}{\sqrt{2\pi}} \int_{-\infty}^x dt e^{-t^2/2} \tag{1.7}$$

This function is not invertible and one cannot apply the previous method. However, if one considers a couple of independent random variables (x, y) = the joint probability distribution is given by $f(x, y) = \exp(-(x^2 + y^2)/2)/(2\pi)$. Using the change of variables $(x, y) \to (r, \theta)$, namely polar coordinates, the joint probability becomes

$$f(r^2)rdrd\theta = \exp(-\frac{r^2}{2})\frac{dr^2}{2}\frac{d\theta}{2\pi}. \tag{1.8}$$

The variable r^2 is a random variable with a exponential probability distribution of average $1/2$, or $\mathcal{E}(1/2)$, and θ is a random variable with a uniform probability distribution on the interval $[0, 2\pi]$.

If u and v are two uniform random variables on the interval $[0, 1]$, or $\mathcal{U}_{[0,1]}$, one has

$$x = \sqrt{-2\ln(u)}\cos(2\pi v)$$
$$y = \sqrt{-2\ln(u)}\sin(2\pi v) \tag{1.9}$$

which are independent random variables with a Gaussian distribution.

1.2.4 Acceptance rejection method

The inverse method or the Box-Muller method can not be used for general probability distribution. The acceptance-rejection method is a general method which gives random numbers with various probability distributions.

This method uses the following property

$$f(x) = \int_0^{f(x)} dt \tag{1.10}$$

Therefore, by considering a couple of random variables with an uniform distribution, one defines the joint probability $g(x,u)$ with the condition $0 < u < f(x)$; the function $f(x)$ is the marginal distribution (of the x variable) of the joint distribution,

$$f(x) = \int du\, g(x,u) \tag{1.11}$$

By using a Monte Carlo method with an uniform sampling, one obtains independent random variables with a distribution, not necessary invertible. The price to pay is illustrated in Fig. 1.1 where the probability distribution $x^\alpha(1-x)^\beta$ (or more formally, a distribution $\mathcal{B}(\alpha,\beta)$) is sampled . For a good efficiency of the method, it is necessary to choose for the variable u an uniform distribution whose interval $\mathcal{U}_{[0,m]}$ with m greater or equal than the maximum of $f(x)$. Therefore, the maximum of $f(x)$ must be determined in the definition of the interval before selecting the range for the random variables. By choosing a maximum value for u equal to the maximum of the function optimizes the method.
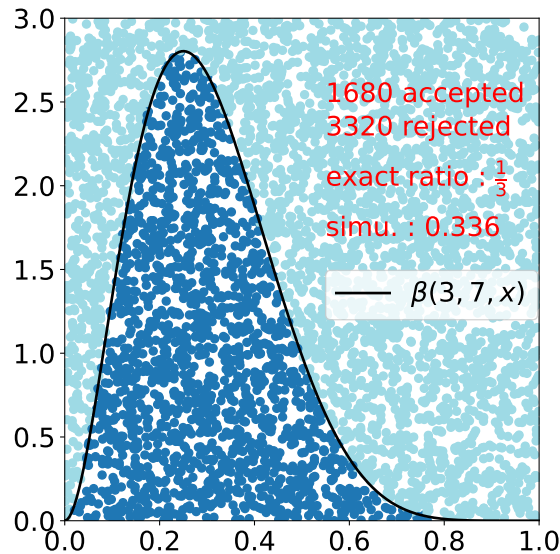

Figure 1.1: Computation of the probability distribution $\mathcal{B}(4,8)$ with the acceptance-rejection method using 5000 random points.

```
"""
Created on Fri Aug 28 12:50:28 2020
@author: viot
"""
import numpy as np
import matplotlib.pylab as plt
from scipy.special import beta

def betad(x,a,b):
    return(x**(a-1)*(1-x)**(b-1)/beta(a,b))

npoints=5000
x,y=np.random.uniform(0,1,size=npoints),np.random.uniform(0,3,size=npoints)
res=y<betad(x,3,7)

point=sum(res)
pointr=npoints-point

plt.figure(figsize=(6,6))
xx=np.linspace(0,1,200)
plt.plot(xx,betad(xx,3,7,),label=r'$\beta(3,7,x)$',color="black",lw=2)
plt.axis([0,1,0,3])
plt.scatter(x,y,c=res,cmap="tab20_r")
plt.text(0.55,2.5,str(point)+"␣accepted",fontsize=20,color="red")
plt.text(0.55,2.3,str(pointr)+"␣rejected",fontsize=20,color="red")
plt.text(0.55,2.0,r"exact␣ratio␣:␣$\frac␣{1}{3}$",fontsize=20,color="red")
plt.text(0.55,1.7,r"simu.␣:␣"+str(point/npoints),fontsize=20,color="red")
plt.legend(fontsize='20',loc=(0.55,0.4))
plt.tick_params(labelsize=20)
plt.tight_layout()
plt.savefig("beta_en.pdf")
plt.show()
```

More precisely, the efficiency of the method is asymptotically given by the ratio of areas: the area whose external boundaries are given by the curve, the x-axis and the two vertical axis over that of the rectangle defined by the two horizontal and vertical axis (in Fig. 1.1, the area of the rectangle is equal to 1). For the probability distribution $\beta(3,7)$ and by choosing a maximum value for the variable u equal to 3, one obtains a ratio of 1/3 (which corresponds to an infinitely large number of trials) between accepted random numbers over total trial numbers (5000 in Fig. 1.1 with 1680 acceptances and 3320 rejections).

The limitations of this method are easy to identify: only probability distribution with a compact support can be well sampled. If not, a truncation of the distribution must be done and when the distribution decreases slowly, the ratio goes to a small value which deteriorates the efficiency of the method.

In order to improve this method, the rectangle can be replaced with a area with an upper boundary defined by a curve. If g is a simple function to sample and if $g > f$ for all values on the interval, one samples random numbers with the distribution g and the acceptance-rejection method is applied for the function $f(x)/g(x)$. The efficiency of the method then becomes the ratio of areas defined by the two functions, respectively, and the number of rejections decreases.

1.3 Markov Chain, Detailed Balance, Metropolis Algorithm

1.3.1 Markov chain for sampling an equilibrium system

Very often, we are interested in the computation of the thermal average of a quantity but not in the partition function itself.

$$\langle A \rangle = \frac{\sum_i A_i \exp(-\beta U_i)}{Z}. \tag{1.12}$$

Let us recall that

$$p_i = \frac{\exp(-\beta U_i)}{Z} \tag{1.13}$$

defines the probability of having the configuration i (at equilibrium). The basic properties of a probability distribution are satisfied: p_i is strictly positive and $\sum_i p_i = 1$. If one were able to generate configurations with this weight, the thermal average of A should be given by

$$\langle A \rangle \simeq \frac{1}{N_r} \sum_i^{N_r} A_i \tag{1.14}$$

where N_r is the total number of configurations where A is evaluated. In this way, the thermal average becomes an arithmetic average.

The trick proposed by Metropolis, Rosenbluth and Teller in 1953 consists of introducing a stochastic Markovian process between successive configurations, and which converges towards the equilibrium distribution p_{eq}.

First, we introduce some useful definitions: To follow the sequence of configurations, one defines a time t equal to the number of "visited" configurations divided by the system size. This time has no relation with the real time of the system. Let us denote $p(i,t)$ the probability of having the configuration i at time t.

Let us explain the meaning of the dynamics: "stochastic" means that going from a configuration to another does not obey a ordinary differential equation but is a random process determined by probabilities; "Markovian" means that the probability of having a configuration j at time $t + dt$, ($dt = 1/N$ where N is the particle number of the system), only depends on the configuration i at time t, but not on previous configurations (the memory is limited to the time t); this conditional probability is denoted by $W(i \rightarrow j)dt$. The master equation of the system is then given (in the thermodynamic limit) by :

$$p(i, t+dt) = p(i,t) + \sum_j \left(W(j \rightarrow i)P(j,t) - W(i \rightarrow j)p(i,t) \right) dt \tag{1.15}$$

This equation corresponds to the fact that at time $t + dt$, the probability of the system of being in the configuration i is equal to the probability of being in a same state at time t, (algebraic) added of the probability of leaving the configuration towards a configuration j and the probability of going from a configuration j towards the configuration i.

At time $t = 0$, the system is in a initial configuration i_0: The initial probability distribution is $p(i) = \delta_{i_0,i}$, which means that we are far from the equilibrium distribution

In order to obtain a stationary solution of the master equation, Eq. (1.15), one obtains the set of conditions

$$\sum_j W(j \rightarrow i)p_{eq}(j) = p_{eq}(i)\sum_j W(i \rightarrow j) \qquad (1.16)$$

A simple solution solution of these equations is given by

$$W(j \rightarrow i)p_{eq}(j) = W(i \rightarrow j)p_{eq}(i) \qquad (1.17)$$

This equation, (1.17), is known as the condition of detailed balance. It expresses that, in a stationary state (as equilibrium state), the probability that the system goes from a stationary state i to a state j is the same that the reverse situation. Let us add this condition is not a sufficient condition, because we have not proved that the solution of the set of equations (1.16) is unique and that the equation (1.17) is a solution with a simple physical interpretation. Because it is difficult to prove that a Monte Carlo algorithm converges towards equilibrium, several algorithms use the detailed balance condition. As we will see later, recently a few algorithms violating detailed balance have been proposed that converges asymptotically towards equilibrium (or a stationary state).

Equation (1.17) can be reexpressed as

$$\frac{W(i \rightarrow j)}{W(j \rightarrow i)} = \frac{p_{eq}(j)}{p_{eq}(j)} = \exp(-\beta(U(j) - U(i))). \qquad (1.18)$$

This implies that $W(i \rightarrow j)$ does not depend on the partition function Z, but only on the Boltzmann factor.

1.3.2 Metropolis algorithm

The choice of a Markovian process in which detailed balance is satisfied is a solution of Eqs. (1.17). In order to obtain solutions of Eqs. (1.17) or, in other words, to obtain the transition matrix ($W(i \rightarrow j)$), note that Monte Carlo dynamics is the sequence of two elementary steps:

1. From a configuration i, one selects randomly a new configuration j, with a priori probability $\alpha(i \rightarrow j)$.

2. This new configuration is accepted with a probability $\Pi(i \rightarrow j)$.

Therefore, one has

$$W(i \rightarrow j) = \alpha(i \rightarrow j)\Pi(i \rightarrow j). \qquad (1.19)$$

In the original algorithm developed by Metropolis (and many others Monte Carlo algorithms), one chooses $\alpha(i \rightarrow j) = \alpha(j \rightarrow i)$; we restrict ourselves to this situation in the remainder of this chapter

Eqs. (1.18) are reexpressed as

$$\frac{\Pi(i \rightarrow j)}{\Pi(j \rightarrow i)} = \exp(-\beta(U(j) - U(i))) \qquad (1.20)$$

The choice introduced by Metropolis *et al.* is

$$\Pi(i \rightarrow j) = \begin{cases} \exp(-\beta(U(j) - U(i))) & \text{if } U(j) > U(i) \\ 1 & \text{if } U(j) \leq U(i) \end{cases} \qquad (1.21)$$

As we will see later, this solution is only efficient far from transitions. Moreover, the implementation is simple and can be used as a benchmark for more sophisticated methods. In chapter 5, specific methods for studying phase transitions will be discussed.

Additional comments for implementing a Monte Carlo algorithm:

Computation of a thermal average only starts when the system reaches equilibrium, namely when $p \simeq p_{eq}$. Therefore, in a Monte Carlo run, there are generally two parts: The first starting from an initial configuration, where a run is performed in order to lead the system close to equilibrium; the second where the system evolves in the vicinity of equilibrium with the computation of thermodynamic quantities.

To estimate the relaxation time towards equilibrium, there are several methods:

1. a naive approach consists of following the evolution of the instantaneous energy of the system and in considering that equilibrium is reached when the energy is stabilized around a quasi-stationary value.

2. A more precise method estimates the relaxation time of a correlation function and one chooses a time significantly larger than the relaxation time. For disordered systems, and at temperature larger the phase transition, this criteria is reasonable in a first approach. More sophisticated estimates will be discussed in the lecture.

We now consider how the Metropolis algorithm can be implemented for several basic models.

1.3.3   Applications

Ising model

Periodic boundary conditions   Since simulation cells are always of finite size, the ratio of the surface times the linear dimension of the particle over the volume of the system is a quite large number. To avoiding large boundary effects, simulations are performed by using periodic boundary conditions. In two dimensions, this means that the simulation cell must tile the plane: due to the geometric constraints, two types of cell are possible: a elementary square and a regular hexagonal. The periodic boundary conditions are implemented as follows: Starting from a given cell, all neighboring cells are drawn with the same configuration of the cell. For each site, one determines all nearest neighbors with the rule: When a spin of a site is flipped, all images are updated in the same time. In other words, the original lattice can be viewed as a lattice on a torus.

Metropolis algorithm   For starting a Monte Carlo simulation, one needs to define a initial configuration, which can be:

1. The ground-state with all aligned spins +1 or −1,

2. A infinite-temperature configuration: on each site, one chooses randomly and uniformly a number between 0 and 1. If this selected number is between 0 and 0.5, the site spin is taken equal to +1; if the selected number is between 0.5 and 1, the site spin is taken equal to −1.

As mentioned previously, Monte Carlo dynamics involves two elementary steps:

First, one selects randomly a trial configuration and secondly, one considers acceptance or rejection by using the Metropolis condition.

In order that the trial configuration can be accepted, this configuration needs to be "close" to the previous configuration; indeed, the acceptance condition is proportional to the exponential of the energy difference of the two configurations. If this difference is large and positive, the probability of acceptance becomes very small and the system can stay "trapped" a long time a local minimum. For a Metropolis algorithm, the single spin flip is generally used which leads to a dynamics where energy changes are reasonable. Because the dynamics must remain stochastic, a spin must be chosen randomly for each trial configuration, and not according to a regular sequence.

In summary, an iteration of the Metropolis dynamics for an Ising model consists of the following:

1. A site is selected by choosing at random an integer i between 1 and the total number of lattice sites.

2. One computes the energy difference between the trial configuration (in which the spin i is flipped) and the old configuration. For short-range interactions, this energy difference involves a few terms and is "local" because only the selected site and its nearest neighbors are considered.

3. If the trial configuration has a lower energy, the trial configuration is accepted. Otherwise, a uniform random number is chosen between 0 and 1 and if this number is less than $\exp(\beta(U(i) - U(j)))$, the trial configuration is accepted. If not, the system stays in the old configuration.

Computation of thermodynamic quantities (mean energy, specific heat, magnetization, susceptibility,…) can be easily performed. Indeed, if a new configuration is accepted, the update of these quantities does not require additional calculation: $E_n = E_o + \Delta E$ where E_n and E_o denote the energies of the new and the old configuration; similarly, the magnetization is given by $M_n = M_o + 2sgn(S_i)$ where $sgn(S_i)$ is the sign of spin S_i in the new configuration. In the case where the old configuration is kept, instantaneous quantities are unchanged, but time must be incremented.

As we discussed in the previous chapter, thermodynamic quantities are expressed as moments of the energy distribution and/or the magnetization distribution. The thermal average can be performed at the end of the simulation when one uses a histogram along the simulation and eventually one stores these histograms for further analysis.

Note that, for the Ising model, the energy spectra is discrete, and computation of thermal quantities can be performed after the simulation run. For continuous systems, it is not equivalent to perform a thermal average "on the fly" and by using a histogram. However, by choosing a sufficiently small bin size, the average performed by using the histogram converges to the "on the fly" value.

Practically, the implementation of a histogram method consists of defining an array with a dimension corresponding the number of available values of the quantity; for instance, the magnetization of the Ising model is stored in an array $histom[2N + 1]$, where N is the total number of spins. (The size of the array could be divided by two, because only even integers are available for the magnetization, but state relabeling is necessary.) Starting with a array whose elements are set to zero at the initial time, magnetization update is performed at each simulation time by the formal code line

$$histom[magne] = histom[magne] + 1 \tag{1.22}$$

where *magne* is the variable storing the instantaneous magnetization.

1.3.4 Simple liquids

Periodic boundary conditions

Calculation of the energy of a new configuration is more sophisticated than for Ising lattice models. Indeed, because the interaction involves all particles of the system, the energy update contains N terms, where N is the total number of particles of the simulation cell. One implements the periodic boundary conditions by covering space by replicating the original simulation unit cell. Therefore, the interaction now involves not only particles inside the simulation cell, but also particles with the simulation cell and particles in all replica.

$$U_{tot} = \frac{1}{2} \sum_{i,j,\mathbf{n}}' u(|\mathbf{r}_{ij} + \mathbf{n}L|) \tag{1.23}$$

where L is the length of the simulation cell and $\mathbf{n}$ is a vector with integer components. For interaction potential decreasing sufficiently rapidly (practically for potentials such that $\int dV\, u(r)$ is finite, where dV is the infinitesimal volume), the summation is restricted to the nearest cells, the so-called minimum image convention.; for calculating of the energy between the particle i and the particle j, a test is performed, for each spatial coordinate if $|x_i - x_j|$ ($|y_i - y_j|$ and $|z_i - z_j|$, respectively) is less than one-half of length size of the simulation cell $L/2$. If $|x_i - x_j|$ ($|y_i - y_j|$ and $|z_i - z_j|$, respectively) is greater than to $L/2$, one calculates $x_i - x_j \bmod L$ ($y_i - y_j \bmod L$ and $z_i - z_j \bmod L$, respectively), which considers particles within the nearest cell of the simulation box. For systems interacting with a long-range interaction, one must compute interaction with all particles, and specific methods have been developped to save comuter time: for instane, see Ewald method in Appendix.

Metropolis algorithm

For an off-lattice system, a trial configuration is generated by moving at random a particle; this particle is obviously chosen at random. In a three-dimensional space a trial move is given by

$$x_i' \to x_i + \Delta(rand - 0.5) \tag{1.24}$$
$$y_i' \to y_i + \Delta(rand - 0.5) \tag{1.25}$$
$$z_i' \to z_i + \Delta(rand - 0.5) \tag{1.26}$$

with the condition that $(x_i' - x_i)^2 + (y_i' - y_i)^2 + (z_i' - z_i)^2 \leq \Delta^2/4$ (this condition corresponds to considering isotropic moves) where rand denotes a uniform random number between 0 and 1. Δ is a a distance of maximum move by step. The value of this quantity must be set at the beginning of the simulation and generally its value is chosen in order to keep a reasonable ratio of new accepted configurations over the total number of configurations.

Note that $x_i' \to x_i + \Delta rand$ would be incorrect because only positive moves are allowed and the detailed balance is then not satisfied (see Eq. (1.17)).

This first step is time consuming, because the energy update requires calculation of $N^2/2$ terms. When the potential decreases rapidly (for instance, the Lennard-Jones potential), at long distance, the density $\rho(r)$ becomes uniform and one can estimate this contribution to the mean energy by the following formula

$$u_i = \frac{1}{2} \int_{r_c}^{\infty} 4r^2 dr u(r) \rho(r) \tag{1.27}$$

$$\simeq \frac{\rho}{2} \int_{r_c}^{\infty} 4r^2 dr u(r) \tag{1.28}$$

This means that the potential is replaced with a truncated potential

$$u^{trunc}(r) = \begin{cases} u(r) & r \le r_c, \\ 0 & r > r_c. \end{cases} \tag{1.29}$$

For a finite-range potential, energy update only involves a summation of a finite number of particles at each time, which becomes independent of the system size. For a Monte Carlo simulation, the computation time becomes proportional to the number of particles N (because we keep constant the same number of moves per particle for all system sizes). In the absence of truncation of potential, the update energy would be proportional to N^2 Note that the truncated potential introduces a discontinuity of the potential. This correction can be added to the simulation results, which gives an "impulse" contribution to the pressure. For the Molecular Dynamics, we will see that this procedure is not sufficient.

In a similar manner to the Ising model (or lattice models), it is useful to store the successive instantaneous energies in a histogram. However, the energy spectra being continuous, it is necessary to introduce a adapted bin size (ΔE). If one denotes N_h the dimension of the histogram array, the energies are stored from E_{min} to $E_{min} + \Delta(E N_t - 1)$. If $E(t)$ is the energy of the system at time t, the index of the array element is given by the relation

$$i = Int(E - E_{min}/\Delta E) \tag{1.30}$$

In this case, the numerical values of moments calculated from the histogram are not exact unlike the Ising model, and it is necessary to choose the bin size in order to minimize this bias.

1.4   Molecular Dynamics : Verlet algorithm, event driven algorithm

1.4.1   Introduction

Monte Carlo simulation has an intrinsic limitation: its dynamics does not correspond to the "real" dynamics. For continuous systems defined from a classical Hamiltonian, it is possible to solve the differential equations of all particles simultaneously. This method provides the possibility of precisely obtaining the dynamical properties (temporal correlations) of equilibrium systems, quantities which are available in experiments, which allows one to test, for instance, the quality of the model.

The efficient use of new tools is associated with knowledge of their ability; first, we analyze the largest available physical time as well as the particle numbers that we can consider for a given system through Molecular Dynamics. For a three dimensional system, one can solve the equations of motion for systems up to several hundred thousands particles. Note that for a simulation with a moderate number of particles, namely 10^4, the average number of particles along an edge of the simulation box is $(10^4)^{(1/3)} \simeq 21$. This means that for a thermodynamic study one needs to use the periodic boundary conditions like in Monte Carlo simulations.

For atomic systems far from the critical region, the correlation length is smaller than the dimensionless length of 21, but Molecular Dynamics is not the best simulation method for a study of phase transitions. The situation is worse if one considers more sophisticated molecular structures, in particular biological systems.

By using a Lennard-Jones potential, it is possible to find a typical time scale from an analysis of microscopic parameters of the system (m mass of the particle, σ diameter, and ϵ energy scale of the interaction potential) is

$$\tau = \sigma \sqrt{\frac{m}{\epsilon}} \qquad (1.31)$$

This time corresponds to the duration for a atom of moving on a distance equal to its linear size with a velocity equal to the mean velocity in the liquid. For instance, for argon, one has the numerical values $\sigma = 3\text{Å}$, $m = 6.63.10^{-23}kg$ and $\epsilon = 1.64.10^{-20}J$, which gives $\tau = 2.8.10^{-14}s$. For solving the equations of motion, the integration step must be much smaller than the typical time scale τ, typically $\Delta t = 10^{-15}s$, even smaller. The total number of steps performed in a run is typically of order of magnitude from 10^5 to 10^7; therefore, the duration of the simulation for an atomic system is $10^{-8}s$.

For many atomic systems, relaxation times are much smaller than $10^{-8}s$ and Molecular Dynamics is a very good tool for investigating dynamic and thermodynamic properties of the systems. For glass-formers, in particular, in for supercooled liquids, one observes relaxation times to the glass transition which increases by several orders of magnitude, where Molecular Dynamics cannot be equilibrated. For conformational changes of proteins, for instance, to the contact of a solid surface, typical relaxation times are of order of a millisecond. In these situations, it is necessary to coarse-graining some of the microscopic degrees of freedom allowing the typical time scale of the simulation to be increased.

1.4.2   Equations of motion

We consider below the typical example of a Lennard-Jones liquid. Equations of motion of particle i are given by

$$\frac{d^2\mathbf{r}_i}{dt^2} = -\sum_{j \neq i} \nabla_{\mathbf{r}_i} u(\mathbf{r}_{ij}). \qquad (1.32)$$

For simulating an "infinite" system, periodic boundary conditions are used. The calculation of the force between two particles i and j can be performed by using the minimum image convention (if the potential decreases sufficiently fast to 0 at large distance. This means that for a given particle i, one needs to find if j or one of its images which is the nearest neighbor of i.

Similarly to a Monte Carlo, simulation, force calculation on the particle i involves the computation of de $(N-1)$ elementary forces between each particle and particle i. By using a truncated potential, one restricts the summation to particles within a sphere whose radius corresponds to the potential trunca-tion.In order that the forces remain finite whatever the particle distance, the truncated Lennard-Jones potential used in Molecular Dynamics is the following

$$u^{trunc}(r) = \begin{cases} u(r) - u(r_c) & r < r_c \\ 0 & r \geq r_c. \end{cases} \qquad (1.33)$$

One has to account for the bias introduced in the potential in the thermodynamics quantities compared to original Lennard-Jones potential.

1.4.3 Discretization. Verlet algorithm

For obtaining a numerical solution of the equations of motion, it is necessary to discretize. Different choices are a priori possible, but as we will see below, it is crucial that the total energy which is constant for a isolated Hamiltonian system remains conserved along the simulation (let us recall that the ensemble is microcanonical). The Verlet's algorithm is one of first methods and remains one most used nowadays.

For the sake of simplicity, let us consider an Hamiltonian system with identical N particles. $\mathbf{r}$, is a vector with $3N$ components: $\mathbf{r} = (\mathbf{r}_1, \mathbf{r}_2, ..., \mathbf{r}_N$, where $\mathbf{r}_i$ denotes the position of particle i. The system formally evolves as

$$m\frac{d^2\mathbf{r}}{dt^2} = \mathbf{f}(\mathbf{r}(t)). \tag{1.34}$$

A time series expansion gives

$$\mathbf{r}(t+\Delta t) = \mathbf{r}(t) + \mathbf{v}(t)\Delta t + \frac{\mathbf{f}(\mathbf{r}(t))}{2m}(\Delta t)^2 + \frac{d^3\mathbf{r}}{dt^3}(\Delta t)^3 + \mathcal{O}((\Delta t)^4) \tag{1.35}$$

and similarly,

$$\mathbf{r}(t-\Delta t) = \mathbf{r}(t) - \mathbf{v}(t)\Delta t + \frac{\mathbf{f}(\mathbf{r}(t))}{2m}(\Delta t)^2 - \frac{d^3\mathbf{r}}{dt^3}(\Delta t)^3 + \mathcal{O}((\Delta t)^4). \tag{1.36}$$

Adding these above equations, one obtains

$$\mathbf{r}(t+\Delta t) + \mathbf{r}(t-\Delta t) = 2\mathbf{r}(t) + \frac{\mathbf{f}(\mathbf{r}(t))}{m}(\Delta t)^2 + \mathcal{O}((\Delta t)^4). \tag{1.37}$$

The position updates are performed with an accuracy of $(\Delta t)^4$. This algorithm does not use the particle velocities for calculating the new positions. One can however determine these as follows:

$$\mathbf{v}(t) = \frac{\mathbf{r}(t+\Delta t) - \mathbf{r}(t-\Delta t)}{2\Delta t} + \mathcal{O}((\Delta t)^2) \tag{1.38}$$

Let us note that most of the computation is spent by the force calculation, and marginally spent on the position updates. As we will see below, we can improve the accuracy of the simulation by using a higher-order time expansion, but this requires the computation of spatial derivatives of forces and the computation time increases rapidly compared to the same simulation performed with the Verlet algorithm.

For the Verlet algorithm, the accuracy of trajectories is roughly given by

$$\Delta t^4 N_t \tag{1.39}$$

where N_t is the total number of integration steps, and the total simulation time is given by $\Delta t N_t$.

It is worth noting that the computation accuracy decreases with simulation time, due to the round-off errors which are not included in Eqs. (1.39).

There are more sophisticated algorithms involving force derivatives; they improve the short-time accuracy, but the long-time precision may deteriorate faster than with a Verlet algorithm. In addition, the computation efficiency is significant lower.

Time symmetry is an important property of the equations of motion. Note that Verlet's algorithm preserves this symmetry. This is, if we change $\Delta t \to -\Delta t$, Eq. (1.37) is unchanged. As a consequence, if at a given time t of the simulation, one inverts the arrow of time , the Molecular Dynamics trajectories

are retraced. The round-off errors accumulative in the simulation limit the the reversibility when the total number of integration steps becomes very large.

For Hamiltonian systems, the volume of phase space is conserved with time, and numerical simulation must preserve this property. Conversely, if an algorithm does not have this property, the total energy is no longer conserved, even for a short simulation. In order to keep this property, it is necessary that the Jacobian of the transformation in phase space, namely between the old and new coordinates in phase space; is equal to one. We will see below that the Verlet algorithm satisfies this property.

An a priori variant of the Verlet algorithm is known as the Leapfrog algorithm and is based on the following procedure: velocities are calculated on half-time intervals, and positions are obtained on integer time intervals. Let us define the velocities at $t + \Delta t/2$ and $t - \Delta t/2$

$$\mathbf{v}(t + \Delta t/2) = \frac{\mathbf{r}(t + \Delta t) - \mathbf{r}(t)}{\Delta t}, \tag{1.40}$$

$$\mathbf{v}(t - \Delta t/2) = \frac{\mathbf{r}(t) - \mathbf{r}(t - \Delta t)}{\Delta t}, \tag{1.41}$$

one immediately obtains

$$\mathbf{r}(t + \Delta t) = \mathbf{r}(t) + \mathbf{v}(t + \Delta t/2)\Delta t \tag{1.42}$$

and similarly

$$\mathbf{r}(t - \Delta t) = \mathbf{r}(t) - \mathbf{v}(t - \Delta t/2)\Delta t. \tag{1.43}$$

By using Eq. (1.37), one gets

$$\mathbf{v}(t + \Delta t/2) = \mathbf{v}(t - \Delta t/2) + \frac{\mathbf{f}(t)}{m}\Delta t + \mathcal{O}((\Delta t)^3). \tag{1.44}$$

Because the Leapfrog algorithm leads to Eq. (1.37), the trajectories are identical to those calculated by the Verlet's algorithm. The computations of velocities for half-integer times are temporary variables, but the positions are identical Some care is necessary when calculating the thermodynamics quantities because the mean potential energy, which is calculated at integer times, and the kinetic energy which is calculated at half-integer times, do not give a constant total energy.

Many attempts to obtain better algorithms have been made, and, in order to overcome the previous heuristic derivation, a more rigorous approach is necessary. From the Liouville formalism, we are going to derive symplectic algorithms, namely algorithms conserving the phase space volume and consequently the total energy of the system. This method provides algorithms with greater accuracy than the Verlet algorithm for a fixed time step Δt. Therefore, more precise trajectories can be obtained.

1.4.4   Hard sphere model: event-driven algorithm

The hard sphere model is defined by the Hamiltonian

$$\mathcal{H}_N = \sum_i^N \frac{1}{2}mv_i^2 + \frac{1}{2}\sum_{i\neq j} u(\mathbf{r}_i - \mathbf{r}_j), \tag{1.45}$$

where the interaction potential is

$$u(\mathbf{r}_i - \mathbf{r}_j) = \begin{cases} +\infty & |\mathbf{r}_i - \mathbf{r}_j| \le \sigma \\ 0 & |\mathbf{r}_i - \mathbf{r}_j| > \sigma \end{cases} \tag{1.46}$$

From this definition, one sees that the Boltzmann factors, which are involved in the configurational integral $\exp(-\beta u(\mathbf{r}_i - \mathbf{r}_j))$ are equal either 0 (when two spheres overlap) or 1 otherwise, which means that this integral does not depend on the temperature, but only on the density. As for systems with a purely repulsive interaction, the hard sphere model does not undergo a liquid-gas transition, but a liquid-solid transition exists.

This model was been intensely studied both theoretically and numerically. A renewal of interest in the two last decades comes in the non equilibrium version, commonly used for granular gases. Indeed, when the packing fraction is small, the inelastic hard sphere is a good reference model. The interaction potential remains the same, but dissipation that occurring during collisions is accounted for in a modified collision rule .

Note that the impulsive character of forces between particles prevents use of the Verlet algorithm and others; all previous algorithms assume that forces are continuous functions of distance, which is not the case here.

For hard spheres, particle velocities are only modified during collisions. Between two collisions, particles follow rectilinear trajectories. Moreover, since the collision is instantaneous, the probability of having three spheres in contact at the same time is infinitesimal. The dynamics is a sequence of binary collisions.

Consider two spheres of identical mass: during the collision, the total momentum is conserved

$$\mathbf{v}_1 + \mathbf{v}_2 = \mathbf{v}_1' + \mathbf{v}_2' \tag{1.47}$$

For an elastic collision, the normal component of the velocity at contact is inverted.

$$(\mathbf{v}_2' - \mathbf{v}_1').(\mathbf{r}_2 - \mathbf{r}_1) = -(\mathbf{v}_1 - \mathbf{v}_2).(\mathbf{r}_2 - \mathbf{r}_1), \tag{1.48}$$

whereas the tangential component of the velocity is unchanged.

$$(\mathbf{v}_2' - \mathbf{v}_1').\mathbf{n}_{12} = (\mathbf{v}_1 - \mathbf{v}_2).\mathbf{n}_{12}, \tag{1.49}$$

where $\mathbf{n}_{12}$ is the normal vector to the collision axis and belonging to the plane defined by the two incoming velocities.

By using Eqs. (1.48) and (1.49), one obtains the post-collisional velocities

$$\mathbf{v}_1' = \mathbf{v}_1 + \frac{(\mathbf{v}_2 - \mathbf{v}_1).(\mathbf{r}_1 - \mathbf{r}_2)}{(\mathbf{r}_1 - \mathbf{r}_2)^2}(\mathbf{r}_1 - \mathbf{r}_2) \tag{1.50}$$

$$\mathbf{v}_2' = \mathbf{v}_2 + \frac{(\mathbf{v}_1 - \mathbf{v}_2).(\mathbf{r}_1 - \mathbf{r}_2)}{(\mathbf{r}_1 - \mathbf{r}_2)^2}(\mathbf{r}_1 - \mathbf{r}_2) \tag{1.51}$$

It is easy to check that the total kinetic energy is constant during the simulation. Indeed, since the algorithm being exact (discarding for the moment the round-off problem), the algorithm is obviously symplectic.

Practically, the hard sphere algorithm is as follows: starting from an initial (non overlapping) configuration, all possible binary collisions are considered, namely for each pair of particles, collision time is calculated.

Between collisions, the positions of i and j are given by

$$\mathbf{r}_i = \mathbf{r}_i^0 + \mathbf{v}_i t \tag{1.52}$$

$$\mathbf{r}_j = \mathbf{r}_j^0 + \mathbf{v}_j t \tag{1.53}$$

where $= \mathbf{r}_i^0$ and $= \mathbf{r}_i^0$ are the particle positions i and j after collision.

The contact condition between two particles is given by relation

$$\sigma^2 = (\mathbf{r}_i - \mathbf{r}_i)^2 = (\mathbf{r}_i^0 - \mathbf{r}_j^0)^2 + (\mathbf{v}_i - \mathbf{v}_j)^2 t^2 + 2(\mathbf{r}_i^0 - \mathbf{r}_j^0)(\mathbf{v}_i - \mathbf{v}_j)t \tag{1.54}$$

Because the collision time is a solution of a quadratic equation, several cases must be considered: if the roots are complex, the collision time is set to a very large value in simulation. If the two roots are real, either they are negative and the collision time is set to a very large value in simulation again. If only one root is positive, the collision time corresponds to this value. If the two roots are positive, the smallest one is selected as the collision time.

A necessary condition for having a positive solution for t (collision in the future) is that

$$(\mathbf{r}_i^0 - \mathbf{r}_j^0).(\mathbf{v}_i - \mathbf{v}_j) < 0 \tag{1.55}$$

Once all pair of particles have been examined, the shortest time is selected, namely the first collision. The trajectories of particles evolve rectilinearly until the new collision occurs (calculation of trajectories is exact, because forces between particles are only contact forces). At the collision time, velocities of the two particles are updated, and one calculates the next collision again.

The algorithm provides trajectories with an high accuracy, bounded only by the round-off errors. The integration step is not constant, contrary to the Verlet's algorithm. This quasi-exact method has some limitation, when the density becomes significant, because the mean time between two collisions decreases rapidly and the system then evolves slowly. In addition, rattling effects occur in isolated regions of the system, which decreases the efficiency of the method.

2.1 Thermodynamics

2.1.1 Monte Carlo

In Monte Carlo simulations, the thermodynamic quantities are obtained by taking averages over moments of the observables. For instance, in a canonical ensemble, the mean energy $\langle E \rangle_\beta$ at the temperature $T = 1/\beta$ is obtained by calculating the integral.

$$\langle E \rangle = \int dE\, E P_\beta(E) \tag{2.1}$$

where $P_\beta(E)$ is the probability distribution of finding an equilibrium configuration at the temperature T.

In a simulation, after a period corresponding the relaxation time, the system evolves at équilibrium and the mean energy is obtained by taking the arithmetic average

$$\langle E \rangle = \frac{1}{N_c} \sum_{i=1}^{N_c} E_i \tag{2.2}$$

where the summation is performed over N_c configurations at equilibrium

The specific heat C_v which is given by $k_b \beta^2 (\langle E^2 \rangle - \langle E \rangle^2)$ is obtained by calculating the first and second moments of the energy distribution.

By using the Ising model, one obtains the mean magnetization $\langle M \rangle = \frac{1}{N_c} \sum_{i=1}^{N_c} M_i$ as a simple arithmetic average. The susceptibility χ is also obtained by the two first moments of the magnetization $\langle M \rangle$ and $\langle M^2 \rangle$. The moments of an observable can be computed along the simulation, ("on the fly" method), whereas the energy (or magnetization) moments can be obtained at the end of the simulation if the energy distribution is stored at the end of the simulation. It is worth noting that the two methods are equivalent when the energy (or magnetization) spectra is discrete. For systems with a continuous spectra, the accurcy of the calculation of the moments from the energy distribution is limited by the with of the bins of the distribution.

2.1.2 Molecular Dynamics

In Molecular Dynamics, the system first relaxes towards equilibrium. Once equilibrated, the trajectories can be used for calculating thermodynamical quantities. One then uses the equivalence between the time average over trajectories and the ensemble average.

$$\langle A \rangle = \lim_{t \to \infty} \frac{1}{t} \int_0^t A(t')dt' \tag{2.3}$$

This property is satisfied if the dynamics is ergodic, which means that, by starting from any initial configuration, the system is able to explore any region of the phase space. The proof of ergodicity breaking is obtained generally in the thermodynamic limit (for instance, long-range interacting systems,

glassy systems,...). Because simulation is performed with finite systems, this should not happen, but the time of the simulation being finite, there exists many situations in which the system can not explore the phase space correctly. For instance, close a first-order phase transition, the relaxation time increases as an exponential of the free energy barrier (which is a monotonous function of the system size) and becomes rapidly larger than the total simulation time, preventing the system to explore the entire phase space.

For a time-driven algorithm (for instance, Verlet, Leapfrog,...) corresponding to a constant timestep, the time average is performed in simulation as follows

$$\langle A \rangle = \frac{1}{N_c} \sum_i^{N_c} A_i \tag{2.4}$$

where N_c is the number of timesteps of the simulation (at equilibrium) and A an observable.

For an event-driven simulation, corresponding to a variable time step, the time average must be performed by using a constant timestep (in order to compute the integral). Either the dynamics is known analytically between collisions and the time integral can be obtained exactly, or the integral can be estimated as

$$\langle A \rangle = \frac{1}{T} \sum_i^{N_c} A_i t_i \tag{2.5}$$

where t_i is time interval between the ith and $i + 1$th event (collision).

2.2 Correlation functions

2.2.1 Introduction

With Monte Carlo or Molecular Dynamics simulation, one can calculate thermodynamic quantities, as seen in previous chapters, but also the spatial correlation functions. These functions characterize the structure of the system and provide more detailed information that thermodynamic quantities. Correlation functions can be directly compared to light or neutron scattering, and/or to several theoretical approaches that have been developed during the last decades (for instance, the integral equations of liquid state).

Time correlation functions can be compared to experiments if the simulation dynamics corresponds to a "real" dynamics, namely a Molecular Dynamics. Monte Carlo dynamics strongly depends of the chosen rule. However, although the Metropolis algorithm does not correspond to a real dynamics, global trends of a real dynamics are generally contained (slowing down for a continuous transition, glassy behavior in glass formers liquids, ...). Using the linear response theory, the transport coefficients can be obtained by integrating the time correlation functions.

In the second part of this chapter, we consider the glassy behavior where simulation showed recently that dynamics of the system is characterized by dynamical heterogeneities. Indeed, while many particles seem to be frozen, isolated regions contain mobile particles. This phenomenon evolves continuously with time where mobile particles becomes frozen and conversely. This feature can be characterized by a high-order correlation function (4-point correlation function). Therefore, specific behavior can be characterized by a more or less sophisticated correlation functions.

2.2.2 Structure

Radial distribution function

We now derive the equilibrium correlation functions as a function of the local density (already defined in Chap. 1). The main interest is to show that these expression are well adapted for simulation. In addition,

we pay special attention to finite size effects; indeed the simulation box containing a finite number of particles, quantities of interest display some differences with the same quantities in the thermodynamic limit and one must account for it.

Let us consider a system of N particles defined by the Hamiltonian

$$\mathcal{H} = \sum_{i=1}^{N} \frac{p_i^2}{2m} + V(\mathbf{r}^N). \tag{2.6}$$

In the canonical ensemble, the density distribution associated with the probability of finding n particles in the elementary volume $\prod_{i=1}^{n} d\mathbf{r}_i$, denoted in the following as $d\mathbf{r}^n$, is given by

$$\rho_N^{(n)}(\mathbf{r}^n) = \frac{N!}{(N-n)!} \frac{\int \cdots \int \exp(-\beta V(\mathbf{r}^N)) d\mathbf{r}^{N-n}}{Z_N(V,T)} \tag{2.7}$$

where

$$Z_N(V,T) = \int \cdots \int \exp(-\beta V(\mathbf{r}^N)) d\mathbf{r}^N. \tag{2.8}$$

Normalization of $\rho_N^{(n)}(\mathbf{r}^n)$ is such that

$$\int \cdots \int \rho_N^{(n)}(\mathbf{r}^n) d\mathbf{r}^n = \frac{N!}{(N-n)!}, \tag{2.9}$$

which corresponds to the number of occurrences of finding n particles among N. In particular, one has

$$\int \rho_N^{(1)}(\mathbf{r}^1) d\mathbf{r}^1 = N \tag{2.10}$$

$$\int \int \rho_N^{(2)}(\mathbf{r}^2) d\mathbf{r}^2 = N(N-1) \tag{2.11}$$

which means for Eqs.(2.10) and (2.11) that one can find N particles and one can find $N(N-1)$ pairs of particles in the total volume, respectively.

The pair distribution function is defined as

$$g_N^{(2)}(\mathbf{r}_1, \mathbf{r}_2) = \frac{\rho_N^{(2)}(\mathbf{r}_1, \mathbf{r}_2)}{(\rho_N^{(1)}(\mathbf{r}_1) \rho_N^{(1)}(\mathbf{r}_2))}. \tag{2.12}$$

For an homogeneous system (which is not the case of liquids in the vicinity of interfaces), one has $\rho_N^{(1)}(r) = \rho$ and the pair distribution function only depends on the relative distance between particles:

$$g_N^{(2)}(\mathbf{r}_1, \mathbf{r}_2) = g(|\mathbf{r}_1 - \mathbf{r}_2|) = \frac{\rho_N^{(2)}(|\mathbf{r}_1 - \mathbf{r}_2|)}{\rho^2} \tag{2.13}$$

where $g(r)$ is called the radial distribution function.

When the distance $|\mathbf{r}_1 - \mathbf{r}_2|$ is large, the radial distribution function goes to $1 - \frac{1}{N}$. To the thermodynamics limit, one recovers that the radial distribution function goes to 1, but in finite size, a correction appears which changes the large distance limit.

Noting that

$$\langle \delta(\mathbf{r} - \mathbf{r}_1) \rangle = \frac{1}{Z_N(V,T)} \int \cdots \int \delta(\mathbf{r} - \mathbf{r}_1) \exp(-\beta V_N(\mathbf{r}^N)) d\mathbf{r}^N \tag{2.14}$$

$$= \frac{1}{Z_N(V,T)} \int \cdots \int \exp(-\beta V_N(\mathbf{r}, \mathbf{r}_2, \ldots, \mathbf{r}_N)) d\mathbf{r}_2 \ldots d\mathbf{r}_N \tag{2.15}$$

the probability density is reexpressed as

$$\rho_N^{(1)}(\mathbf{r}) = \langle \sum_{i=1}^{N} \delta(\mathbf{r} - \mathbf{r}_i) \rangle. \tag{2.16}$$

Similarly, one infers

$$\rho_N^{(2)}(\mathbf{r}, \mathbf{r}') = \langle \sum_{i=1}^{N} \sum_{j=1, j \neq i}^{N} \delta(\mathbf{r} - \mathbf{r}_i) \delta(\mathbf{r}' - \mathbf{r}_j) \rangle. \tag{2.17}$$

By using microscopic densities, the radial distribution function is expressed as

$$g^{(2)}(\mathbf{r}_1, \mathbf{r}_2) \rho(\mathbf{r}_1)) \rho(\mathbf{r}_2) = \langle \sum_{i=1}^{N} \sum_{j=1, j \neq i}^{N} \delta(\mathbf{r} - \mathbf{r}_i) \delta(\mathbf{r}' - \mathbf{r}_j) \rangle. \tag{2.18}$$

For a homogeneous and isotropic system, the radial distribution function only depends on the module of relative distance $|\mathbf{r} - \mathbf{r}'|$. Integrating over the volume, one obtains that

$$\rho g(|\mathbf{r}|) = \frac{1}{N} \langle \sum_{i=1}^{N} \sum_{j=1, j \neq i}^{N} \delta(\mathbf{r} - \mathbf{r}_i + \mathbf{r}_j) \rangle. \tag{2.19}$$

In a simulation using periodic boundary conditions (with cubic symmetry), one cannot obtain the structure of the system beyond a distance equal to $L/2$, because of the spatial periodicity of each main directions of the box. Computation of the radial distribution function lies on a space discretization. Practically, one starts with an empty distance histogram of spatial step of Δr, one calculates the number of pairs whose distance is between r and $r + \Delta r$, one performs integration of Eq. (2.19) on the shell labeled by the index j of thickness Δr by using the approximate formula:

$$\rho g(\Delta r(j + 0.5)) = \frac{1}{N(V_{j+1} - V_j)} 2N_p(r), \tag{2.20}$$

where $N_p(r)$ is the number of distinct pairs whose center to center distances are between $j\Delta r$ and $(j + 1)\Delta r$ and where $V_j = \frac{4\pi}{3}((j + 1)\Delta r)^3$.

This formula is accurate if the radial distribution smoothly varies between the distance r and $r + \Delta r$. By decreasing the spatial steps, one can check a posteriori that this condition is satisfied. However, by decreasing the spatial step of the histogram, the statistical accuracy in each bin diminishes. Therefore, a compromise must be found for the step, based in part on a rule of thumb.

Last, note that computation of this correlation function (for a given configuration) involves all pairs, namely the square of the particle number, a intrinsic property of the correlation function. Because a correct average needs to consider a sufficient number of different configurations, only configurations where all particles have been moved will be considered instead of all configurations. The part of computation time spent for the correlation is then divided by N. In summary, calculation of the correlation
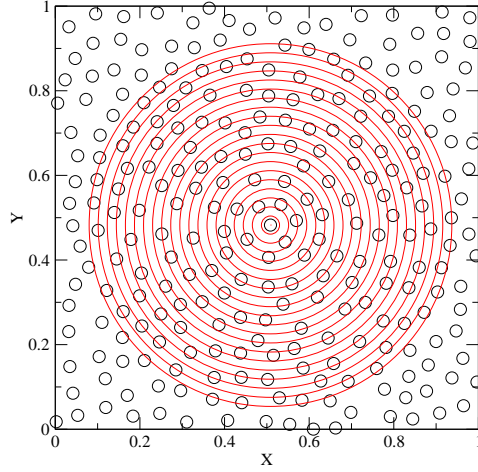
Figure 2.1: Basics of the computation of the radial distribution function: starting from a particle, one determines the pair number whose distance is between the successive built from the discretization given by Eq. (2.20).

function scales as N and is comparable to this of the simulation dynamics. The computation time can be decreased if only the short distance structure is either significant or of interest.

By expressing the radial distribution function with the local density, note that the distribution function is then defined in a statistical manner. The ensemble average is not restricted to equilibrium. We will see later (Chapter 7) that it is possible to calculate this function for out of equilibrium systems (random sequential addition) where the process is not described by a Gibbs distribution.

Structure factor

The static structure factor, $S(\mathbf{k})$, is a quantity available experimentally from light or neutron scattering; this is the Fourier transform of the radial distribution function $g(r)$.

For a simple liquid, the static structure factor is defined as

$$S(\mathbf{k}) = \frac{1}{N}\langle \rho_{\mathbf{k}}\rho_{-\mathbf{k}}\rangle \tag{2.21}$$

where $\rho_{\mathbf{k}}$ is the Fourier transform of the microscopic density $\rho(\mathbf{r})$. This reads

$$S(\mathbf{k}) = \frac{1}{N}\left\langle \sum_{i=1}^{N}\sum_{j=1}^{N}\exp(-i\mathbf{k}\mathbf{r}_i)\exp(i\mathbf{k}\mathbf{r}_j)\right\rangle. \tag{2.22}$$

By using δ distributions, $S(k)$ is expressed as

$$S(\mathbf{k}) = 1 + \frac{1}{N}\left\langle \int\int \exp(-i\mathbf{k}(\mathbf{r}-\mathbf{r}'))\sum_{i=1}^{N}\sum_{j=1,i\neq j}^{N}\delta(\mathbf{r}-\mathbf{r}_i)\delta(\mathbf{r}-\mathbf{r}_j)d\mathbf{r}d\mathbf{r}'\right\rangle \tag{2.23}$$

23

which gives

$$S(\mathbf{k}) = 1 + \frac{1}{N} \int \int \exp(-i\mathbf{k}(\mathbf{r} - \mathbf{r}'))\rho(\mathbf{r}, \mathbf{r}')d\mathbf{r}d\mathbf{r}'. \tag{2.24}$$

For a homogeneous fluid (isotropic and uniform)

$$S(\mathbf{k}) = 1 + \frac{\rho^2}{N} \int \int \exp(-i\mathbf{k}(\mathbf{r} - \mathbf{r}'))g(\mathbf{r}, \mathbf{r}')d\mathbf{r}d\mathbf{r}' \tag{2.25}$$

For an isotropic fluid, the radial distribution function only depends on $|\mathbf{r} - \mathbf{r}'|$. One then obtains

$$S(\mathbf{k}) = 1 + \rho \int \exp(-i\mathbf{k}\mathbf{r})g(r)d\mathbf{r}. \tag{2.26}$$

Because the system is isotropic, the Fourier transform only depends on the modulus k of wave vector, $|\mathbf{k}|$, which gives in three dimensions

$$S(k) = 1 + 2\pi\rho \int r^2 g(r) \int_0^\pi \exp(-ikr\cos(\theta))\sin(\theta)d\theta dr \tag{2.27}$$

and, after some calculation

$$S(k) = 1 + 4\pi\rho \int_0^\infty r^2 g(r)\frac{\sin(kr)}{kr}dr. \tag{2.28}$$

Finally, calculation of the static structure factor requires a one-dimensional sine-Fourier transform on the positive axis. Efficient codes of fast Fourier transforms calculate $S(k)$ very rapidly.

In a simulation, one can calculate either $g(r)$ and obtain $S(k)$ by a Fourier transform or $S(k)$ from Eq. (2.22) and obtain $g(r)$ by an inverse Fourier transform. In both cases, knowledge of correlations is limited to a distance equal to the half length of the simulation box.

For the static structure factor, this yields an infrared cut-off (π/L). The simulation cannot provide information for smaller wave vectors. Because the computation of the spatial correlation function over pairs of particles for a given configuration, the number of terms of the summation is proportional to N^2 (times the number of configurations used for the average in the simulation). In the direct calculation of the static structure factor $S(k)$, the number of terms to consider is proportional to N multiplied by the number of wave numbers which are the components of the structure factor (and finally multiplied by the number of configurations used in the simulation.

Repeated evaluation of trigonometric functions in Eq. (2.22) can be avoided by tabulating complex exponentials in an array at the beginning of the simulation

Basically, computation of $g(r)$, followed of the Fourier transform, should give the same result than the direct computation of the structure factor. However, because of the finite duration of the simulation as well as the finite size of the simulation box, statistical errors and round-off errors can give differences between the two manners of computation.

2.2.3   Dynamics

Spatial correlation functions are relevant probes of the presence or absence of the order at many lenghtscales. Similarly, knowledge of equilibrium fluctuations is provided by time correlation functions. Indeed, let us recall that equilibrium does not mean absence of particle dynamics: the system undergoes continuously fluctuations and how a fluctuation is able to disappear is a essential characteristic associated with to macroscopic changes, observed in particular in the vicinity of a phase transition.

Time correlation functions

Let us consider two examples of time correlation functions using simple models introduced in the first chapter of these lecture notes.

For the Ising model, one defines the spin-spin time correlation function

$$C(t) = \frac{1}{N} \sum_{i=1}^{N} < S_i(0)S_i(t) > \tag{2.29}$$

where the brackets denote equilibrium average and $S_i(t)$ is the spin variable of site i at time t. This function measures the system looses memory of a configuration at time t. At time $t = 0$, this function is equal to 1 (value which can not exceeded, by definition), then decreases and goes to 0 when the elapsed time is much larger than the equilibrium relaxation time.

For a simple liquid made of point particles, one can monitor the density autocorrelation function

$$C(t) = \frac{1}{V} \int d\mathbf{r} \langle \delta\rho(\mathbf{r}, t)\delta\rho(\mathbf{r}, 0)\rangle \tag{2.30}$$

where $\delta\rho(\mathbf{r}, t)$ denotes the local density fluctuation. This autocorrelation function measures the evolution of the local density along the time. It goes to zero when the elapsed time is much larger to the relaxation times of the system.

Computation of the time correlation function

We now go in details for implementing the time autocorrelation function, for a basic example, namely the spin correlation in the Ising model. This function is defined in Eq. (2.29)[1]

Time average of a correlation function (or others quantities) in the equilibrium simulation (Molecular Dynamics or Monte Carlo) is calculated by using a fundamental property of equilibrium systems, namely, time translational invariance: in other words, if one calculates $< S_i(t')S_i(t' + t) >$, the results is independent of t'. In order to have a statistical average well defined, one must iterate this computation for many different t'.

$$C(t) = \frac{1}{NM} \sum_{j=1}^{M} \sum_{i=1}^{N} S_i(t_j)S_i(t_j + t). \tag{2.31}$$

where the initial instant is a time where the system is already at equilibrium.

We have assumed that the time step is constant. When the later is variable, one can add a constant time step for the correlation function (in general, slightly smaller than the mean value of variable time step) and the above method can be then applied. For the computation of the correlation function, the time step Δt is generally a multiple of the time step of the simulation dynamics δt.

For practical computation of $C(t)$, one first defined a matrix of N_c columns and N raws (N is the total number of spins) and once equilibrated, one defines a real vector of N_c components and a integer vector of N_c components. Matrix and vectors are initially set to 0.

- At $t = 0$, the spin configuration is stored in the first column of the matrix vector and the scalar product $\sum_i S_i(t_0)S_i(t_0)$ is performed and the result is added to the first component of the real N_c component vector and the first component of the integer vector is incremented by one.

---

[1] Ising model does now own a Hamiltonian dynamics, and must be simulated by a Monte Carlo simulation, but the method described here can be applied for all sorts of dynamics, Monte Carlo or Molecular Dynamics.

- At $t = \Delta t_c$, the spin configuration is stored in the second column of the matrix, scalar products $\sum_i S_i(t_1)S_i(t_1)$ and $\sum_i S_i(t_0)S_i(t_1)$ are performed and added to the first and second component of the real N_c component vector. The first and second component of the integer vector are increased by one.

- For $t = k\Delta t_c$ with $k < N_c$, the same procedure is iterated and $k+1$ scalar products are performed and added in the $k+1$ components of the real N_c component vector.

- When $t = N_c\Delta t_c$, the first column of the matrix is erased and replaced with the new configuration. N_C scalar products can be performed and added to the N_c real vector. Similarly, all components of the integer vectors are increased by one. For $t = (N_c+1)\Delta t_c$, the second column of the matrix is replaced with the new configuration and so on.

- Finally, this procedure is stopped at time $t = T_f$, and because number of configurations involved in averaging the correlation function are not equal, the integer vector of N_c is used as a histogram of configuration average.

- Finally Eq. (2.31) is used for calculating the correlation function.)

A last remark concerns the delicate choice of the time step as well the number of components of the correlation function. First, the correlation function is calculated for a duration equal to $(N_c - 1)\Delta t$, which is bounded

$$\tau_{eq} << N_c\Delta t_c << T_{sim} \tag{2.32}$$

Indeed, configuration averaging needs that $N_c\Delta t_c$ is less than the total simulation time, but much larger than the equilibrium relaxation. Therefore, Δt_c which is a free parameter, is chosen a multiple of the time step of the simulation.

Linear response theory: results and transport coefficients

When a equilibrium system is slightly perturbed by an external field, the linear response theory provides the following result: the response of the system and return to equilibrium are directly related to the ability of the equilibrium system (namely in the absence of a external field) to answer to fluctuations (Onsager assumption of fluctuation regression).

In a simulation, it is easier to calculate a correlation function than a linear response function for several reasons: i) Computation of a correlation function is done at equilibrium. Practically, the correlation function is obtained simultaneously with other thermodynamic quantities along the simulation. ii) For computing response functions, it is necessary to perform different simulations for each response functions. Moreover, for obtaining the linear part of the response function (response of a quantity $B(t)$ to a external fieldΔF), one needs to ensure that the ratio $\langle \Delta B(t)\rangle / \Delta F$ is independent of ΔF: this constraint leads to choose a small value of ΔF, but if the perturbative field is too weak, the function $\langle \Delta B(t)\rangle$ will be small and could be of the same order of magnitude of statistical fluctuations of the simulation. In the last chapter of these lecture notes, we will introduce a recent method allowing to calculate response functions without perturbing the system. However, this method is restricted to Monte Carlo simulations. For Molecular Dynamics, fluctuations grow very rapidly with time[2].

In summary, by integrating the correlation function $C(t)$ over time, on obtains the system susceptibility.

---

[2]It exists some cases where the response function is easier to calculate than the correlation function, namely viscosity for liquids.

Consider a system at equilibrium described by the Hamiltonian $\mathcal{H}_0$. At time $t = 0$, this system is submitted to an external force and the Hamiltonian $\mathcal{H}'$ is given by

$$\mathcal{H}' = -A(\mathbf{r}^N)F(t) \tag{2.33}$$

where $F(t)$ is an external time-dependent force and $A(\mathbf{r}^N)$ is the variable conjugate to the force F. One assumes that this force goes to zero when $t \to \infty$ such that the system goes to equilibrium. It is possible to consider a space-dependent force, but for sake of simplicity, we restrict here the analysis to a uniform force.

The time evolution of the system is described by the Liouville equation

$$\frac{\partial f^{(N)}(\mathbf{r}^N, \mathbf{p}^N, t)}{\partial t} = -i\mathcal{L}f^{(N)}(\mathbf{r}^N, \mathbf{p}^N, t)$$

$$= \{\mathcal{H}_0 + \mathcal{H}', f^{(N)}(\mathbf{r}^N, \mathbf{p}^N, t)\}$$

$$= -i\mathcal{L}_0 f^{(N)}(\mathbf{r}^N, \mathbf{p}^N, t) - \{A, f^{(N)}(\mathbf{r}^N, \mathbf{p}^N, t)\}F(t)$$

where $\mathcal{L}_0$ denotes the Liouville operator associated with $\mathcal{H}_0$, $\mathcal{L}_0 = i\{\mathcal{H}_0, \}$.
Because the system was initially at equilibrium, one has

$$f^{(N)}(\mathbf{r}^N, \mathbf{p}^N, 0) = C\exp(-\beta\mathcal{H}_0(\mathbf{r}^N, \mathbf{p}^N)), \tag{2.34}$$

where C is a normalization constant. Since the external force is weak, one performs a perturbative expansion of $f^{(N)}(\mathbf{r}^N)$ around equlibrium. One writes

$$f^{(N)}(\mathbf{r}^N, \mathbf{p}^N, t) = f_0^{(N)}(\mathbf{r}^N, \mathbf{p}^N) + f_1^{(N)}(\mathbf{r}^N, \mathbf{p}^N, t) \tag{2.35}$$

To the lowest order in , one has

$$\frac{\partial f_1^{(N)}(\mathbf{r}^N, \mathbf{p}^N, t)}{\partial t} = -i\mathcal{L}_0 f_1^{(N)}(\mathbf{r}^N, \mathbf{p}^N, t) - \{A(\mathbf{r}^N), f_0^{(N)}(\mathbf{r}^N, \mathbf{p}^N)\}F(t). \tag{2.36}$$

Equation (2.36) is solved formally with the initial condition given by equation (2.34). This gives

$$f_1^{(N)}(\mathbf{r}^N, \mathbf{p}^N, t) = -\int_{-\infty}^t \exp(-i(t-s)\mathcal{L}_0)\{A, f_0^{(N)}\}F(s)ds. \tag{2.37}$$

Therefore, the variable $\langle \Delta B(t) \rangle = \langle B(t) \rangle - \langle B(-\infty) \rangle$ evolves as

$$\langle \Delta B(t) \rangle = \int\int d\mathbf{r}^N d\mathbf{p}^N \left(f^{(N)}(\mathbf{r}^N, \mathbf{p}^N, t) - f_0^{(N)}(\mathbf{r}^N, \mathbf{p}^N) \right) B(\mathbf{r}^N) d\mathbf{r}^N d\mathbf{p}^N. \tag{2.38}$$

To lowest order, the difference of Liouville distributions is given by equation (2.37) and equation (2.38) becomes

$$\langle \Delta B(t) \rangle = -\int\int d\mathbf{r}^N d\mathbf{p}^N \int_{-\infty}^t \exp(-i(t-s)\mathcal{L}_0)\{A, f_0^{(N)}\}B(\mathbf{r}^N)F(s)ds$$

$$= -\int\int d\mathbf{r}^N d\mathbf{p}^N \int_{-\infty}^t \{A, f_0^{(N)}\}\exp(i(t-s)\mathcal{L}_0)B(\mathbf{r}^N)F(s)ds \tag{2.39}$$

by using the fact that the Liouville operator is Hermitian.

Calculating the Poisson bracket, one obtains that

$$
\begin{aligned}
\{A, f_0^{(N)}\} &= \sum_{i=1}^{N} \left(\frac{\partial A}{\partial \mathbf{r}_i} \frac{\partial f_0^{(N)}}{d\mathbf{p}_i} - \frac{\partial A}{\partial \mathbf{p}_i} \frac{\partial f_0^{(N)}}{d\mathbf{r}_i} \right) \\
&= -\beta \sum_{i=1}^{N} \left(\frac{\partial A}{\partial \mathbf{r}_i} \frac{\partial \mathcal{H}_0^{(N)}}{d\mathbf{p}_i} - \frac{\partial A}{\partial \mathbf{p}_i} \frac{\partial \mathcal{H}_0^{(N)}}{d\mathbf{r}_i} \right) f_0^{(N)} \\
&= -\beta i \mathcal{L}_0 A f_0^{(N)} \\
&= -\beta \frac{dA(0)}{dt} f_0^{(N)}
\end{aligned}
\tag{2.40}
$$

By inserting equation (2.40) in Eq. (2.39), one obtains

$$
\langle \Delta B(t) \rangle = \beta \int \int d\mathbf{r}^N d\mathbf{p}^N f_0^{(N)} \int_{-\infty}^{t} \frac{dA(0)}{dt} \exp(-i(t-s)\mathcal{L}_0) B(\mathbf{r}^N) F(s) ds
\tag{2.41}
$$

By using the fact that

$$
B(\mathbf{r}^N(t)) = \exp(it\mathcal{L}_0) B(\mathbf{r}^N(0))
\tag{2.42}
$$

Eq. (2.41) becomes

$$
\langle \Delta B(t) \rangle = \beta \int_{-\infty}^{t} ds \left\langle \frac{dA(0)}{dt} B(t-s) \right\rangle F(s)
\tag{2.43}
$$

One defines the linear response function of B with respect to F as

$$
\langle \Delta B(t) \rangle = \int_{-\infty}^{\infty} ds \chi(t,s) F(s) + \mathcal{O}(F^2)
\tag{2.44}
$$

With Eq. (2.43), one finds the following properties

1. By equating Eqs. (2.43) and (2.44), one obtains the fluctuation-dissipation theorem

$$
\chi(t) = \begin{cases} -\beta \frac{d}{dt} \langle A(0)B(t) \rangle & t > 0 \\ 0 & t < 0 \end{cases}
\tag{2.45}
$$

2. A system cannot respond to a perturbation before it is applied. This property is a consequence of the causality.

$$
\chi(t,s) = 0, \qquad t - s \leq 0
\tag{2.46}
$$

3. The equilibrium response function is translationally invariant in time

$$
\chi(t,s) = \chi(t-s)
\tag{2.47}
$$

When $A = B$, one denotes the autocorrelation function as

$$
C_A(t) = \langle A(0)A(t) \rangle,
\tag{2.48}
$$

and we have

$$\chi(t) = \begin{cases} -\beta \dfrac{dC_A(t)}{dt} & t > 0 \\ 0 & t < 0 \end{cases} \tag{2.49}$$

By defining the linear response as

$$R(t) = \int_0^t \chi(s)ds \tag{2.50}$$

The fluctuation-dissipation theorem is expressed as

$$R(t) = \begin{cases} \beta(C_A(0) - C_A(t)) & t > 0 \\ 0 & t < 0 \end{cases} \tag{2.51}$$

2.2.4 Space-time correlation functions

To go further in correlation study, one can follow correlations both in space and time. This information is richer, but the price to pay is the calculation of a two-variable correlation function, at least. We introduce these functions because they are also available in experiments, essentially form neutron scattering.

Van Hove function

Let us consider the density correlation function which depends both on space and time

$$\rho G(\mathbf{r}, \mathbf{r}'; t) = \langle \rho(\mathbf{r}' + \mathbf{r}, t)\rho(\mathbf{r}', 0) \rangle \tag{2.52}$$

This function can be expressed from the microscopic densities as

$$\rho G(\mathbf{r}, \mathbf{r}'; t) = \left\langle \sum_{i=1}^{N} \sum_{j=1}^{N} \delta(\mathbf{r}' + \mathbf{r} - \mathbf{r}_i(t))\delta(\mathbf{r} - \mathbf{r}_j(0)) \right\rangle \tag{2.53}$$

For a homogeneous system, $G(\mathbf{r}, \mathbf{r}'; t)$ only depends on the relative distance. Integrating over volume, one obtains

$$G(\mathbf{r}, t) = \frac{1}{N} \left\langle \sum_{i=1}^{N} \sum_{j=1}^{N} \delta(\mathbf{r} - \mathbf{r}_i(t) + \mathbf{r}_j(0)) \right\rangle \tag{2.54}$$

At $t = 0$, the Van Hove function $G(\mathbf{r}, t)$ is simplified and one obtains

$$G(\mathbf{r}, 0) = \frac{1}{N} \left\langle \sum_{i=1}^{N} \sum_{j=1}^{N} \delta(\mathbf{r} + \mathbf{r}_i(0) - \mathbf{r}_j(0)) \right\rangle$$

$$= \delta(\mathbf{r}) + \rho g(\mathbf{r}) \tag{2.55}$$

Except a singularity at the origin, at $t = 0$, the Van Hove function is proportional to the pair distribution function $g(\mathbf{r})$. On can separate this function in two parts, self and distinct

$$G(\mathbf{r}, t) = G_s(\mathbf{r}, t) + G_d(\mathbf{r}, t) \tag{2.56}$$

with

$$G_s(\mathbf{r}, t) = \frac{1}{N} \left\langle \sum_{i=1}^{N} \delta((\mathbf{r} + \mathbf{r}_i(0) - \mathbf{r}_i(t)) \right\rangle \tag{2.57}$$

$$G_d(\mathbf{r}, t) = \frac{1}{N} \left\langle \sum_{i \neq j}^{N} \delta(\mathbf{r} + \mathbf{r}_j(0) - \mathbf{r}_i(t)) \right\rangle \tag{2.58}$$

These correlation functions have the physical interpretation: the Van Hove function is the probability density of finding a particle i in the vicinity of $\mathbf{r}$ at time t knowing that a particle j is in the vicinity of the origin at time $t = 0$. $G_s(\mathbf{r}, t)$ is the probability density of finding a particle i at time t knowing that this particle was at the origin at time $t = 0$; finally, $G_d(\mathbf{r}, t)$ corresponds to the probability density of finding a particle j different of i at time t knowing that the particle i was at the origin at time $t = 0$.

Normalization of these two functions reads

$$\int d\mathbf{r} G_s(\mathbf{r}, t) = 1 \tag{2.59}$$

and corresponds to be certain that the particle is in the volume at any time (namely, particle conservation).

Similarly, one has

$$\int d\mathbf{r} G_d(\mathbf{r}, t) = N - 1 \tag{2.60}$$

with the following physical meaning: by integrating over space, the distinct correlation function is able to count the remaining particles.

In the long time limit, the system looses memory of the initial configuration and the correlation functions becomes independent of the distance $\mathbf{r}$.

$$\lim_{r \to \infty} G_s(\mathbf{r}, t) = \lim_{t \to \infty} G_s(\mathbf{r}, t) \simeq \frac{1}{V} \simeq 0 \tag{2.61}$$

$$\lim_{r \to \infty} G_d(\mathbf{r}, t) = \lim_{t \to \infty} G_s(\mathbf{r}, t) \simeq \frac{N-1}{V} \simeq \rho \tag{2.62}$$

Intermediate scattering function

Instead of considering correlations in space, one can see in reciprocal space, namely in Fourier components. Let us define a correlation function so called intermediate scattering function, which is the Fourier transform of the Van Hove function

$$F(\mathbf{k}, t) = \int d\mathbf{k} G(\mathbf{r}, t) e^{-i\mathbf{k} \cdot \mathbf{r} t} \tag{2.63}$$

In a similar manner, one defines self and distinct parts of the function

$$F_s(\mathbf{k}, t) = \int d\mathbf{k} G_s(\mathbf{r}, t) e^{-i\mathbf{k} \mathbf{r} t} \tag{2.64}$$

$$F_d(\mathbf{k}, t) = \int d\mathbf{k}\, G_d(\mathbf{r}, t) e^{-i\mathbf{k}\mathbf{r}t} \tag{2.65}$$

The physical interest of splitting the function is related to the fact that coherent and incoherent neutron scattering provide the total $F(\mathbf{k}, t)$ and self $F_s(\mathbf{k}, t)$ intermediate scattering functions.

Dynamic structure factor

The dynamics structure factor is defined as the time Fourier transform of the intermediate scattering function

$$S(\mathbf{k}, \omega) = \int dt\, F(\mathbf{k}, t) e^{i\omega t} \tag{2.66}$$

Obviously, one has the following sum rule: integrating the dynamic structure factor over ω gives the static structure factor.

$$\int d\omega\, S(\mathbf{k}, \omega) = S(\mathbf{k}) \tag{2.67}$$

3

3.1   Introduction

One very interesting application of simulations is to the study of phase transitions, even though they can occur only in infinite systems (namely in the thermodynamic limit). This apparent paradox can be resolved as follows: in a continuous phase transition (unlike a first-order transition), fluctuations occur at increasing length scales as the temperature approaches the critical point. In a simulation box, when fluctuations are smaller than the linear dimension of the simulation cell, the system does not realize that the simulation cell is finite and its behavior (and the thermodynamic quantities) is close to an infinite system. When the fluctuations are comparable to the system size, the behavior differs from the infinite system close the critical temperature, but the finite size behavior is similar to the infinite system when the temperature is far from the critical point.

Finite size scaling analysis which involves simulations with different system sizes[1] provides an efficient tool for determining the critical exponents of the system.

Many simulations investigating the critical phenomena (continuous phase transitions) were performed with lattice models. Studies of continuous systems are less common. the critical phenomena theory show that phase transitions are characterized by scaling laws (algebraic laws) whose exponents are universal quantities independent of a underlying lattice. This is due to the fact that a continuous phase transition is associated with fluctuations of all length scales at the critical point. Therefore, microscopic details are irrelevant in the universal behavior of the system, but the space dimension of the system as well as the symmetry group of the order parameter are essential.

Phase transitions are characterized by critical exponents which define universality classes. Studies can therefore be realized accurately on simple models. For example, the liquid-gas transition for liquids interacting with a pairwise potential belongs to the same universality class as the para-ferromagnetic transition of the Ising model.

As we will see below, simulations must be performed with different sizes in order to determine the critical exponents. If we compare lattice and continuous systems, the former requires less simulation time. Indeed, varying the size of a continuous system over several orders of magnitude is a challenging problem, whereas it is possible with lattice systems.

Finally, let us note that the critical temperature obtained in simulations varies weakly with the system size in continuous systems, whereas a strong dependence can be observed in lattice models. Consequently, with a modest size, a rather good estimate of the critical temperature can be obtained with a simulation.

---

[1]For a good accuracy for the critical exponents, one must choose large simulation cells (and the accuracy of critical exponents are restricted by the computer powers). Indeed, scaling laws used for the critical exponent calculation corresponds to asymptotic behaviors, whose validity is for large simulation cells. To have accurate critical exponents, scaling law corrections can be included, which introduces additional parameters to be estimated.

3.2 Scaling laws

3.2.1 Critical exponents

Scaling law assumptions were made in the sixties and were subsequently precisely derived with the renormalization group theory, which provides a general framework for studying critical phenomena. Detailed presentation of this theory goes beyond the scope of these lecture notes, and we only introduce the basic concepts useful for studying phase transitions in simulations

For the sake of simplicity, we consider the Ising model whose Hamiltonian is given by

$$\mathcal{H} = -J \sum_{<i,j>}^{N} S_i S_j - H \sum_{i=1}^{N} S_i \tag{3.1}$$

where $< i, j >$ denotes a summation over nearest sites, J is the ferromagnetic interaction strength, and H a uniform external field.

In the vicinity of the critical point (namely, for the Ising model, $H = 0$, $T_c/J = 2.2691\ldots$ in two dimensions), thermodynamic quantities, as well as spatial correlation functions behave according to scaling laws. The magnetization per spin is defined by

$$m(t,h) = \frac{1}{N} \sum_{i=1}^{N} \langle S_i \rangle, \tag{3.2}$$

where $t = (T - T_c)/T_c$ is the dimensionless temperature and $h = H/k_B T$ the dimensionless external field.

Magnetization (Eq. (3.2)) is defined as

$$m(t,h) = \lim_{N \to \infty} m_N(t,h). \tag{3.3}$$

In the absence of an external field, the scaling law is

$$m(t, h = 0) = \begin{cases} 0 & t > 0 \\ A|t|^\beta & t < 0 \end{cases} \tag{3.4}$$

where the exponent β characterizes the spontaneous magnetization in the ferromagnetic phase.

Similarly, along the critical isotherm, one has

$$m(t = 0, h) = \begin{cases} -B|h|^{1/\delta} & h < 0 \\ B|h|^{1/\delta} & h > 0 \end{cases} \tag{3.5}$$

where δ is the exponent of the magnetization in the presence of an external field.

The specific heat c_v is given by

$$c_v(t, h = 0) \begin{cases} C|t|^{-\alpha} & t < 0 \\ C'|t|^{-\alpha'} & t > 0 \end{cases} \tag{3.6}$$

where α and α' are the exponents associated with the specific heat.

Experimentally, one always observes that $\alpha = \alpha'$. The amplitude ratio C/C' is also a universal quantity. Similarly, one can define a pair of exponents for each quantity for positive or negative dimensionless temperature, but exponents are always identical and we only consider an exponent for each quantity. Isothermal susceptibility in zero external field diverges at the critical point as

$$\chi_T(h=0) \sim |t|^{-\gamma}, \tag{3.7}$$

where γ is the susceptibility exponent.

The spatial correlation function, denoted by $g(r)$, behaves in the vicinity of the critical point as

$$g(r) \sim \frac{\exp(-r/\xi)}{r^{d-2+\eta}}, \tag{3.8}$$

where ξ is the correlation length, which behaves as

$$\xi \sim |t|^{-\nu}, \tag{3.9}$$

where ν is the exponent associated with the correlation length.

This correlation function decreases algebraically at the critical point as follows

$$g(r) \sim \frac{1}{r^{d-2+\eta}} \tag{3.10}$$

where η is the exponent associated with the correlation function.

These six exponents $(\alpha, \beta, \gamma, \delta, \nu, \eta)$ are not independent! Assuming that the free energy per volume unit and the pair correlation function obey a scaling function, it can be shown that only two exponents are independent.

3.2.2 Scaling laws

Landau theory neglects the fluctuations of the order parameter (relevant in the vicinity of the phase transition) and expresses the free energy as an analytical function of the order parameter. The phase transition theory assumes that the neglected fluctuations of the mean-field approach make a non analytical contribution to the thermodynamic quantities, e.g. the free energy density, denoted $f_s(t,h)$:

$$f_s(t,h) = |t|^{2-\alpha} F_f^{\pm}\left(\frac{h}{|t|^{\Delta}}\right) \tag{3.11}$$

where $F_f^{\pm}$ are functions defined below and above the critical temperature and which approach a non zero value when $h \to 0$ and have an algebraic behavior when the scaling variable goes to infinity,

$$F_f^{\pm}(x) \sim x^{\lambda+1}, \qquad x \to \infty. \tag{3.12}$$

Properties of this non analytical term give relations between critical exponents. Therefore, magnetization is obtained by taking the derivative of the free energy density with respect to the external field h,

35

$$m(h,t) = -\frac{1}{k_B T}\frac{\partial f_s}{\partial h} \sim |t|^{2-\alpha-\Delta} F_f^{\pm'}\left(\frac{h}{|t|^\Delta}\right). \tag{3.13}$$

For $h \to 0$, one identifies exponents of the algebraic dependence in temperature:

$$\beta = 2 - \alpha - \Delta. \tag{3.14}$$

Similarly, by taking the second derivative of the free energy density with respect to the field h, one obtains the isothermal susceptibility

$$\chi_T(t,h) \sim t^{2-\alpha-2\Delta} F_f^{\pm''}\left(\frac{h}{|t|^\Delta}\right). \tag{3.15}$$

For $h \to 0$, one identifies exponents of the algebraic dependence in temperature:

$$-\gamma = 2 - \alpha - 2\Delta. \tag{3.16}$$

By eliminating Δ, one obtains a first relation between exponents α, β and γ, called Rushbrooke scaling law

$$\alpha + 2\beta + \gamma = 2. \tag{3.17}$$

This relation does not depend on the space dimension d. Moreover, one has

$$\Delta = \beta + \gamma. \tag{3.18}$$

Let us consider the limit when t goes to zero when $h \neq 0$. One then obtains for the magnetization, along the critical isotherm:

$$m(t,h) \sim |t|^\beta \left(\frac{h}{|t|^\Delta}\right)^\lambda \tag{3.19}$$

$$\sim |t|^{\beta-\Delta\lambda} h^\lambda. \tag{3.20}$$

In order to recover Eq. (3.5), magnetization must be finite when $t \to 0$, i.e. does not diverge or vanish. This yields

$$\beta = \Delta\lambda, \tag{3.21}$$

By identifying exponents of h in Eqs. (3.5) and (3.20) one infers

$$\lambda = \frac{1}{\delta}. \tag{3.22}$$

Eliminating Δ and λ in Eqs. (3.21), (3.22) and (3.18), one infers the following relation

$$\beta\delta = \beta + \gamma. \tag{3.23}$$

The next two relations are inferred from the scaling form of the free energy density and of the spatial correlation relation $g(r)$. By considering that the relevant macroscopic length scale of the system is the correlation length, the singular free energy density has the following expansion

$$\frac{f_s}{k_B T} \sim \xi^{-d}\left(A + B_1\left(\frac{l_1}{\xi}\right) + \ldots\right) \tag{3.24}$$

where l_1 is a microscopic length scale. When $t \to 0$, subdominant corrections can be neglected and one has

$$\frac{f_s}{k_B T} \sim \xi^{-d} \sim |t|^{\nu d}. \tag{3.25}$$

Taking the second derivative of this equation with respect to the temperature, one obtains for the specific heat

$$c_v = -T\frac{\partial^2 f_s}{\partial T^2} \sim |t|^{\nu d - 2}. \tag{3.26}$$

By using Eq. (3.6), one infers the Josephson relation (so called the hyper scaling relation),

$$2 - \alpha = d\nu, \tag{3.27}$$

which involves the space dimension. Knowing that the space integral of $g(r)$ is proportional to the susceptibility, one performs the integration of $g(r)$ over a volume whose linear dimension is ξ, which gives

$$\int_0^\xi d^d r\, g(r) = \int_0^\xi d^d r\, \frac{\exp(-r/\xi)}{r^{d-2+\eta}} \tag{3.28}$$

With the change of variable $u = r/\xi$ in Eq. (3.28), it comes

$$\int_0^\xi d^d r\, g(r) = \xi^{2-\eta} \int_0^1 d^d u\, \frac{\exp(-u)}{u^{d-2+\eta}} \tag{3.29}$$

On the right-hand side of Eq. (3.29), the integral is a finite value. By using the relation between the correlation length ξ and the dimensionless temperature t (Eq. (3.9)), one obtains that

$$\chi_T(h = 0) \sim |t|^{-(2-\eta)\nu}, \tag{3.30}$$

By considering Eq. (3.7), one infers

$$\gamma = (2 - \eta)\nu. \tag{3.31}$$

Finally, since there are four relations between critical exponents that implies only two are independent [2].

An significant feature of the critical phenomena theory is the existence of a upper and lower critical dimensions: At the upper critical dimension d_{sup} and above, the mean-field theory (up to some logarithmic subdominant corrections) describes the critical phase transition. Below lower critical dimension d_{inf}, no phase transition can occur. For the Ising model, $d_{inf} = 1$ and $d_{sup} = 4$. This implies that in three-dimensional Euclidean space, a mean-field theory cannot describe accurately the para-ferromagnetic phase transition, in particular the critical exponents. Because the liquid-gas transition belongs to the universality class of the Ising model, a similar conclusion applies to the phase transition.

After this brief survey of critical phenomena, we now apply scaling laws for finite size systems to develop a method which gives the critical exponents of the phase transition as well as non universal quantities in the thermodynamic limit.

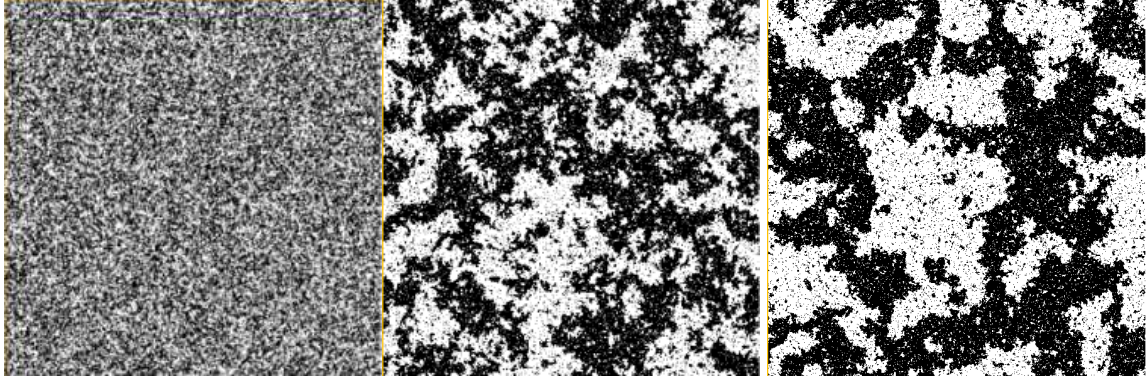[2]This property does not apply to quenched disordered systems.

Figure 3.1: Spin configurations of the Ising model in 2 dimensions: (a) at high temperature. (b) close to the critical temperature (c) below the critical temperature

3.3 Finite size scaling analysis

3.3.1 Specific heat

A close examination of spin configuration in Fig. 3.1 merely illustrates that a system close to the phase transition shows domains of spins of the same sign. The size of domains increases as the transition is approached. The group renormalization theory showed that, close to the critical point, the thermodynamic quantities of a finite system of linear size L for a dimensionless temperature t, and a dimensionless field $h,\dots$, are the same of a system of size L/l for a dimensionless temperature tl^{y_t} and a dimensionless field $hl^{y_h},\dots$, which gives

$$f_s(t,h,\dots L^{-1}) = l^{-d} f_s(tl^{y_t}, hl^{y_h},\dots,(l/L)^{-1}).\tag{3.32}$$

where y_t and y_h are the exponents associated with the fields.

A phase transition occurs when all variables of f_s go to 0. In zero field, one has

$$f_s(t,\dots L^{-1}) = |t|^{2-\alpha} F_f^{\pm}(|t|^{-\nu}/L).\tag{3.33}$$

If the correlation length ξ is smaller than L, the system behaves like an infinite system. But, in simulation, the limit $t \to 0$ can be taken before than $L \to \infty$, and ξ can be larger than L, the linear dimension of the simulation cell; in other words, this corresponds to the fact that the variable of the function F_f (Eq. (3.33)) then goes to infinity; this means, one moves away the critical point. Below and above the critical point of the infinite and for a vicinity which shrinks with increasing sizes of simulation cells, the system behaves like an infinite system whereas in the region where the correlation length is equal to size of the simulation cell, one observes a size-dependence (See Fig. 3.2). If we denote by F_c the scaling function associated with the specific heat, which depends on the scaling variable $|t|^{-\nu}/L$, one has

$$c_v(t,L^{-1}) = |t|^{-\alpha} F_c^{\pm}(|t|^{-\nu}/L).\tag{3.34}$$

Because $|t|^{-\alpha}$ goes to infinity when $t \to 0$, $F_c^{\pm}(x)$ must go to zero when x goes to zero. Reexpressing this function as

$$F_c^{\pm}(|t|^{-\nu}/L)) = (|t|^{-\nu}/L)^{-\kappa} D^{\pm}(Lt^{\nu})\tag{3.35}$$

with $D^{\pm}(0)$ finite. Since the specific heat does not diverge when $|t|$ goes to zero, one requires that
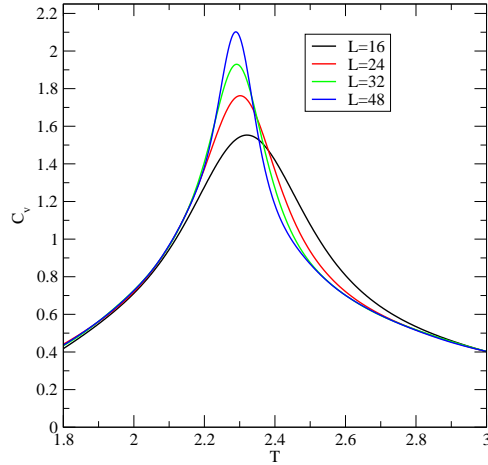
$$\kappa = \alpha/\nu\tag{3.36}$$

Figure 3.2: Specific heat versus temperature of the Ising model in two dimensions, The simulation results correspond to different system sizes where L is the linear dimension of the lattice.

which gives for the specific heat

$$c_v(t, L^{-1}) = L^{\alpha/\nu} D(L|t|^{\nu}). \tag{3.37}$$

The function D goes to zero when the scaling variable is large and is always finite and positive. D is a continuous function, and displays a maximum for a finite value of the scaling variable, denoted x_0. Therefore, for a finite size system, one obtains the following result

- The maximum of the specific heat occurs at a temperature $T_c(L)$ which is shifted with respect to that of the infinite system

$$T_c(L) - T_c \sim L^{-1/\nu}. \tag{3.38}$$

- The maximum of the specific heat of a finite size system L is given by the scaling law

$$C_v(T_c(L), L^{-1}) \sim L^{\alpha/\nu}. \tag{3.39}$$

3.3.2 Other quantities

Similar results can be obtained for other thermodynamic quantities, available in simulations. For instance, let us consider the absolute value of the magnetization

$$\langle |m| \rangle = \frac{1}{N} \langle | \sum_{i=1}^{N} S_i | \rangle \tag{3.40}$$

and the isothermal susceptibility

$$k_B T \chi = N(\langle m^2 \rangle - \langle m \rangle^2). \tag{3.41}$$

It is possible to calculate a second susceptibility

$$k_B T \chi' = N(\langle m^2 \rangle - \langle |m| \rangle^2) \tag{3.42}$$

χ increases as N when $T \to 0$, due to the existence of two peaks in the magnetization distribution and does not display a maximum at the transition temperature. Conversely, χ' goes to 0 when $T \to 0$ and has a maximum at the critical point. At high temperature, both susceptibilities are related in the thermodynamic limit by the relation $\chi = \chi'(1 - 2/\pi)$. At the critical point, both susceptibilities χ and χ' diverge with the same exponent, but χ' has a smaller amplitude.

Another quantity, useful in simulation, is the Binder parameter

$$U = 1 - \frac{\langle m^4 \rangle}{3 \langle m^2 \rangle^2} \tag{3.43}$$

The reasoning leading to the scaling function of the specific heat can be used for other thermodynamic quantities and scaling laws for finite size systems are given by the relations

$$\langle |m(t, 0, L^{-1})| \rangle = L^{-\beta/\nu} F_m^{\pm}(t L^{1/\nu}) \tag{3.44}$$

$$k_B T \chi(t, 0, L^{-1}) = L^{\gamma/\nu} F_\chi^{\pm}(t L^{1/\nu}) \tag{3.45}$$

$$k_B T \chi'(t, 0, L^{-1}) = L^{\gamma/\nu} F_{\chi'}^{\pm}(t L^{1/\nu}) \tag{3.46}$$

$$U(t, 0, L^{-1}) = F_U^{\pm}(t L^{1/\nu}) \tag{3.47}$$

where $F_m^{\pm}$, $F_\chi^{\pm}$, $F_{\chi'}^{\pm}$, and $F_U^{\pm}$ are 8 scaling functions (with different maxima).

Practically, by plotting Binder's parameter as a function of temperature, all curves $U(t, 0, L^{-1})$ intersect at the same abscissa (within statistical errors), which determines the critical temperature of the system in the thermodynamic limit. Once the temperature of the transition obtained, one can compute β/ν from $\langle |m| \rangle$, then γ/ν from χ (or χ'). By considering the maximum of C_v or other quantities, one derives the value of the exponent $1/\nu$.

Note that in simulation more information is available than the two independent exponents and the critical temperature. Indeed, because of uncertainty and sub-dominant corrections to scaling laws,[3] by comparing results, one can determine more accurately critical exponents.

Monte Carlo simulation, combined with finite size scaling, is a powerful method for calculating critical exponents. Moreover, one also obtains non-universal quantities, like the critical temperature, that no analytical treatment is able to provide with sufficient accuracy until now. Indeed, the renormalization group can only give critical exponents and is unable to provide a reasonable value of the critical temperature. Only the functional or non perturbative approach can give quantitative results, but with a high price to pay in terms of computation time.

3.4   Critical slowing down

The nice method, developed in the previous section, uses the idea that the Metropolis algorithm remains efficient even in the vicinity of the critical region. This is not the case, and in order to obtain equilibrium, fluctuations must be sampled at all scales. But, close to the critical point, large scale fluctuations are present and relaxation times increase accordingly; these times are related to the growing correlation length by the scaling relation

$$\tau \sim (\xi(t))^z \tag{3.48}$$

---

[3]Scaling laws correspond to asymptotic behavior for very large system sizes: in order to increase the accuracy of the simulation, one needs to include subdominant corrections.

where z is a new exponent, the so-called dynamical exponent. It typically varies between 2 and 5 (for a Metropolis algorithm). For a infinite system, knowing that $\xi \sim |t|^{-\nu}$, the relaxation time then diverges as

$$\tau \sim |t|^{-\nu z}. \tag{3.49}$$

For a finite system, the correlation length is bound by the linear system size L and the relaxation time increases as

$$\boxed{\tau \sim L^z;} \tag{3.50}$$

Simulation time then becomes prohibitive!

3.5   Reweighting Method

To obtain a complete phase of a given system, a large number of simulations are required for scanning the entire range of temperatures, or for the range of external fields. When one attempts to locate a phase transition precisely, the number of simulation runs can become prohibitive. The reweighting method is a powerful techniques that estimates the thermodynamic properties of the system by using the simulation data performed at a temperature T, for a set of temperatures between $[T - \Delta T, T + \Delta T]$ (or for an external field H, within a set of values of the external field $[H - \Delta H, H + \Delta H]$).

The method relies on the following results: Consider the partition function [6, 7, 5],

$$
\begin{aligned}
Z(\beta, N) &= \sum_{\{\alpha\}} \exp(-\beta H(\{\alpha\})) \\
&= \sum_{i=1} g(i) \exp(-\beta E(i))
\end{aligned} \tag{3.51}
$$

where $\{\alpha\}$ denotes all available states, the index i runs over all available energies of the system, $g(i)$ denotes the density of states of energy $E(i)$. For a given inverse temperature $\beta' = 1/(k_B T')$, the partition function can be expressed as

$$
\begin{aligned}
Z(\beta', N) &= \sum_i g(i) \exp(-\beta' E(i)) \\
&= \sum_i g(i) \exp(-\beta E(i)) \exp(-(\beta' - \beta) E(i)) \\
&= \sum_i g(i) \exp(-\beta E(i)) \exp(-(\Delta \beta) E(i)),
\end{aligned} \tag{3.52}
$$

where $\Delta \beta = (\beta' - \beta)$.
Similarly, a thermal average, like the mean energy, is expressed as:

$$
\begin{aligned}
\langle E(\beta', N) \rangle &= \frac{\sum_i g(i) E(i) \exp(-\beta' E(i))}{\sum_i g(i) \exp(-\beta' E(i))} \\
&= \frac{\sum_i g(i) E(i) \exp(-\beta E(i)) \exp(-(\Delta \beta) E(i))}{\sum_i g(i) \exp(-\beta E(i)) \exp(-(\Delta \beta) E(i))}.
\end{aligned} \tag{3.53}
$$

In a Monte Carlo simulation, at equilibrium, one can monitor an energy histogram associated with visited configurations.
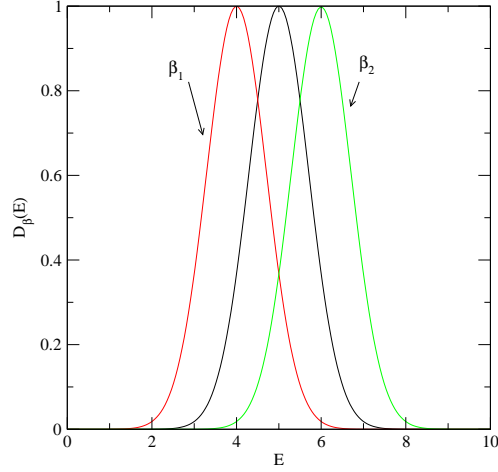
Figure 3.3: Energy histogram, $D_\beta(E)$ of a Monte Carlo simulation (middle curve) to the inverse temperature β; ,$D_{\beta_1}(E)$ and $D_{\beta_2}(E)$ are obtained by a reweighting method.

This histogram, denoted $D_\beta(i)$, is proportional to the density of states $g(i)$ weighted by the Boltzmann factor,

$$D_\beta(i) = C(\beta)g(i)\exp(-\beta E(i)) \tag{3.54}$$

where $C(\beta)$ is a temperature dependent constant. One can easily see that Eq. (3.53) can be reexpressed as

$$\langle E(\beta', N)\rangle = \frac{\sum_i D_\beta(i)E(i)\exp(-(\Delta\beta)E(i))}{\sum_i D_\beta(i)\exp(-(\Delta\beta)E(i))}. \tag{3.55}$$

An naive (or optimistic) view would consist in believing that a single simulation at given temperature could give the thermodynamic quantities of the entire range of temperature[4]. As shown in the schematic of Fig. 3.3, when the histogram is reweighted with a lower temperature than the temperature of the simulation, $(\beta_1 > \beta)$, energy histogram is shifted towards to lower energies. Conversely, when reweighted energy histogram with a higher temperature $(\beta_2 > \beta)$, energy histogram is shifted towards the higher energies.

In a Monte Carlo simulation, the number of steps is finite, which means that for a given temperature, states of energy significantly lower or larger than the mean energy are weakly sampled, or not sampled at all. Reweighting leads to an exponential increase of errors with the temperature difference. Practically, when the reweighted histogram has a maximum at a distance larger than the standard deviation of the simulation data, the accuracy of the reweighted histogram, and of the thermodynamic quantities is poor.

We briefly summarize the results of a more refined analysis of the reweighting method

For a system with a continuous phase transition, the energy histogram $D_\beta(i)$ is bell-shaped, and can be approximated by a Gaussian far from a phase transition. This is associated with the fact that at equilibrium, available energy states are around the mean energy value. Far from the critical point, the histogram width corresponds to fluctuations and is then proportional to $1/\sqrt{N}$ where N is the site number or the particle number. This shows that the efficiency of this reweighting method decreases

---

[4]By using a system of small dimensions, one can obtain an estimate for a large range of temperatures.

when the system size increases. In the critical region, the width of the energy histogram increases, and if simulation sampling is done correctly, an increasing range of temperatures is estimated by the reweighting method.

In summary, this method is accurate in the vicinity of the temperature of the simulation and allows one to build a complete phase diagram rapidly, because the number of simulations to perform is quite limited. By combining several energy histograms (multiple reweighting method), one can improve the estimates of thermodynamic quantities for a large range of temperatures.

The principle of the method developed by considering energy and the conjugate variable β can be generalized for all pairs of conjugate variables, e.g. the magnetization M and an external uniform field H.

3.6 Conclusion

Phase transitions can be studied by simulation, by using several results of statistical physics. Indeed, the renormalization group theory has provided the finite size analysis, which permits the extrapolations of the critical exponents of the system in the thermodynamic limit by using simulation results of different systems size. Cluster methods are required for decreasing the dynamic exponent associated with the phase transition. By combining simulation results with a reweighting method, one drastically reduces the number of simulations. If the accuracy of simulation results are comparable to the theoretical methods for simple systems, like the Ising model, it is superior for almost more complicated models.

4.1 Molecular dynamics: Symplectic algorithms

4.1.1 Liouville formalism

In the Gibbs formalism, the phase space distribution is given by an N-particle probability distribution $f^{(N)}(\mathbf{r}^N, \mathbf{p}^N, t)$ (N is the total number of particles of the system) $\mathbf{r}^N$ denotes the coordinate set and $\mathbf{p}^N$ that of the impulses. If $f^{(N)}(\mathbf{r}^N, \mathbf{p}^N, t)$ is known, the average of a macroscopic quantity can be calculated [24, 8]. By writing the local conservation of the probability distribution, one obtains

$$\frac{\partial f^{(N)}(\mathbf{r}^N, \mathbf{p}^N, t)}{\partial t} + \sum_{i=1}^N \left(\frac{\partial}{\partial \mathbf{r}_i} \left(\frac{d\mathbf{r}_i}{dt} f^{(N)}(\mathbf{r}^N, \mathbf{p}^N, t) \right) + \frac{\partial}{\partial \mathbf{p}_i} \left(\frac{d\mathbf{p}_i}{dt} f^{(N)}(\mathbf{r}^N, \mathbf{p}^N, t) \right) \right) = 0, \tag{4.1}$$

irrespective of the nature of the dynamics. If the dynamics is Hamiltonian

$$\left(\frac{\partial \mathcal{H}_N}{\partial \mathbf{p}_i} \right) = \mathbf{v}_i = \frac{d\mathbf{r}_i}{dt} \tag{4.2}$$

$$\left(\frac{\partial \mathcal{H}_N}{\partial \mathbf{r}_i} \right) = -\mathbf{f}_i = -\frac{d\mathbf{p}_i}{dt}. \tag{4.3}$$

one obtains, on obtient

$$\frac{\partial}{\partial \mathbf{r}_i} \left(\frac{d\mathbf{r}_i}{dt} \right) = -\frac{\partial}{\partial \mathbf{p}_i} \left(\frac{d\mathbf{p}_i}{dt} \right) \tag{4.4}$$

which gives the Liouville equation ce qui donne l'équation de Liouville

$$\frac{\partial f^{(N)}(\mathbf{r}^N, \mathbf{p}^N, t)}{\partial t} + \sum_{i=1}^N \left(\frac{d\mathbf{r}_i}{dt} \frac{\partial f^{(N)}}{\partial \mathbf{r}_i} + \frac{d\mathbf{p}_i}{dt} \frac{\partial f^{(N)}}{\partial \mathbf{p}_i} \right) = 0, \tag{4.5}$$

In the following, we only consider Hamiltonian dynamics. The time evolution of the distribution probability can be expressed as

$$\frac{\partial f^{(N)}(\mathbf{r}^N, \mathbf{p}^N, t)}{\partial t} - \{\mathcal{H}_N, f^{(N)}\} = 0, \tag{4.6}$$

where $\mathcal{H}_N$ denotes the Hamiltonian of the system of N particles, and the bracket $\{A, B\}$ corresponds the Poisson bracket[1]

---

[1] If A and B are two functions of $\mathbf{r}^N$ and $\mathbf{p}^N$, the Poisson bracket between A and B is defined as

$$\{A, B\} = \sum_{i=1}^{N} \left(\frac{\partial A}{\partial \mathbf{r}_i} \frac{\partial B}{\partial \mathbf{p}_i} - \frac{\partial B}{\partial \mathbf{r}_i} \frac{\partial A}{\partial \mathbf{p}_i} \right)$$

The Liouville operator is defined as

$$\mathcal{L} = i\{H_N, \} = \sum_{i=1}^{N} \left(\left(\frac{\partial \mathcal{H}_N}{\partial \mathbf{r}_i} \right) \frac{\partial}{\partial \mathbf{p}_i} - \left(\frac{\partial \mathcal{H}_N}{\partial \mathbf{p}_i} \right) \frac{\partial}{\partial \mathbf{r}_i} \right) \tag{4.7}$$

Therefore, Eq. (4.6) is reexpressed as

$$\frac{\partial f^{(N)}(\mathbf{r}^N, \mathbf{p}^N, t)}{\partial t} = -i\mathcal{L} f^{(N)}, \tag{4.8}$$

and one gets the formal solution

$$f^{(N)}(\mathbf{r}^N, \mathbf{p}^N, t) = \exp(-i\mathcal{L}t) f^{(N)}(\mathbf{r}^N, \mathbf{p}^N, 0). \tag{4.9}$$

Similarly, if A is a function of positions $\mathbf{r}^N$, and impulses, $\mathbf{p}^N$, (but without explicit time dependence) obeys

$$\frac{dA}{dt} = \sum_{i=1}^{N} \left(\frac{\partial A}{\partial \mathbf{r}_i} \frac{d\mathbf{r}_i}{dt} + \frac{\partial A}{\partial \mathbf{p}_i} \frac{d\mathbf{p}_i}{dt} \right). \tag{4.10}$$

Using the Liouville operator, this equation becomes

$$\frac{dA}{dt} = i\mathcal{L}A, \tag{4.11}$$

which gives formally

$$A(\mathbf{r}^N(t), \mathbf{p}^N(t)) = \exp(i\mathcal{L}t) A(\mathbf{r}^N(0), \mathbf{p}^N(0)). \tag{4.12}$$

Unfortunately (or fortunately, because, if not, the world would be too simple), exact expression of the exponential operator is not possible in general case. However, one can obtain it in two important cases: the first expresses the Liouville operator as the sum of two operators

$$\mathcal{L} = \mathcal{L}_r + \mathcal{L}_p \tag{4.13}$$

where

$$i\mathcal{L}_r = \sum_i \frac{d\mathbf{r}_i}{dt} \frac{\partial}{\partial \mathbf{r}_i} \tag{4.14}$$

and

$$i\mathcal{L}_p = \sum_i \frac{d\mathbf{p}_i}{dt} \frac{\partial}{\partial \mathbf{p}_i} \tag{4.15}$$

In a first case, one assumes that the operator $\mathcal{L}_p$ is equal to zero. Physically, this corresponds to the situations where particle impulses are conserved during the evolution of the system and

$$i\mathcal{L}_r^0 = \sum_i \frac{d\mathbf{r}_i}{dt}(0) \frac{\partial}{\partial \mathbf{r}_i} \tag{4.16}$$

Time evolution of $A(t)$ is given by

$$A(\mathbf{r}(t), \mathbf{p}(t)) = \exp(i\mathcal{L}_r^0 t) A(\mathbf{r}(0), \mathbf{p}(0)) \tag{4.17}$$

Expanding the exponential, one obtains

$$A(\mathbf{r}^N(t), \mathbf{p}^N(t)) = A(\mathbf{r}^N(0), \mathbf{p}^N(0)) + i\mathcal{L}_r^0 A(\mathbf{r}^N(0), \mathbf{p}^N(0)) + \frac{(i\mathcal{L}_r^0)^2}{2!} A(\mathbf{r}^N(0), \mathbf{p}^N(0)) + \dots$$

$$= \sum_{n=0}^{\infty} \sum_i \frac{\left(\frac{d\mathbf{r}_i}{dt}(0)t\right)^n}{n!} \left(\frac{\partial^n}{\partial \mathbf{r}_i^n}\right) A(\mathbf{r}(0), \mathbf{p}(0)) \tag{4.18}$$

$$A(\mathbf{r}^N(t), \mathbf{p}^N(t)) = A\left(\left(\mathbf{r}_i + \frac{d\mathbf{r}_i}{dt}(0)t\right)^N, \mathbf{p}^N(0)\right) \tag{4.19}$$

The solution is a simple translation of spatial coordinates, which corresponds to a free streaming of particles without interaction, as expected.

The second case uses a Liouville operator where $\mathcal{L}_r^0 = 0$. Applying to A, $\mathcal{L}_p^0$ defined like $\mathcal{L}_r^0$ in the first case, one obviously obtains the solution of the Liouville equation which corresponds to a simple impulse translation.

4.1.2 Discretization of the Liouville equation

In the previous section, we expressed the Liouville operator as the sum of two operators $\mathcal{L}_r$ and $\mathcal{L}_p$. These two operators do not commute

$$\exp(\mathcal{L}t) \neq \exp(\mathcal{L}_r t)\exp(\mathcal{L}_p t). \tag{4.20}$$

The key point of the reasoning uses the Trotter identity

$$\exp(B + C) = \lim_{P \to \infty} \left(\exp\left(\frac{B}{2P}\right)\exp\left(\frac{C}{P}\right)\exp\left(\frac{B}{2P}\right)\right)^P. \tag{4.21}$$

For a finite number P of iterations, one obtains

$$\exp(B + C) = \left(\exp\left(\frac{B}{2P}\right)\exp\left(\frac{C}{P}\right)\exp\left(\frac{B}{2P}\right)\right)^P \exp\left(\mathcal{O}\left(\frac{1}{P^2}\right)\right) \tag{4.22}$$

When truncating after P iterations, the approximation is of order $1/P^2$. Therefore, by using $\Delta t = t/P$, by replacing the formal solution of the Liouville equation by a discretized version, and by introducing

$$\frac{B}{P} = \frac{i\mathcal{L}_p t}{P} \tag{4.23}$$

and

$$\frac{C}{P} = \frac{i\mathcal{L}_r t}{P}, \tag{4.24}$$

one obtains for an elementary step

$$e^{i\mathcal{L}_p \Delta t/2} e^{i\mathcal{L}_r \Delta t} e^{i\mathcal{L}_p \Delta t/2}. \tag{4.25}$$

Because the operators $\mathcal{L}_r$ and $\mathcal{L}_p$ are hermitian, the exponential operator is unitary, and by using the Trotter formula, one gets a method for which we may derive symplectic algorithms namely algorithms preserving the volume of the phase space.

$$e^{i\mathcal{L}_p \Delta t/2} A\left(\mathbf{r}^N(0), \mathbf{p}^N(0)\right) =$$
$$A\left(\mathbf{r}^N(0), \left(\mathbf{p}(0) + \frac{\Delta t}{2}\frac{d\mathbf{p}(0)}{dt}\right)^N\right) \tag{4.26}$$

then

$$e^{i\mathcal{L}_r \Delta t} A\left(\mathbf{r}^N(0), \left(\mathbf{p}(0) + \frac{\Delta t}{2}\frac{d\mathbf{p}(0)}{dt}\right)^N\right) =$$
$$A\left(\left(\mathbf{r}(0) + \Delta t\frac{d\mathbf{r}(\frac{\Delta t}{2})}{dt}\right)^N, \left(\mathbf{p}(0) + \frac{\Delta t}{2}\frac{d\mathbf{p}(0)}{dt}\right)^N\right) \tag{4.27}$$

and lastly, applying $e^{i\mathcal{L}_p \Delta t/2}$, we have

$$A\left(\left(\mathbf{r}(0) + \Delta t\frac{d\mathbf{r}(\frac{\Delta t}{2})}{dt}\right)^N, \left(\mathbf{p}(0) + \frac{\Delta t}{2}\frac{d\mathbf{p}(0)}{dt} + \frac{\Delta t}{2}\frac{d\mathbf{p}(\Delta t)}{dt}\right)^N\right) \tag{4.28}$$

In summary, one obtains the global transformations

$$\mathbf{r}(\Delta t) = \mathbf{r}(0) + \Delta t\frac{d\mathbf{r}(\Delta t/2)}{dt} \tag{4.29}$$

$$\mathbf{p}(\Delta t) = \mathbf{p}(0) + \frac{\Delta t}{2}\left(\mathbf{f}(\mathbf{r}(0)) + \mathbf{f}(\mathbf{r}(\Delta t))\right) \tag{4.30}$$

By expanding the velocity of Eq. (4.30) at the second order one obtains

$$\mathbf{r}(\Delta t) = \mathbf{r}(0) + \Delta t\frac{d\mathbf{r}(0)}{dt} + \frac{\Delta t^2}{2m}\mathbf{f}(\mathbf{r}(0)) \tag{4.31}$$

Finally, one obtains

$$\mathbf{r}(\Delta t) = \mathbf{r}(0) + \Delta t\frac{\mathbf{p}(0)}{m} + \frac{\Delta t^2}{2m}\mathbf{f}(\mathbf{r}(0)) \tag{4.32}$$

$$\mathbf{p}(\Delta t) = \mathbf{p}(0) + \frac{\Delta t}{2}\left(\mathbf{f}(\mathbf{r}(0)) + \mathbf{f}(\mathbf{r}(\Delta t))\right) \tag{4.33}$$

which corresponds to the the Velocity Verlet algorithm. For starting the simulation, one needs the positions and velocities at the same time ($t = 0$). The first equation updates the positions by using the forces and the velocities at the same time. The second equation updates the velocities by using the forces at two times.

Note that it is possible of restarting a new derivation by inverting the roles of operators $\mathcal{L}_r$ and $\mathcal{L}_p$ in the Trotter formula and to obtains new evolution equations. Once again, the discretized equations of trajectories are those of Position Verlet algorithm.

In summary, the product of the three unitary operators is also a unitary operator which leads to a symplectic algorithm. In other words, the Jacobian of the transformation, Eq. (4.25), is the product of three Jacobian and is equal to 1. Expansion can be performed to the next order in the Trotter formula: More accurate algorithms can be derived, which are always symplectic, but they involve force derivatives. Since force calculation is always very demanding, calculation of force derivatives would add a large penalty of the computing performance and are only used when short-time accuracy is a crucial need.

4.2 Molecular Dynamics in other ensembles

As discussed above, Molecular Dynamics corresponds to a simulation in the microcanonical ensemble. Generalizations exist in other ensembles, for instance, in canonical ensemble. Let us note that the thermal bath introduces random forces which changes dynamics with an ad hoc procedure. Because the dynamics then depends on a adjustable parameter, different dynamics can generated that are different from the "real" dynamics obtained in a microcanonical ensemble. The methods consist of modifying the equations of motion so that the velocity distribution reaches a Boltzmann distribution. However, this condition is not sufficient for characterizing a canonical ensemble. Therefore, after introducing a heuristic method, we will see how to build a more systematic method for performing Molecular Dynamics in generalized ensembles.

4.2.1 Andersen algorithm

The Andersen algorithm is a method where the coupling of the system with a bath is done as follows: a stochastic process modifies velocities of particles by the presence of instantaneous forces. This mechanism can be interpreted as Monte Carlo-like moves between isoenergy surfaces. Between these stochastic "collisions", the system evolves with the usual Newtonian dynamics. The coupling strength is controlled by the collision frequency denoted by ν. In addition, one assumes that the stochastic "collisions" are totally uncorrelated, which leads to a Poissonian distribution of collisions, $P(\nu, t)$

$$P(\nu, t) = e^{-\nu t} \tag{4.34}$$

Practically, the algorithm is composed of three steps

- The system follows Newtonian dynamics over one or several time steps, denoted Δt.

- On chooses randomly a number of particles for stochastic collisions. The probability of choosing a particle in a time interval Δt is $\nu \Delta t$.

- When a particle is selected, its velocity is chosen randomly in a Maxwellian distribution with a temperature T. Other velocities are not updated.

This procedure ensures that the velocity distribution goes to equilibrium, but obviously, real dynamics of the system is deeply disturbed. Moreover, the full distribution obtained with the Andersen thermostat is not a canonical distribution: This can be shown by considering the fluctuation calculation. In particular, correlation functions relax at a rate which strongly depends on coupling with the thermostat.

4.2.2 Nosé-Hoover algorithm

Refs.[[18, 14]]

As discussed above, the Andersen algorithm biases dynamics of the simulation, which is undesirable, because the main purpose of the Molecular Dynamics is to provide a real dynamics. To overcome this problem, a more systematic approach, introduced by Nosé enlarges the system by introducing additional degrees of freedom. This procedure modifies the Hamiltonian dynamics by adding a coupling between particle velocities and a fictive particle.

One considers the Hamiltonian

$$\mathcal{H} = \sum_{i=1}^{N} \frac{(\mathbf{p}_i)^2}{2m_i s^2} + U(\mathbf{r}^N) + \frac{p_s^2}{2Q} + \frac{L}{\beta} \ln(s) \tag{4.35}$$

Let us reexpress the microcanonical partition function of this system made of N interacting particles and of this additional degree of freedom interacting with N particles.

$$Q = \frac{1}{N!} \int dp_s ds d\mathbf{p}^N d\mathbf{r}^N \delta(\mathcal{H} - E) \tag{4.36}$$

The partition function corresponds to N indistinguishable particles and to the additional variable in the microcanonical ensemble where microstates of isoenergy are considered equiprobable.

Let us introduce $\mathbf{p}' = \mathbf{p}/s$. One obtains that

$$Q = \frac{1}{N!} \int dp_s ds s^{3N} d\mathbf{p}'^N d\mathbf{r}^N \delta(\sum_{i=1}^{N} \frac{(\mathbf{p}'_i)^2}{2m_i} + U(\mathbf{r}^N) + \frac{p_s^2}{2Q} + \frac{L}{\beta} \ln(s) - E) \tag{4.37}$$

One defines $\mathcal{H}'$ as

$$\mathcal{H}' = \sum_{i=1}^{N} \frac{(\mathbf{p}'_i)^2}{2m_i} + U(\mathbf{r}^N) \tag{4.38}$$

the partition function becomes

$$Z = \frac{1}{N!} \int dp_s ds s^{3N} d\mathbf{p}'^N d\mathbf{r}^N \delta(\mathcal{H}' + \frac{p_s^2}{2Q} + \frac{L}{\beta} \ln(s) - E) \tag{4.39}$$

By using the property

$$\delta(h(s)) = \frac{\delta(s - s_0)}{h'(s_0)} \tag{4.40}$$

where $h(s)$ is a function with only one zero on the x-axis at the value $s = s_0$.

One integrates over the variable s and one obtains

$$\delta(\mathcal{H}' + \frac{p_s^2}{2Q} + \frac{L}{\beta} \ln(s) - E) = \frac{\beta s}{L} \delta(s - \exp(-\frac{\beta}{L}(\mathcal{H}' + \frac{p_s^2}{2Q} - E))) \tag{4.41}$$

This gives for the partition function

$$Z = \frac{\beta \exp(E(3N+1)/L)}{LN!} \int dp_s d\mathbf{p}'^N d\mathbf{r}^N \exp\left(\frac{-\beta(3N+1)}{L}(\mathcal{H}' + \frac{p_s^2}{2Q})\right) \tag{4.42}$$

50

Setting $L = 3N + 1$, and integrating over the additional degree of freedom, the partially integrated partition function Q of the microcanonical ensemble of the full system (N particles and the additional degree of freedom), becomes a canonical partition function of a system with N particle.

It is worth noting that variables used are r, p' and t'. Discretizing the equations of motion would give a variable time step which is not easy to control in Molecular Dynamics. It is possible to return to a constant time step by using additional changes of variable. This work was done by Hoover.

Finally, the equations of motion are

$$\dot{\mathbf{r}}_i = \frac{\mathbf{p}_i}{m_i} \tag{4.43}$$

$$\dot{\mathbf{p}}_i = -\frac{\partial U(\mathbf{r}^N)}{\partial \mathbf{r}_i} - \xi \mathbf{p}_i \tag{4.44}$$

$$\dot{\xi} = \left(\sum_{i=1}^{N} \frac{\mathbf{p}_i^2}{2m_i} - \frac{L}{\beta} \right) \frac{1}{Q} \tag{4.45}$$

$$\frac{\dot{s}}{s} = \xi \tag{4.46}$$

The two first equations are a closed set of equations for N particles. The last equation controls the evolution of the additional degree of freedom in the simulation.

4.3 Monte Carlo: Cluster algorithm, Tempering and Wang-Landau methods

When a system undergoes a continuous phase transition, Monte Carlo methods which consists of flipping (or moving) a single spin (or particle) converge more slowly in the critical region than the cluster algorithm (when it exists). The origin of this slowing down is associated with real physical phenomena, even if Monte Carlo dynamics can never to be considered as a true dynamics. The rapid increase of the relaxation time is related to the existence of fluctuations of large sizes (or the presence of domains) which are difficult to sample by a local dynamics: indeed, cluster algorithms accelerate the convergence in the critical region, but not far away.

For a first-order transition, the convergence of Monte Carlo methods based on a local dynamics is weak because close to the transition, there exists two or more metastable states: the barriers between metastable states increase with the system size, and the relaxation time has an exponential dependence of system size which rapidly exceeds a reasonable computing time. Finally, the system is unable to explore the phase space and is trapped in a metastable region. The replica exchange method provides a efficient way for crossing metastable regions, but this method requires a fine tuning of many parameters (temperatures, exchange frequency between replica).

New approaches have been proposed in the last decade based on the computation of the density of states. These methods are general in the sense that the details of dynamics are not imposed. Only a condition similar to the detailed balance is given. The goal of these new methods is to obtain the key quantity which is the density of states.

4.3.1 Cluster algorithm

Let us recall that the Metropolis algorithm is a Markovian dynamics for particle motion (or spin flips in lattices). A reasonable acceptance ratio is obtained by choosing a single particle (or spin) in order to have a product $|\beta \Delta E|$ which is relatively small. A major advance of twenty years ago consists of generating

methods where a large number of particles (or spins) are moved (or flipped) simultaneously, and keeping a quite high acceptance ratio (or even equal to 1), as well as by reaching a equilibrium state.[22].

We consider below the Ising model, but be generalized the method can be done for all locally symmetric Hamiltonian (for the Ising model, this corresponds to the up/down symmetry).

Ideally, a global spin flip should have a acceptance ratio equal to 1. The proposed method adds a new step to the Metropolis algorithm: from a given spin configuration, one characterizes the configuration by means of bonds between spins. The detailed balance equation (1.18) Chap. 2 is modified as follows

$$\frac{P_{gc}(o)W(o \to n)}{P_{gc}(n)W(n \to o)} = \exp(-\beta(U(n) - U(o))) \tag{4.47}$$

where $P_{gc}(o)$ is the probability of generating a bond configuration from o to n (o and n denote the old and new configurations, respectively). If one wishes to accept all new configurations ($W(i \to j) = 1$), whatever configurations i and j, one must have the following ratio

$$\frac{P_{gc}(o)}{P_{gc}(n)} = \exp(-\beta(U(n) - U(o))) \tag{4.48}$$

In order to build such an algorithm, let us note that energy is simply expressed as

$$U = (N_a - N_p)J \tag{4.49}$$

where N_p is the number of pairs of nearest neighbor spins of the same sign and N_a the number of pairs of nearest neighbor spins of the opposite sign. This formula, beyond its simplicity, has the advantage of being exact whatever the dimensionality of the system. The method relies on rewriting of the partition function given by Fortuyn and Kasteliyn (1969), but exploiting this idea for simulation occurred almost twenty years later with the Swendsen and Wang[22] work.

For building clusters, one defines bonds between nearest neighbor spins with the following rules

1. If two nearest neighbor spins have opposite signs, they are not connected.

2. If two nearest neighbor spins have the same sign, they are connected with a probability p and disconnected with a probability $(1 - p)$.

This rule assumes that J is positive (ferromagnetic system). When J is negative, spins of same sign are always disconnected and spins of opposite signs are connected with a probability p, and disconnected with a probability $(1 - p)$. Let consider a configuration of N_p pairs of spins of same sign, the probability of having n_c pairs connected (and consequently $n_b = N_p - n_c$ pairs of spins are disconnected) is given by the relation

$$P_{gc}(o) = p^{n_c}(1 - p)^{n_b}. \tag{4.50}$$

Once bonds are set, a cluster is a set of spins connected by at least one bond between them. If one flips a cluster ($o \to n$), the number of bonds between pairs of spins of same and opposite signs is changed and one has

$$N_p(n) = N_p(o) + \Delta \tag{4.51}$$

and similarly

$$N_a(n) = N_a(o) - \Delta. \tag{4.52}$$

The energy of the new configuration $U(n)$ is simply related to the energy of the old configuration $U(o)$ by the equation:

$$\mathcal{U}(n) = \mathcal{U}(o) - 2J\Delta. \tag{4.53}$$

Let us now consider the probability of the inverse process. One wishes to generate the same cluster structure, but one starts from a configuration where one has $N_p + \Delta$ parallel pairs and $N_a - \Delta$ antiparallel pairs. Antiparallel bonds are assumed broken. One wishes that the bond number n_c' is equal to n_c because one needs to have the same number of connected bonds for generating the same cluster. The difference with the previous configuration is the number of bonds to break. Indeed, one obtains

$$N_p(n) = n_c' + n_b' \tag{4.54}$$
$$N_p(o) = n_c + n_b \tag{4.55}$$
$$N_p(n) = N_p(o) + \Delta$$
$$= n_c + n_b + \Delta, \tag{4.56}$$

which immediately gives

$$n_b' = n_b + \Delta. \tag{4.57}$$

The probability of generating the new bond configuration from the old configuration is given by

$$P_{gc}(n) = p^{n_c}(1-p)^{n_b+\Delta} \tag{4.58}$$

Inserting Eqs. (4.50) and (4.58) in Eq. (4.48), one obtains

$$(1-p)^{-\Delta} = \exp(2\beta J\Delta) \tag{4.59}$$

One can solve this equation for p, which gives

$$(1-p) = \exp(-2\beta J), \tag{4.60}$$

Finally, the probability p is given by

$$p = 1 - \exp(-2\beta J). \tag{4.61}$$

Therefore, if the probability is chosen according Eq. (4.61), new configuration is always accepted!

The virtue of this algorithm is not only its ideal acceptance rate, but one can also show that, in the vicinity of the critical point, the critical slowing down drastically decreases. For example, the critical exponent of the two-dimensional Ising model is equal to 2.1 with the Metropolis algorithm while it is 0.2 with a cluster algorithm. Therefore, a cluster algorithm becomes quite similar to the Metropolis algorithm in term of relaxation time far from the critical point.

More generally, Monte Carlo dynamics is accelerated when one finds a method able to flip large clusters corresponding to the underlying physics. In the Swendsen-Wang method, one selects spin sets which correspond to equilibrium fluctuations; conversely, in a Metropolis method, by choosing randomly a spin, one generally creates a defect in the bulk of a large fluctuation, and this defect must diffuse from the bulk to the cluster surface in order that the system reaches equilibrium. Knowing that diffusion is like a random walk and that the typical cluster size is comparable to the correlation length,

the relaxation time is then given by $\tau \sim \xi^2$, which gives for a finite size system $\tau \sim L^2$, and explains why the dynamical exponent is close to 2.

Note that the necessary ingredient for defining a cluster algorithm is the existence of a symmetry. C. Dress et W. Krauth [4] generalized these methods when the symmetry of the Hamiltonian has a geometric origin. For lattice Hamiltonians, where the up-down symmetry does not exist, J. Heringa and H. Blote generalized the Dress and Krauth method by using the discrete symmetry of the lattice [11, 12].

4.4 Density of states

4.4.1 Definition and physical meaning

For a classical systems described by a Hamiltonian $\mathcal{H}$, the microcanonical partition function is given by (see Chap. 1)

$$Z(E) = \sum_\alpha \delta(\mathcal{H} - E) \tag{4.62}$$

where E denotes the energy of the system and the index α runs over all available configurations. The symbol δ denotes the Kronecker symbol where the summation is discrete; an analogous formula can be written for the microcanonical partition function when the energy spectra is continuous; the sum is replaced with an integral and the Kronecker symbol with a δ distribution.

Equation (4.62) means that the microcanonical partition function is a sum over all microstates of total energy E, each state has a identical weight. Introducing the degeneracy of the system for a given energy E, the function $g(E)$ is defined as follows: in the case of a continuous energy spectra, $g(E)dE$ is the number of states available of the system for a total energy between E and $E + dE$. The microcanonical partition function is then given as

$$Z(E) = \int du\, g(u)\delta(u - E) = g(E) = \exp(S(E)) \tag{4.63}$$

Therefore, the density of states is nothing else than the microcanonical partition function of the system and its logarithm is equal to the entropy of the system.

4.4.2 Properties

The integral (or the sum) over all energies of the density of states gives the following rule

$$\int dE\, g(E) = \mathcal{N} \tag{4.64}$$

where $\mathcal{N}$ is the total number of configurations (for a lattice model).

For a Ising model, this number $\mathcal{N}$ is equal to 2^N where N is the total number of spins of the system. This value is then very large and grows exponentially with the system size. From a numerical point of view, one must use the logarithm of this function $\ln(g(E))$ for avoiding overflow problem.

For simple models, one can obtain analytical expressions for small or moderate system sizes, but combinatorics becomes rapidly a tedious task. Some results can not obtained easily: Indeed, for the Ising model, there are two ground states corresponding to full ordered states. The first nonzero value of the density of states is equal to $2N$ which correspond to the number of possibilities of flipping one spin on the lattice of N sites.

Figure (4.1) shows the logarithm of the density of states of the two-dimensional Ising model on a square lattice with a total number of sites equal to 1024. The shape of this curve is the consequence of
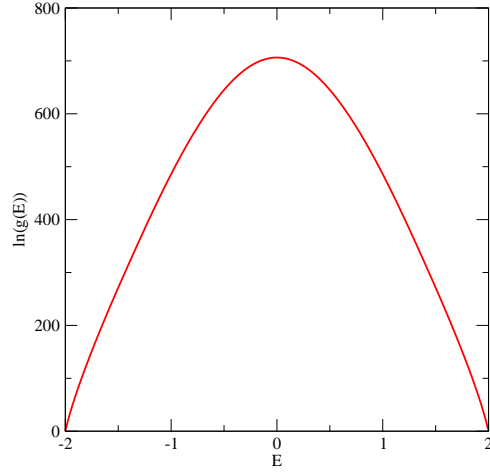
Figure 4.1: Logarithm of the density of states $\ln(g(E))$ as a function of energy E for a two-dimensional Ising model on a square lattice of linear size $L = 32$.

specific and universal features that we now detail: for all systems where the energy spectra is discrete, the range of energy has a lower bound given by the ground state of the system. In case of simple liquids, the density of states does not have an upper bound, because overlap between particles which interact with a Lenard-Jones potential is always possible, which gives very large values of the energy; however the equilibrium probability of having such configurations is weak.

The shape of the curve which displays a maximum is a characteristic of all simple systems, but the Oy-symmetry is a consequence of the up-down symmetry of the corresponding Hamiltonian. This symmetry is also present in thermodynamic quantities, like magnetization versus temperature (see Chapter 1).

For Monte Carlo algorithms based on the density of states, one can simply remark: With the Metropolis algorithm, the acceptance probability of a new configuration satisfies detailed balance, namely $\Pi(i \to j)P_{eq}(i) = \Pi(j \to i)P_{eq}(j)$ where $P_{eq}(j)$ is the probability of having the configuration j at equilibrium and $\Pi(i \to j)$ is the transition probability of going from the state i towards the state j. One then rewrites detailed balance in energy variable.

Let us denote $H_\beta(E)$ the energy histogram associated to successive visits of the simulation. Consequently, one has

$$H_\beta(E) \propto g(E)\exp(-\beta E) \tag{4.65}$$

Assume that one imposes the following biased detailed balance

$$\Pi(E \to E')\exp(-\beta E + w(E)) = \Pi(E' \to E)\exp(-\beta E' + w(E')) \tag{4.66}$$

energy histogram then becomes proportional to

$$H_\beta(E) \propto g(E)\exp(-\beta E + w(E)) \tag{4.67}$$

It immediately appears that, when $w(E) \sim \beta E - \ln(g(E))$, the energy histogram becomes a flat his-

togram and independent of the temperature. The detailed balance then becomes

$$\frac{\Pi(E \rightarrow E')}{g(E)} = \frac{\Pi(E' \rightarrow E)}{g(E')} \tag{4.68}$$

The stochastic process corresponds to a random walk in energy space. The convergence of this method is related to the fact that the available interval of the walker is bounded. For the Ising model, these bounds exist, for other models, it is possible of restricting the range of the energy interval in a simulation.

This very interesting result is at the origin of multicanonical methods (introduced for the study of first-order transition). However, it is necessary to know the function $w(E)$, namely to know the function $g(E)$. In multicanonical method, a guess for $w(E)$ is provided from the density of states obtained (by simulation) with small system sizes. By extrapolating an expression for larger system sizes, the simulation is performed and by checking the deviations of the flatness of the energy histogram, one can correct the weight function, in order to flatten the energy histogram in a second simulation run.

Performing this kind of procedure consisting of suppressing the free energy barriers which exist in a Metropolis algorithm, and which vanishes here by the introduction of an appropriate weight function. The difficulty of this method is to obtain an good extrapolation of the weight function for large system sizes. Indeed, a bias of the weight function can insert new free energy barriers and simulations converge slowly again.

For obtaining a simulation method that computes the density of states without knowledge of a good initial guess, one needs to add an ingredient to the multicanonical algorithm. A new method has been proposed in 2001 by J.S. Wang et D.P. Landau[27, 26], which we detail below.

4.5 Wang-Landau algorithm

The basics of the algorithm are:

1. A change of the initial configuration is proposed (generally a local modification)

2. One calculates the energy associated with the modified configuration E'. This configuration is accepted with a Metropolis rule $\Pi(E \rightarrow E') = Min(1, g(E)/g(E'))$, if not the configuration is rejected and the old configuration is kept (and added as in an usual Metropolis algorithm)

3. The accepted configuration modifies the density of states as follows: $\ln(g(E')) \leftarrow \ln(g(E')) + \ln(f)$

This iterative scheme is repeated until the energy histogram is sufficiently flat: practically, the original algorithm proposes the histogram is flat when each value of the histogram must be larger than 80% of the mean value of this histogram.

f is called the modification factor. Because the density of states changes continuously in time, it is not a stationary quantity. The accuracy of the density of states depends on the statistical quantity of each value of $g(E)$. Because the density of states increases with time, the asymptotic accuracy is given by $\sqrt{\ln(f)}$. To this first stage, the precision is not sufficient for calculating the thermodynamic quantities.

Wang and Landau completed the algorithm as follows: One resets the energy histogram (but, obviously not the histogram of the density of states). One restart a new simulation described above, but with a new modification factor equal to $\sqrt{f}$. Once this second stage achieved, the density of states is refined with respect to the previous iteration, because the accuracy of the density is given by $\sqrt{\ln(f)/2}$.

In order to have an accurate density of states, the simulation is continued by dishing the modification factor by the relation

$$f \leftarrow \sqrt{f} \tag{4.69}$$

When $\ln(f) \sim 10^{-8}$, the density of states does not longer evolve, the dynamics becomes a random walk in energy space and the simulation is then stopped.

Once the density of states obtained, one can easily derive all thermodynamic quantities from this alone function. A additional virtue in this kind of simulation is that if the accuracy is not reached, the simulation can be easily prolongated by using the previous density of states until a sufficient accuracy is reached. Contrary to other methods based on one or several values of the temperature, one can here calculate the thermodynamic quantities for all temperatures (corresponding to the energy scale used in the simulation).

Considering that the motion in the energy space is purely diffusive (what is only true for the last iterations of the algorithm, namely values of the modification factor close to one), the computer time which is necessary is proportional to $(\Delta E)^2$, where ΔE represents the energy interval. This means that computer time increases as the square of the system size. The computer time of this king of simulation is then larger than this of Metropolis algorithm, but for the second case, one obtains the thermodynamic quantities for one temperature (or by using a reweighting method a small interval of temperature), whereas for only one Wang-Landau simulation, one can obtains these quantities for a large range of temperatures (as shown below) and the accuracy is much better.

For decreasing the computing time, it is judicious to reduce the energy interval in the simulation, and eventually to perform several simulations for different (overlapping) energy ranges. In the second case, the total duration of all simulations is divided by two compared to an unique simulation over the complete energy space. One can then match the density of states of each simulation. However, this task is subtle, even impossible, if the energy interval belongs to the region of a transition. Indeed, it occurs errors in the density of states at the ends of each density of states forbidding a complete rebuilding of the density of states. With limitations, the method is very efficient for lattice systems with discrete energy spectra (additional problems occur with continuous energy spectra. In any case, free energy barriers disappear for first order transition, and it allows for an efficient exploration of phase space.

4.6   Thermodynamics recovered!

Once obtained the density of states (to an additive constant), one obtains the mean energy (in a canonical ensemble) a posteriori by computing the ratio of following integrals

$$<E> = \frac{\int E \exp(-\beta E + \ln(g(E))) dE}{\int \exp(-\beta E + \ln(g(E))) dE} \tag{4.70}$$

The practical computation of these integrals requires some caution. The arguments of these exponentials can be very large and lead to overflows. For avoiding these problems, let us note that for a given temperature (or β), the expression

$$-\beta E + \ln(g(E)) \tag{4.71}$$

is a function which admits one or several maxima (but close) and which decreases rapidly toward negative values when the energy is much smaller or greater to these minima. Without changing the result,

one can multiply each integral by $\exp(-Max(-\beta E + \ln(g(E))))^2$, the exponentials of each interval have an argument always negative or equal to zero. On can then truncate the bounds of each integral when the arguments of each exponential become equal to -100 and the computation of each interval is safe, without any overflows (or underflows).

The computation of the specific heat is done with the usual formula

$$C_v = k_B \beta^2 \left(\langle E^2 \rangle - \langle E \rangle^2 \right) \tag{4.72}$$

It is easy to see that the procedure skechted for the computation of the energy can be transposed identically for the computation of the specific heat. One can calculate the thermodynamic quantities for any value of the temperature and obtain an accurate estimate of the maximum of the specific heat as well as the associated temperature.

A last main advantage of this method is to obtain the free energy of the system for all temperatures as well as the entropy of the system, a different situation of a Monte Carlo simulation in the canonical ensemble.

One can also obtain the thermodynamic magnetic quantities with a modest computational effort. Indeed, one obtained the density of states, it is possible to run a simulation where the modification factor is equal to 1 (the density of states does not evolve) and therefore the simulation corresponds to a random walk in the space energy: one stores a magnetization histogram $M(E)$ as well as the square magnetization $M^2(E)$, even higher moments $M^n(E)$.... From these histograms and the density of states $g(E)$, one can calculate the mean magnetization of the system as a function of the temperature by using the following formula

$$< M(\beta) > = \frac{\int \frac{M(E)}{H(E)} \exp(-\beta E + \ln(g(E))) dE}{\int \exp(-\beta E + \ln(g(E))) dE} \tag{4.73}$$

and one can obtain the critical exponent associated to the magnetization for a finite size scaling.

Similarly, one can calculate the magnetic susceptibility as a function of the temperature.

Therefore, one can write a minimal program for studying a system by calculating the quantities involving the moments of energy in order to determine the region of the phase diagram where the transition takes place and what is the order of the transition. Secondly, one can calculate other thermodynamic quantities by performing an additional simulation in which the modification factor is equal to 1. Conversely, for a simulation in a canonical ensemble, a complete program must be written for calculating all quantities from the beginning.

To simply summarize the Monte Carlo simulations based on the density of states, one can say that an efficient method for obtaining thermodynamics of a system consists in performing a simulation where thermodynamics is not involved.

Indeed, simulation is focussed on the density of states which is not a thermodynamic quantity, but a statistical quantity intrinsic of the system.

It is possible to perform simulations of Wang-Landau with a varying number of particles. It allows one to obtain the thermodynamic potential associated with a grand canonical ensemble. On can also perform simulation of simple lquids and build the coexistence curves with accuracu. Let us note that additional difficulties occur when the energy spectra is continuous and some refinements with respect to the original algorithm have been proposed by several authors correcting in part the drawbacks of the method. Because this method is very recent , improvements are expected in the near future, but this method represents a breakthough and can alllow studies of systems where standard methods fail

---

[2]When there are several maxima, one chooses the maximum which gives the largest value.

to obtain reliable thermodynamic quantities. There is an active fied for bringing modifications to the original method (see e.g. the references [29, 19]).

4.7   Monte Carlo method with multiple Markov chains

The free energy barriers prevent the exploration of the phase diagram in a reasonable computer time. The convergence of Metropolis-like algorithms becomes very slow, because the typical relaxation time is proportional to the exponential of the free energy barriers, which grow with the system size.

To calculate a coexistence curve, or to obtain a well equilibrated system below the critical temperature, one has to perform a series of simulations for a sequence of temperature (and/or chemical potentials for a liquid)

The "parallel tempering" method (or replica exchange method) is inspired by the following remark: when the temperature decreases, equilibrium is more and more difficult to reach, due to the presence of large free energy barriers. Conversely, phase diagram is easily explored at high temperatures. The method consists of propagating from high temperature toward low temperature configurations and conversely.

For the sake of simplicity, we consider a system where one only changes the temperature, but the method is easy generalized to other intensive quantities (chemical potential, modification of the Hamiltonian,...): the canonical partition function of a system to the temperature T_i is given by the relation

$$Q_i = \sum_\alpha \exp(-\beta_i U(\alpha)) \tag{4.74}$$

where α is an index running over all configurations available to the system and β_i the inverse of the temperature.

Let us consider the direct product of all systems evolving to different temperatures, the corresponding partition function of this new ensemble is equal to

$$Q_{total} = \prod_{i=1}^{N} Q_i \tag{4.75}$$

where N denotes the total number of temperatures used in all simulation boxes.

A great advantage of the method is that the simulations can be performed in parallel. The parallel tempering method introduces an additional Markov chain between simulation boxes, the internal Markov chain of each simulation box are unchanged. In order to ensure convergence towards equilibrium, a detailed balance rule must be added between simulation boxes. A global exchange of particles between two simulation boxes is possible only if the two temperatures are close. This means that exchange is only proposed between two consecutive boxes .

The detailed balance is expressed as

$$\frac{\Pi((i,\beta_i),(j,\beta_j) \rightarrow (j,\beta_i),(i,\beta_j))}{\Pi((i,\beta_j),(j,\beta_i) \rightarrow (i,\beta_i),(j,\beta_j))} = \frac{\exp(-\beta_j U(i)) \exp(-\beta_i U(j))}{\exp(-\beta_i U(i)) \exp(-\beta_j U(j))} \tag{4.76}$$

where $U(i)$ et $U_(j)$ are the total energies of the boxes i and j, respectively.

The algorithm consists of two kinds of move:

- Particle motion in each box, which can be performed in parallel according to a Metropolis rule. The acceptance probability for a single move within a simulation box is given by

$$\min(1, \exp(-\beta_i(U_i(n) - U_i(o)))) \tag{4.77}$$

  where n and o denote the new and old configurations, respectively.

- Particle exchange between two consecutive boxes. The acceptance probability is then given by

$$\min(1, \exp(-(\beta_i - \beta_j)(U_j - U_i))) \tag{4.78}$$

The exchange fraction beween boxes must to be set to optimize the simulation, as well as the temperature interval.

A very simple illustration of this algorithm will be given with the following toy model: Consider a particle in a one dimensional space undergoing to the external potential $V(x)$
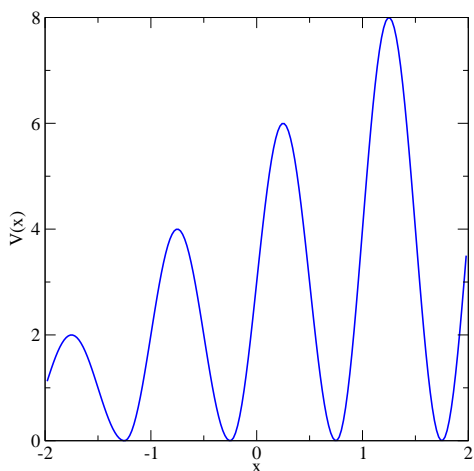
$$V(x) = \begin{cases} +\infty & \text{si } x < -2 \\ 1 + \sin(2\pi x) & \text{si } -2 \leq x \leq 1.25 \\ 2 + 2\sin(2\pi x) & \text{si } -1.25 \leq x \leq -0.25 \\ 3 + 3\sin(2\pi x) & \text{si } -0.25 \leq x \leq 0.75 \\ 4 + 4\sin(2\pi x) & \text{si } 0.75 \leq x \leq 1.75 \\ 5 + 5\sin(2\pi x) & \text{si } 1.75 \leq x \leq 2.0 \end{cases}$$

Figure 4.2: One-dimensional potential $V(x)$.

The equilibrium probabilities $P_{eq}(x, \beta)$ can be calculated exactly

$$P_{eq}(x, \beta) = \frac{\exp(-\beta V(x))}{\int_{-2}^{2} dx \exp(-\beta V(x))} \tag{4.79}$$

Figure 4.3 show equilibrium probabilities for three different temperatures. Note that, because the minima of potential energy are identical, maxima of equilibrium probabilities are the same. When the temperature is decreased, the probability of passing between two energy minima becomes very small.

Figure 4.3a shows simulation results with a Metropolis algorithm for three different temperatures, whereas figure 4.3b is for a parallel tempering algorithm. The total number of configurations used in both simulations are the same.

With a Metropolis algorithm, the system is only equilibrated for the highest temperature. For $T = 0.3$, the system cannot reach the third potential minimum (knowing that the initial position of the particle was in the left region. For $T = 0.1$, the particle is unable to cross an energy barrier during the simulation run. By using the parallel tempering method, the system reaches equilibrium for all temperatures, in particular even for the lowest temperature.
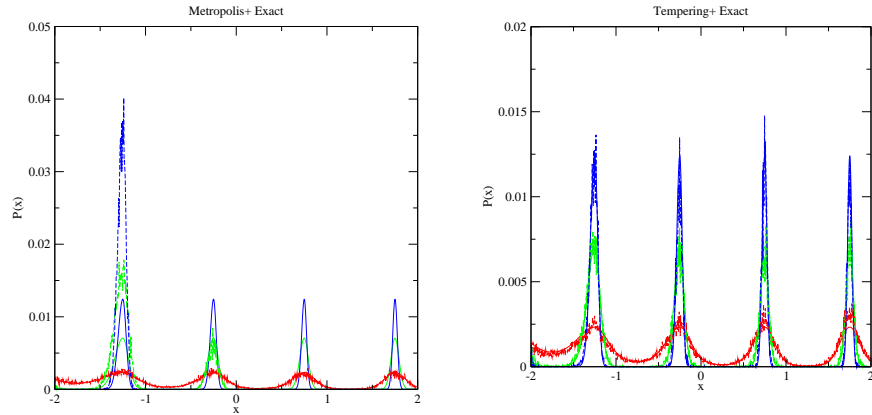
Figure 4.3: Equilibrium probabilities (full curves) and probabities obtained from simulations for the particle undergoing to the external one dimensional potential for three different temperatures $T = 0.1, 0.3, 2$. (a) Metropolis (b) parallel tempering.

For an N body system, the parallel tempering algorithm must be performed by using a number of simulation boxes which increases with the system size. Moreover, this method introduces several parameters to be set in order that the simulation is efficient: the temperature interval must be set in a subtle manner: if the interval is too large, the acceptance probability for particle exchange is very small and the simulation boxes at low temperatures are not sufficiently equilibrated. The temperature interval is not necessarily constant (a constant interval in the inverse temperature is more efficient). Once a particle exchange is performed, the system must relax at a given temperature, which means that the frequency exchange must be smaller than the inverse of the relaxation time of each simulation box.

4.8 Conclusion

Monte Carlo methods can be used in various physical situations and can be adapted and/or optimized by considering the specific properties of a systems to be studied. This chapter is a simple overview of a rapidly growing literature, but we hope to give some elements for building more specific methods.

5

5.1 Introduction

The classical point of view in thermodynamics is focused on the mean quantities of large systems; indeed, in the thermodynamical limit, the mean quantities per particle are well defined because the fluctuations of these later decrease as long as the central limit theorem holds. In other words, fluctuations were considered as a pebble in one's shoe., and their random behavior seemed to be useless.

Whereas fluctuations have a time evolution which appears stochastic, their statistical properties exhibit strong constraints and are the signature of intrinsic properties of the system. A first approach has revealed this feature through the linear response theory. Basically, at equilibrium, the response of a system to a small ("infinitesimal") external field is intimately related to how fluctuations of the quantity (conjugate to the field) vanishes when the system relaxes to equilibrium.

The renewed interest in studying fluctuations is associated with many physical situations where a thermodynamic limit cannot be taken: for instance, biological systems, colloidal particles driven by tweezers, biological motors... For these systems, the large molecule undergoes collisions with bath particles, whose dynamics can be modeled as a stochastic process. Along a trajectory, the large particle exchanges work and heat with its environment in the presence of fluctuations which cannot be neglected. Definitions of thermodynamic quantities have to be adapted to the stochastic dynamics, and this topic is called stochastic thermodynamics. To define these new quantities, we first consider the trajectories of a particle at a microscopic level surrounded by a environment of small particles and a external operator able to modify the potential in which the particle evolves. A convenient approach consists in using a Langevin equation, namely a stochastic differential equation. One first introduce some definitions and properties of this mathematical field. Second, two paradigmatic models of Langevin are then defined, allowing us to introduce the basic concepts of the stochastic thermodynamics more physically and finally to consider the different fluctuation theorems.

In linear response theory, the role of fluctuations is well understood when the system is close to equilibrium. Several major steps have been done on fluctuations by the findings of different relations, so called fluctuation theorems.

We review some of these results in this chapter, but recent exhaustive reviews[20] and books[21] help readers to go beyond this basic introduction.

5.2 Brownian dynamics

5.2.1 Stochastic differential equations

Let us consider the stochastic differential equation

$$\frac{dx(t)}{dt} = a(x,t) + b(x,t)\xi(t)$$

(5.1)

where $\xi(t)$ is a Gaussian white noise, $< \xi(t) >= 0$ and $< \xi(t)\xi(t') >= 2\delta(t-t')$.
A formal solution of the stochastic differential equation in the time interval Δt reads

$$x(t + \Delta t) = x(t) + \int_t^{t+\Delta t} dt'(a(x,t') + b(x,t'))\xi(t') \tag{5.2}$$

$$= x(t) + \int_t^{t+\Delta t} dt' a(x,t') + \int_t^{t+\Delta t} dW(t)b(x,t') \tag{5.3}$$

where $w(t)$ is a Wiener process, such that $dW(t) = \xi(t)dt$. The Wiener process is a Markovian process at continuous time such that $\langle W(t) \angle = 0$ (equivalent to a random walk where the left and right direction have the same direction) and $\langle W(t)W(t') \rangle = \text{Min}(t,t')$. (An elementary proof consists in writing $\langle W(t)W(t') \rangle = \langle W(t)(W(t') - W(t) + W(t)) \rangle$ and if $t' > t$, the first is equal to zero and the second term to t (diffusion term)).

Stochastic calculus

In order to solve the Langevin equation previously introduced, we have to calculate integrals as

$$\int_{t_0}^t f(t)dW(t) \tag{5.4}$$

where $W(t)$ is a Wiener process and $f(t)$ an unspecified function A standard way of calculating this integral consists of discretizing the time with a constant timestep and performing a Riemann integration. Therefore, one has

$$S_n = \sum_{i=1}^n f(\tau_i)(W(t_i) - W(t_{i-1})) \tag{5.5}$$

where τ_i is a intermediate time between t_{i-1} and t_i.

By choosing $f(t) = W(t)$, one calculates the average of the integral over all realizations of the Wiener process.

$$< S_n >= \sum_{i=1}^n (\text{Min}(\tau_i, t_i) - \text{Min}(\tau_i, t_{i-1})) \tag{5.6}$$

$$= \sum_{i=1}^n (\tau_i - t_{i-1}) \tag{5.7}$$

If one chooses τ_i as the barycenter of the time interval

$$\tau_i = \alpha t_i + (1 - \alpha)t_{i-1} \tag{5.8}$$

with α between 0 and 1, one obtains for the mean value of S_n

$$< S_n >= \alpha(t - t_0) \tag{5.9}$$

which leads to a result depending on the intermediate point, even after the average over all realization! For defining the value of a stochastic integral, it is necessary to choose the intermediate point and the Ito's choice corresponds to $\alpha = 0$. Thereforce, one has

$$\int_{t_0}^t f(t)dW(t) = \lim_{n \to \infty} \sum_{i=1}^n f(t_{i-1})(W(t_i) - W(t_{i-1})) \tag{5.10}$$

The Ito's choice corresponds to the fact that the integral is calculated by taking a value of the function f indépendent of the behavior of the Wiener process in the future. A principle similar to the causality

principle! However, it yields $< f(t).dW(t) >=< f(t) >< dW(t) >= 0$ and raises question for the computation of the work along a stochastic trajectory.

The Stratonovitch's choice implies that $< f(t).dW(t) >\neq< f(t) >< dW(t) >\neq 0$, which leads to adopt this choice in the stochastic thermodynamics.

Change of variable in Ito calculus

Let the change of variable $y = f(x(t), t)$. Performing an expansion to the second order in en dx, one obtains

$$dy(t) = f(x(t + dt)) - f(x(t)) = \frac{\partial f(x, t)}{\partial t}dt + \frac{\partial f(x, t)}{\partial x}dx(t) + \frac{\partial^2 f(x, t)}{2\partial x^2}dx(t)^2... \qquad (5.11)$$

Contrary to the ordinary differential equation, one keeps the term in dx^2, because the $dW(t)^2 \equiv dt$. Using the differential expression of the Langevin equation, one has $dx(t)^2 = (a(x, t)dt + b(x, t)dW(t))^2$. Performing the expansion of $dx(t)^2$, the terms dt^2, $dWdt$ can be neglected, but it remains a term $dW(t)^2$ and one gets $dx^2 = b^2(x, t)dt$. Therefore, collecting all terms, one obtains the result

$$dy(t) = \left(\frac{\partial f(x, t)}{\partial t} + a(x, t)\frac{\partial f(x, t)}{\partial x} + \frac{\partial^2 f(x, t)}{2\partial x^2}b^2(x, t) \right)dt + b(x, t)f'(x).dW(t) \qquad (5.12)$$

Stratonovitch calculus

Let us introduce the Stratonovitch calculus and the usual notation, one has

$$f(x, t) \circ dW = f(x + dx/2, t + dt/2)dW$$
$$= (f(x, t) + f'(x, t)dx/2)dW \qquad (5.13)$$

Higher terms are negligible.

Comparaison of the two rules

In order to obtain the same trajectory either calculated by the Ito calculus or by the Stratonovitch calculus, one has to compare with the stochastic differential equation $dx = a(x)dt + b(x)dW$.

For the Stratonovitch calculus, one has

$$b(x, t) \circ dW(t) = (b(x, t) + \frac{\partial b(x, t)}{2\partial x}dx)dW$$

$$(5.14)$$

At the lowest order $dx = b(, x, t)dW$ and $dW^2 = dt$, one gets

$$b(x, t) \circ dW(t) = b(x, t)dW(t) + \frac{b(x, t)}{2}\frac{\partial b(x, t)}{\partial x}dt \qquad (5.15)$$

Finally, the Langevin equation of the Ito calculus $dx(t) = a(x, t)dt + b(x, t)dW$ can be expressed as

$$dx(t) = \left(a(x) - \frac{b(x, t)}{2}\frac{\partial b(x, t)}{\partial x} \right)dt + b(x) \circ dW(t) \qquad (5.16)$$

with the Stratanovich calculus.

Note that when $b(x)$ is constant (corresponding to a white noise for the stochastic differential equation), the drift term cancels.

Therefore, one can obtain the same trajectory by using the Ito calculus or the Stratonovitch calculus, if the Langevin equation is modified as above. Note that when b is independent of x, both equations have the same expressions. However, when one computes integrals which involves the stochastic variable $x(t)$ (namely work and/or heat, see below), the result depends the choice of Ito or Stratonovitch.

5.2.2 Langevin dynamics

Underdamped motion

Let us consider a particle in one dimension with an applied force deriving from a potential energy $U(x, \lambda)$ and in thermal environment, where λ is a parameter which depends on time in general.

$$
\begin{cases}
\frac{dp}{dt} = -\frac{\partial U(x,\lambda)}{\partial x} - \gamma \frac{p}{m} + \xi(t) \\
\frac{dx}{dt} = \frac{p}{m}
\end{cases}
$$

where $\xi(t)$ is a Gaussian white noise characterized by the two first moments

$$
\langle \xi(t) \rangle = 0, \quad \langle \xi(t)\xi(t') \rangle = 2\gamma k_b T \delta(t - t') \tag{5.17}
$$

and $-\gamma \frac{p}{m}$ is a viscous damping force coming from the thermal environment. In the absence of the external force, one easily checks that the system obeys the Einstein relation, and leads the system to equilibrium. It is easy to show that $\langle \frac{p^2}{m} \rangle = k_B T$.

Overdamped motion

If one assumes that the variation of λ is slow, and the time step Δt for solving the equation of motion is larger than m/γ, the velocity distribution of the particle is always at equilibrium and the derivative of the momentum in the Langevin is much smaller than $\gamma p/m$. The motion is then overdamped and the Langevin equation becomes

$$
0 = -\frac{\partial U(x, \lambda)}{\partial x} - \gamma \frac{p}{m} + \xi(t) \tag{5.18}
$$

which can be reexpressed as

$$
\frac{dx}{dt} = \frac{1}{\gamma} \left(-\frac{\partial U(x, \lambda)}{\partial x} + \xi(t) \right) \tag{5.19}
$$

5.2.3 Fokker-Planck and Kramers equations

Whereas the Langevin equation is well adapted for obtaining information for a single trajectory, the Fokker-Planck and Kramers equation describe the evolution of the probability $P(x, p, t)$ which corresponds to an average over a large number of trajectories.

For underdamped motion, one has

$$
\frac{\partial P(x, p, t)}{\partial t} = \left[-\frac{\partial}{\partial x} \frac{p}{m} + \frac{\partial}{\partial p} \left(\frac{\partial U(x, \lambda)}{\partial x} + \gamma \frac{p}{m} \right) + \frac{\partial^2}{\partial p^2} \gamma k_B T \right] P(x, p, t) \tag{5.20}
$$

Note that the Kramers equation can be interpreted as an equation of continuity in the phase space.

$$\frac{\partial P(x,p,t)}{\partial t} = -\frac{\partial J_x}{\partial x} - \frac{\partial J_p}{\partial p} = -\vec{\nabla}.\vec{J} \tag{5.21}$$

with

$$\vec{J} = \begin{cases} J_x &= \frac{p}{m}P(x,p,t) \\ J_p &= \left(-\frac{\partial U(x,\lambda)}{\partial x} - \gamma\frac{p}{m}\right)P(x,p,t) - \frac{\partial}{\partial p}(\gamma k_B T P(x,p,t)) \end{cases} \tag{5.22}$$

is the flux of probability at point (x,p).

Note that when λ and T are constant, the Kramers equation evolves to equilibrium, which means that the stationary probability is given as $P(x,v) = f(x)g(p)$ Inserting the ansatz in Eq. 5.2.3, one obtains

$$0 = -\frac{p}{m}g(p)\frac{df(x)}{dx} + f(x)\frac{\partial U(x)}{\partial x}\frac{dg(p)}{dp} + \frac{\gamma}{m}f(x)\frac{dpg(p))}{dp} + f(x)\gamma k_B T\frac{d^2g(v)}{dv^2} \tag{5.23}$$

By dividing the above equation by $f(x)g(p)$, one obtains

$$\frac{p}{m}\frac{d\ln(f(x))}{dx} - \frac{\partial U(x)}{\partial x}\frac{d\ln(g(p))}{dp} = \frac{\gamma}{mg(p)}\frac{dpg(p))}{dp} + \frac{\gamma k_B T}{g(p)}\frac{d^2g(v)}{dv^2} \tag{5.24}$$

Both sides of the equation must be equal to 0 in the stationary state (because at equilibrium, no flux is present in the system). One first obtains that

$$\frac{p}{m}g(p) + k_B T\frac{dg(p)}{dp} = 0 \tag{5.25}$$

which gives

$$g(p) \propto e^{-\frac{p^2}{2mk_BT}} \tag{5.26}$$

Inserting this solution in Eq.5.23, the differential equation for $f(x)$ is then given by

$$\frac{p}{m}\left(\frac{d\ln(f(x))}{dx} + \frac{1}{k_B T}\frac{\partial U(x)}{\partial x}\right) = 0 \tag{5.27}$$

with the solution $f(x) \propto e^{-\beta U(x)}$.

By using the normalization of P, the equilibrium probability is given by

$$P_{eq}(x,p) = \frac{\exp\left(-\beta\left(\frac{p^2}{2m} + U(x,\lambda)\right)\right)}{\sqrt{2\pi m/\beta}\int dx\exp\left(-\beta\left(\frac{p^2}{2m} + U(x,\lambda)\right)\right)} \tag{5.28}$$

For an overdamped motion, the velocity distribution is always at equilibrium and the position distribution obeys the Fokker-Planck equation

$$\frac{\partial P(x,t)}{\partial t} = \frac{\partial}{\partial x}\left(\frac{1}{\gamma}\left[\frac{\partial U(x,\lambda)}{\partial x} + \frac{\partial}{\partial x}k_B T\right]\right)P(x,t) = -\frac{\partial J}{\partial x} \tag{5.29}$$

where J is the probability flux

$$J = -\frac{1}{\gamma}\left(\frac{\partial U(x,\lambda)}{\partial x} + \frac{\partial}{\partial x}k_B T\right)P(x,p,t) \tag{5.30}$$

It is worth noting that the position distribution also reaches equilibrium at long times by cancelling the flux J.

$$P_{eq}(x) = \frac{\exp\left(-\beta U(x,\lambda)\right)}{\int dx \exp\left(-\beta U(x,\lambda)\right)} \tag{5.31}$$

5.3   Path integral approach

A third approach for the stochastic processes can be done by using the formalism of path ensemble. $\xi(t)$ is a Gaussian white noise, with the two first moments $\langle\xi(t)\rangle = 0$ and $\langle\xi(t)\xi(t')\rangle = 2\gamma k_b T$. The probability of having a path $\xi(t)$ between 0 and t is given by

$$P[\xi] \propto \exp\left(-\frac{1}{4\gamma k_B T}\int_0^t du\, \xi^2(u)\right) \tag{5.32}$$

The probability $P[\xi]$ is normalized by summing over paths:

$$\int d[\xi]P[\xi] = 1 \tag{5.33}$$

For an overdamped motion, the Langevin equation can be expressed as

$$\gamma\frac{dx}{dt} + \frac{\partial U(x,\lambda)}{\partial x} = \xi(t) \tag{5.34}$$

which can be interpreted as follows: when one solves the stochastic differential equation, the noise is converted in position fluctuations of the particle. Therefore, the probability of having a trajectory $x(t)$ is given by

$$P[x] \propto \exp\left(-\frac{1}{4\gamma k_B T}\int_0^t du\left\{\left[\gamma\frac{dx}{dt} + \frac{\partial U}{\partial x}\right]^2 - 2k_B T\frac{\partial^2 U}{\partial x^2}\right\}\right) \tag{5.35}$$

such that

$$\int d[x]P[x] = 1 \tag{5.36}$$

The seconde derivative of the potential which appears in Eq.5.35 comes from the Jacobian of the change of variable $\xi(t)$ to $x(t)$ in the path integral. Indeed, taking a finite time step, the Langevin equation is expressed as

$$\gamma((x_{n+1} - x_n) = -U'(x_n')\delta t + \sqrt{2\gamma k_B T}(W_{n+1} - W_n) \tag{5.37}$$

where x_n' is a point choosing betwenn x_n and x_{n+1}. By choosing a Stratonovitch rule (trapezoidal rule), we have $U'(x_n' = (U'(x_n) + \frac{1}{2}U''(x_n)(x_{n+1} - x_n)$ which gives a Jacobian of the elementary transformation equal to

$$\frac{\partial(W_{n+1} - W_n)}{\partial(x_{n+1} - x_n)} = \frac{\gamma}{\sqrt{2\gamma k_B T}}(1 + \frac{\delta t}{2\gamma}U''(x_n)) \tag{5.38}$$

Finally, one takes the limit $\Delta t \to 0$, and one obtains

$$\prod_{n=0}^{\frac{t}{\Delta t}}(1 + \frac{\delta t}{2\gamma}U''(x_n)) \to \exp\left(\frac{1}{2\gamma}\int_0^t U''(x)ds\right) \tag{5.39}$$

Contrary to Hamiltonian systems, the Langevin equation breaks the time-reversal symmetry (for a single trajectory). However, one can see that the time-reversal process $\xi(-t)$ occurs with the same probability. When a Langevin process described a motion at equilibrium, the probability of having the time-reversal trajectory $x(-t)$ is equal to the probability of having $x(t)$. This symmetry is called detailed balance. Consequently, no work can be extracted from the stochastic motion of the particle, corresponding to the prescription of the second law of thermuodynamics.

5.4   Stochastic thermodynamics
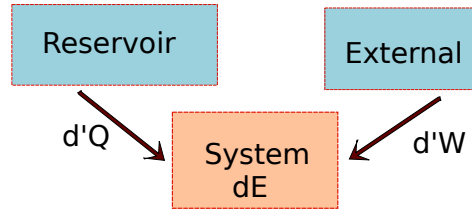
Figure 5.1: Scheme of the energy fluxes between the three parts of the world. The arrows indicate positive fluxes.

In order to define the fluctuating thermodynamic quantities of a stochastic process, one first defines the world consists in three parts: the system, the thermal environnement and the external operator. (See Fig. (5.1))

As for macroscopic systems, when the system receives heat from the reservoir (thermal environment), it is considered as positive. For an infinitesimal timestep dt. The force exerced by the thermal environment is $-\gamma\frac{dx}{dt} + \xi(t)$ and the heat received is $d'Q$

$$d'Q = \left(-\gamma\frac{dx}{dt} + \xi(t)\right) \circ dx(t) \tag{5.40}$$

Note that the product is performed by the Stratonovitch rule for physical reasons. The notation d' recalls that the integrated heat depends on the trajectory (or on the external force) and not only on the initial and final states like thermodynamic potentials

For an underdamped motion, the heat is given by $-\gamma\frac{dp}{dt} + \xi(t)$ times the displacement. By using the

equation of motion, the heat can be written as

$$d'Q = \left(\frac{dp}{dt} + \frac{\partial U(x,\lambda)}{\partial x} \right) \circ dx(t) \tag{5.41}$$

5.4.1 First law of thermodynamics

The work brought to the system corresponds to a change performed by the external operator, one has

$$d'W = \frac{\partial U(x,\lambda)}{\partial \lambda} \circ d\lambda(t) \tag{5.42}$$

For a underdamped motion, one uses two identities

$$\frac{dp}{dt} \circ dx(t) = \frac{dp}{dt} \circ \frac{p}{m} dt = d\left(\frac{p^2}{2m} \right)$$

$$\frac{\partial U(x,\lambda)}{\partial x} \circ dx = dU(x,\lambda) - \frac{\partial U(x,\lambda)}{\partial \lambda} \circ d\lambda$$

which gives

$$dE = d'Q + d'W \tag{5.43}$$

where E is the total energy of the system

$$E = \left(\frac{p^2}{2m} + U(x,\lambda) \right) \tag{5.44}$$

Eq.(5.43) expresses the conservation of the energy of the system.

For an overdamped motion, by using the Langevin equation and Eq.(5.40), the heat is given by

$$d'Q = \frac{\partial U(x,\lambda)}{\partial x} \circ dx(t) \tag{5.45}$$

and one immediately obtains

$$dU(x,\lambda) = \delta'Q + \delta'W \tag{5.46}$$

Because the motion is overdamped, the mean kinetic energy stays at equilibrium and only the internal energy is modified when work and/or heat are brought to the system.

The thermodynamics quantities have been defined for a single trajectory, and it is also interesting to calculate an ensemble average of these fluctuating observables. It is convenient to use the Fokker-Planck and/or Kramers equations.

For a underdamped motion, the mean heat variation can be rewritten as

$$\langle d'Q \rangle = \int \int \left(\frac{dp}{dt} + \frac{\partial U(x,\lambda)}{\partial x} \right) \circ \frac{dx}{dt} P(x,p) dx dp dt \tag{5.47}$$

$$= \int \int \left(\frac{p}{m} \circ \frac{dp}{dt} + \frac{\partial U(x,\lambda)}{\partial x} \circ \frac{dx(t)}{dt} \right) P(x,p) dt dx dp \tag{5.48}$$

This can be reexpressed as

$$\langle d'Q \rangle = \int \left(\frac{\partial E}{\partial x} J_x + \frac{\partial E}{\partial p} J_p \right) dx \, dp \, dt$$

$$\langle d'Q \rangle = \int \left(\vec{\nabla} E \vec{J} \right) dx \, dp \, dt \tag{5.49}$$

where

$$\vec{J} = \left(\frac{dx}{dt} P(x,p), \frac{dp}{dt} P(x,p) \right)$$

is the flux of probability in the phase space.

Similarly, for an overdamped motion, one has

$$\langle d'Q \rangle = \int \frac{\partial E}{\partial x} J_x \, dx \, dt \tag{5.50}$$

5.4.2 Entropy and second law of thermodynamics

It is now possible to define a stochastic entropy which comes from the particle trajectory We restrict here to an overdamped motion

$$s(t) = -\ln(P((x(t,\lambda),t))) \tag{5.51}$$

where $P((x(t,\lambda),t)$ is the probability provided by the Fokker-Planck equation associated with the Langevin equation and calculated along the particle trajectory x_t. As a consequence, the stochastic entropy depends both on the trajectory and on the ensemble. Taking the time derivative of the stochastic entropy, one has

$$\frac{ds(t)}{dt} = -\frac{1}{P(x,t)} \left(\frac{\partial P(x,t)}{\partial t} + \frac{\partial P(x,t)}{\partial x} \frac{dx}{dt} \right) \tag{5.52}$$

By using Eq.(5.30)

$$\frac{\partial P(x,t)}{\partial x} = -\beta \left(\gamma J(x,t) + \frac{\partial U(x,t)}{\partial x} P(x,t) \right) \tag{5.53}$$

one obtains

$$\frac{ds(t)}{dt} = -\frac{\partial_t P(x,t)}{P(x,t)} + \left(\frac{\beta \gamma J(x,t)}{P(x,t)} + \beta \partial_x U(x,t) \right)_{x_t} \frac{dx}{dt} \tag{5.54}$$

where one introduces the short-hand notation $\partial_x = \frac{\partial}{\partial x}$

An second contribution of the entropy creation comes from the entropy dissipated into the environment: the heat released in the environnement is equal to the opposite heat received by the system and the entropy rate is given by

$$\frac{ds_m(x(t))}{dt} = \beta \frac{-dq(x(t))}{dt} \tag{5.55}$$

By using Eq.(5.45)

$$\frac{ds_m(x(t))}{dt} = -\beta \partial_x U(x,t) \frac{dx}{dt} \tag{5.56}$$

By summing the two contributions to the total entropy, one obtains the total entropy

$$\frac{ds_{tot}(t)}{dt} = -\frac{\partial_t P(x,t)}{P(x,t)} + \left(\frac{J(x,t)}{DP(x,t)} \right)_{x_t} \frac{dx}{dt} \tag{5.57}$$

where $D = 1/\beta\gamma$.

The rate of the total entropy is now averaged over all trajectories. For a given function $f(x,t)$, the brackets denoting the average mean

$$\langle f(x,t) \rangle = \int dx f(x,t) P(x,t) \tag{5.58}$$

Consequently, one has

$$\left\langle f(x,t) \frac{dx}{dt} \right\rangle = \int dx f(x,t) J(x,t) \tag{5.59}$$

where $J(x,t)$ is the flux of probability

The mean rate of the total entropy is then given by

$$\frac{dS_{tot}(t)}{dt} = \left\langle \frac{ds_{tot}(t)}{dt} \right\rangle$$

$$= -\int dx \frac{\partial P(x,t)}{\partial t} + \int dx \frac{J^2(x,t)}{DP(x,t)} \tag{5.60}$$

Due to the conservation of the probability, one has $\int dx \frac{\partial P(x,t)}{\partial t} = 0$ and finally the mean rate of the total entropy is

$$\frac{dS_{tot}(t)}{dt} = \int dx \frac{J^2(x,t)}{DP(x,t)} \geq 0 \tag{5.61}$$

because the integrand $\frac{J^2(x,t)}{Dp(x,t)}$ is positive. Therefore, one recovers that the total entropy increases with time as expected by the second law of the thermodynamics.

5.5 Large deviation functions

For a random variables A_n parameterized by n which is an increasing index, the theory of large deviations says (for a large class of systems) that the probability $P(A_n = a)$ behaves as $\approx e^{-I(a)n}$ for large n. $I(a)$ is called the rate function. In other words, the leading behavior can be expressed as

$$\lim_{n \to \infty} -\frac{\ln(P(A_n))}{n} = I(a) \tag{5.62}$$

This theory encompasses various situations occurring in statistical physics, stochastic processes, probability theory. The goal of this introduction is to show by using simple examples that this quantity can be obtained analytically and/or numerically from simulations.

5.5.1 Independent and Identically Distributed variables

Let us consider a probability distribution $p(x)$, and let us define the mean value of n variables

$$S_n = \frac{1}{n} \sum_{i=1}^{n} x_i \tag{5.63}$$

where x_i are random variables chosen with the probability distribution $p(x)$.

The probability of having $S_n = s$ is given by

$$P(S_n = s) = \int dx_1 \int dx_2 \cdots \int dx_n p(x_1) p(x_2) \cdots p(x_n) \delta(x_1 + x_2 + \cdots + x_n - sn) \tag{5.64}$$

72

where δ is the Dirac function.

By introducing the Laplace transform of P and the change of variable $s \to ns$

$$\tilde{P}(u) = \int_0^\infty e^{-us} P(s) ds \tag{5.65}$$

one obtains

$$\tilde{P}(u) = \tilde{p}^n(u/n) \tag{5.66}$$

With an exponential distribution $p(x) = \lambda \exp(-\lambda x)$, one obtains

$$\tilde{P}(u) = \frac{\lambda^n}{(\lambda + u/n)^n} \tag{5.67}$$

which gives

$$P(s) = \frac{\lambda^n (ns)^n}{n!} e^{-\lambda ns} \tag{5.68}$$

By using the Stirling formula , $n! \sim n^n e^{-n} \sqrt{2\pi n}$, the probability $P(s)$ behaves at large n as

$$P(s) \approx \exp(-I(s)n) \tag{5.69}$$

where $I(s)$ is the rate function is given by

$$I(x) = \lambda x - \ln(\lambda x) - 1 \tag{5.70}$$

The rate function $I(x)$ is maximum and cancels when $\lambda x = 1$, which corresponds to the mean value $\lambda s = 1$. Expanding to second-order at the maximum of the function, one obtains

$$I(x) = \frac{1}{2}(\lambda x - 1)^2 \tag{5.71}$$

and we recover the law of large numbers, which gives a Gaussian distribution of $P(x)$ around the mean value.

Figure 5.2 shows the theoretical rate function $I(x)$, the law of large numbers and the simulation results for the mean of 20 exponentially IID variables. Clearly, the law of large numbers overestimates the smallest mean values and underestimates the largest values. It also appears that the rate function is a difficult task to obtain in simulations, because the large values of the rate function corresponds to rare events. It exists some methods which permits to sample rare events by introducing simulation methods which biases generated configurations.

5.5.2 Gartner-Ellis theorem

For a random variable A_n where n is a positive integer, one defines the scaled cumulant generating function

$$\lambda(k) = \lim_{n \to \infty} \frac{1}{n} \ln \langle e^{nkA_n} \rangle \tag{5.72}$$

If $\lambda(k)$ exists and is differentiable for all real values k then the probability $P(A_n)$ is given as a large deviation function

$$P(a) \approx e^{-nI(a)} \tag{5.73}$$

Inserting Eq.(5.73) in Eq.(5.72), one obtains that

$$\langle e^{nkA_n} \rangle \approx \int da\, e^{n(ka - I(a))} \tag{5.74}$$

73
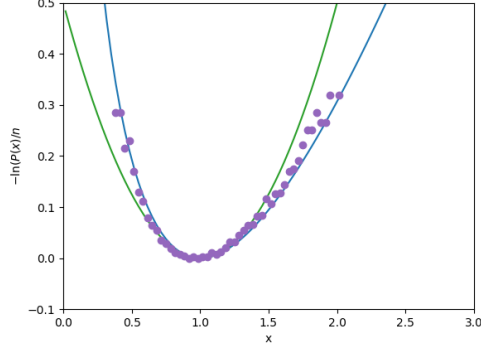
Figure 5.2: Rate functions of IID variables for the exponential distribution: theoretical prediction (full curve) and simulation results (dots). The green curve corresponds to the Gaussian approximation (law of large numbers.

By using the saddle-point method (or Laplace's method), one obtains that

$$\lambda(k)) = \sup_{a \in R}(ka - I(a)) \tag{5.75}$$

where sup means "supremum of". The Legendre-Fenchel transform of the rate function gives the scaled cumulant generating function. If $\lambda(k)$ is a differentiable function, the inverse transform holds and the rate function is then given by

$$I(a) = \sup_{k \in R}(ka - \lambda(k)) \tag{5.76}$$

5.5.3 Application in Statistical Mechanics

The thermodynamic potentials satisfy a large deviation principle. The partition functions associated with the different ensembles: for the microcanonical ensemble, the partition function has a large deviation principle, where the rate function is the opposite of the mean entropy per particle (or per lattice site)

$$Z(E, V, N) \approx e^{Ns(e,\rho)} \tag{5.77}$$

The canonical partition function has a large deviation principle

$$Z(V, N, T) \approx e^{-N\beta f(\rho,\beta)} \tag{5.78}$$

where $\beta = 1/T$ is the inverse temperature (for the sake of simplicity, the Boltzmann constant k_B is set to 1) and f is the free energy per particle.

For concave entropy, the free energy can be obtained from a Legendre-Fenchel transform

$$\beta(f(\rho,\beta) = \sup_{e \in R}(\beta e - s(e,\rho)) \tag{5.79}$$

Conversely, if the free energy is differentiable for all temperatures, one can obtain the entropy as

$$s(e,\rho) = \inf_{\beta \in R^+}(\beta e - f(\rho,\beta)) \tag{5.80}$$

where inf is the "infimum of".

For a more detailed introduction to the large deviation functions, see [?].

5.6 Fluctuation theorems

The different fluctuation theorems express the universal properties of the probability distribution of the thermodynamic quantities. This corresponds to a generalisation of thermodynamics by including the fluctuations. Three classes of properties have been proved under specific assumptions. Let us introduce a variable $\Lambda(x,t)$ which depends on x and t.

5.6.1 Integral fluctuation theorem

If $\Lambda(x,t)$ is a non dimensional functional, one says that Λ obeys the integral fluctuation theorem iff

$$\langle \exp(-\Lambda) \rangle = \int d\Lambda\, p(\Lambda) \exp(-\Lambda) = 1 \tag{5.81}$$

where $p(\Lambda)$ is the distribution probability. Several properties can be infered from the IFT

-
$$\langle \Lambda \rangle \geq 0 \tag{5.82}$$

  By using the inequality $e^{-x} \geq 1 - x$, one obtains that

  $$-\langle \Lambda \rangle < 0$$

  which leads to Eq.(5.81)

- The integral being equal to 1, there are trajectories where Λ is negative. There is an apparent violation of the second law of thermodynamics. In fact, this corresponds to fluctuations which can lead to negative values of Λ.

-
$$P(\Lambda < -\lambda) \leq \int_{-\infty}^{-\lambda} d\Lambda\, p(\Lambda) e^{-\lambda-\Lambda} \leq e^{-\lambda} \tag{5.83}$$

  To prove the inequality, one writes

  $$
  \begin{aligned}
  P(\Lambda < -\lambda) &= \int_{-\infty}^{-\lambda} d\Lambda\, p(\Lambda) \\
  &\leq \int_{-\infty}^{-\lambda} d\Lambda\, p(\Lambda) e^{-\lambda-\Lambda} \\
  &\leq \int_{-\infty}^{\infty} d\Lambda\, p(\Lambda) e^{-\lambda} e^{-\Lambda} \\
  &\leq e^{-\lambda} \tag{5.84}
  \end{aligned}
  $$

- When the probability distribution is Gaussian and satisfies an IFT, this imposes a constraint between the variance and the mean of Λ

  $$\langle (\Lambda - \langle \Lambda \rangle)^2 \rangle = 2\langle \Lambda \rangle \tag{5.85}$$

if $p(\Lambda) = \frac{1}{\sqrt{2\pi}\sigma} exp(-\frac{(\Lambda-\langle\Lambda\rangle)^2)}{2\sigma^2}$ with $\sigma^2 = \langle (\Lambda - \langle\Lambda\rangle)^2 \rangle$ one has

$$\int e^{-\Lambda} p(\Lambda) = e^{\sigma^2/2 - \langle\Lambda\rangle}$$

which leads to Eq.(5.85)

5.6.2 Detailed fluctuation theorem

The detailed fluctuation theorem provides a relation between the probability of obtaining the quantity Λ and the opposite $-\Lambda$:

$$\frac{p(-\Lambda)}{p(\Lambda)} = \exp(-\Lambda) \tag{5.86}$$

Several properties can be also infered from this theorem
When a quantity Λ satisfies this relation, the IFT is also satisfied.

$$\int d\Lambda \exp(-\Lambda)p(\Lambda) = \int d\Lambda p(-\Lambda) \tag{5.87}$$

$$= \int d\Lambda p(\Lambda) = 1 \tag{5.88}$$

5.6.3 Generalized Crooks fluctuation theorem

The generalized Crooks fluctuation theorem provides a relation comparing the probability distribution function $p(\Lambda)$ with the probability $p^\dagger(\Lambda)$ of the same quantity Λ for a "conjugate" process (generally one considers a time-reversed process)

$$\frac{p^\dagger(-\Lambda)}{p(\Lambda)} = \exp(-\Lambda) \tag{5.89}$$

5.6.4 Work fluctuation theorems

We first consider work fluctuations when the initial configuration is in equilibrium whereas the final configuration is not necessarily in equilibrium. The system evolves between the two states due to a driving force.

Jarzynski relation

Jarzynski showed the work which allows to drive the system from the initial equilibrium state by using a time-dependent potential $V(x, \lambda)$ for a time t satisfies the relation

$$\left\langle \exp\left(-\frac{w}{T}\right) \right\rangle = \exp\left(-\frac{\Delta\mathcal{F}}{T}\right) \tag{5.90}$$

where $\Delta\mathcal{F}$ is the difference of the free energy between the final state where the control parameter is equal to λ_t and the initial state with a control parameter λ_0. This can be viewed as a IFT relation for the dimensionless dissipated work.

$$w_d = \frac{w - \Delta\mathcal{F}}{T} \tag{5.91}$$

Therefore, experimentally and/or in simulation, it becomes possible to obtain the free energy difference $\Delta\mathcal{F} = \mathcal{F}(\lambda_t) - \mathcal{F}(\lambda_0)$, namely a equilibrium property, from non equilibrium measurements.

Crooks fluctuation theorem

The Crooks fluctuation theorem states that the probability distribution $p(w)$ for work spent in the process is related to the probability distribution $\tilde{p}$ for work in the reverse process. The control parameter of the reversed process is given by $\tilde{\lambda}(\tau) = \lambda(t - \tau)$ and the initial state of the reversed process is an equilibrium state where $\tilde{\lambda}(0) = \lambda(t)$.

$$\frac{\tilde{p}(w)}{p(w)} = \exp\left(-\frac{w - \Delta\mathcal{F}}{T}\right) \tag{5.92}$$

Note that for a system where the Crooks relation holds, the Jarzynski theorem is satisfied. Indeed, knowing that $\tilde{p}(w)$ is normalized, one immediately infers that the JR holds.

5.6.5 Entropy production

The entropy production along a trajectory is the sum of two terms as previously seen

$$\Delta s_{tot} = \Delta s_m + \Delta s \tag{5.93}$$

with

$$\Delta s = -\ln(p(x_t, \lambda_t)) + \ln(p(x_0, \lambda_0)) \tag{5.94}$$

The total entropy obeys the IFT

$$\langle \exp(-\Delta s_{tot}) \rangle = 1 \tag{5.95}$$

By using the convexity of the exponential function, one infers that $\langle \Delta s_{tot} \rangle \geq 0$ wich shows that the entropy production is obviously compatible with the second law of thermodynamics.

6.1 Introduction

We consider here the large domain of out-of-equilibrium statistical physics. Physical situations where a system evolves without reaching equilibrium are very frequent. There are different reasons: i) a system is not isolated, for instance in contact with a thermostat, or surrounded by several particle reservoirs,... which prevents to reach equilibrium; ii) the relaxation times may be much larger than the typical experiment time, and the system cannot reach equilibrium (for instance, protein adsorption at liquid-solid interfaces, polymers, glassformers, spin glasses); iii) The system has an intrinsic irreversibility (for instance, collisional dynamics for granular matter) for which one needs to introduce an appropriate out of equilibrium statistical description (granular matter, fragmentation, growing phenomena, avalanches, earthquakes)[25, 13, 23].

These systems can be separated in three large classes which describe their out of equilibrium evolution: First, relaxation times are very large (significantly larger than the experimental time), second, the evolution is driven towards non equilibrium states. Lastly, systems evolve under external constraints towards stationary states, with a microscopic dynamics that may or may not be Hamiltonian.

The relevance of this approach is illustrated by considering several toy models of non equilibrium statistical physics. Special attention will be devoted to algorithms of numerical simulation of these systems.

A numerical approach is justified by the absence of a general theoretical framework of out-of-equilibrium systems. Numerical results allow us to understand the physics of such systems and are an efficient tool for developing theoretical methods.

6.2 Random sequential addition

6.2.1 Motivation

When a solution of macromolecules (proteins, colloids) is placed in contact with a solid surface, one observes a surface adsorption as a monolayer of macromolecules. This process is slow; the adsorption can take from several minutes to several weeks. Once adsorption performed, if one replaces the solution with a buffer solution, little or no desorption is observed and there are few changes in the structure of the adsorbed monolayer. When the experiment is repeated with different concentrations of macromolecules, the saturation coverage is always the same[23].

Considering the typical time scales and the microscopic complexity of molecules, it is not possible to perform Molecular Dynamics describing the process. A first step consists of coarse-graining the system with a "mesoscopic" length scale. The typical size of molecules is from $10nm$ to some mm, and therefore the range of interaction between particles is smaller than the particle size. The shape of these particles does not change during the process and particles cannot overlap. As a first approach, the interaction potential can be taken as a hard core potential (for instance for colloids).

When the particle is in the neighborhood of the surface, the interaction with the surface is strongly attractive on a short distance and strongly repulsive when the particle goes into the surface. The interaction potential can be approximated as a strongly attractive contact potential. Once adsorbed, particles

cannot desorb or move on the surface. Because particles in solution follow Brownian trajectories, one can assume that particles reach the surface randomly. If the particle first reaches an adsorbed particle, it is pushed away from the surface and returns to the bulk. If the particle reaches the solid surface, without overlapping other adsorbed particles, it is "glued" to the surface, definitively.

6.2.2   Definition

Once the system has been coarse-grained, the particle adsorption can be described by the following model, called, Random Sequential Adsorption (or Addition), RSA.

Consider a space of dimension d. One sequentially drops hard particles onto a $d - 1$ surface, randomly, with the following condition: if the trial particle does not overlap any adsorbed particles, this particle is placed in this position definitively; otherwise, the trial particle is removed and a new attempt is performed.

Such a model contains two essential features characterizing the adsorption kinetics: exclusion effects and irreversibility of the kinetics.

When one considers spherical particles, this means that in one dimension one places hard rods onto a line, in two dimensions, one places discs onto a plane and in three dimensions balls in the three-dimensional space.

As seen in chapter 2, Monte Carlo dynamics with a detailed balance condition corresponds to a Markovian process converging to equilibrium. For the RSA model, without detailed balance (or balance condition), the Markovian process does not converge to equilibrium, but approaches a saturation state. A Monte Carlo algorithm can be used for describing this model and is detailed below.

6.2.3   Algorithm

The basic algorithm of the Monte Carlo simulation is independent of the space dimension. Because the primary motivation is particle adsorption onto a surface, we consider hard discs (which represent the projected volume onto the plane). The length size of the simulation cell is set to unity. Two arrays of maximum size equal to $4/(\pi\sigma^2)$ are initialized to zero (σ denotes the particle diameter), and are used for storing particle positions during the process.

These arrays are void at time $t = 0$, because the surface does not contain particles initially. A kinetic time step is the following:

1. One selects randomly and uniformly positions of a trial particle within the simulation cell.

$$\begin{cases} x_0 = & rand \\ y_0 = & rand \end{cases} \tag{6.1}$$

   Time is increased by 1: $t = t + 1$.

2. One checks if the trial particle does not overlap already adsorbed (a true condition at $t = 0$, because the surface is empty) One has to check that $(\mathbf{r}_0 - \mathbf{r}_i)^2 > \sigma^2$ wih i running from 1 to the index of the last adsorbed particle (at time t) denoted n_a. If this test is false, one can stop the nested loop, and the trial particle is rejected and one selects a new trial particle. Oppositely, when the test is true for all adsorbed particles, one increments the index n_a ($n_a = n_a + 1$), one inserts the particle positions in the coordinate arrays:

$$\begin{cases} x[n_a] = & x_0 \\ y[n_a] = & y_0. \end{cases} \tag{6.2}$$
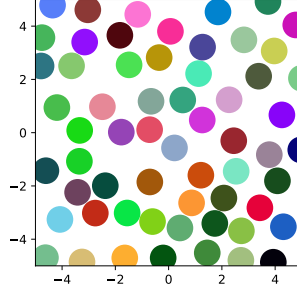
80

Figure 6.1: Adsorbed disks in a RSA kinetics: the trial particle is at the center of the figure. The cell associated with the trial particle is in red. The 24 cells to be considered for the overlapping test are in orange.

Because the attempt number for filling the surface is not known initially, one sets the maximum of attempts and in other words the computer time of a run.

The basic algorithm is correct, but very slow in the final stages of the kinetics. Indeed, at each time step, it is necessary to perform n_a overlapping tests for determining if the trial particle can be inserted onto the surface. When we are close to the saturation coverage, a lot of computer time is spent performing useless tests, because practically all trial particles are rejected.

Knowing that a disc can be surrounded by six particles at maximum, it is easy to see that overlapping tests are useless with particles far from the trial particle.

A solution can be found by listing cells where particles can overlap with the trial particle. If on chooses a grid whose elementary cell has a linear size strictly smaller than the particle diameter, this means that in each cell, one can put one or zero disc. One defines a two dimensional array whose indices i and j correspondent to elementary cells. This array is initialized to 0. The algorithm is then modified as follows:

1. The first step is unchanged.

2. One determines indices corresponding to the elementary cell associated to the trial particle.

$$\begin{cases} i_0 = & Int(x_0/\sigma) \\ j_0 = & Int(y_0/\sigma). \end{cases} \tag{6.3}$$

If the cell is occupied ($cell[i_0][j_0] \neq 0$), the trial particle is immediately rejected and one restarts with a new particle. If the cell is empty, one needs to test the neighboring 24 cells cellules. The nested loop is only performed on occupied cells (see Fig 6.1). For an occupied cell, ($cell[i][j] \neq 0$), a test for overlap between the trial particle and the particle of the cell is performed. If overlap, the loop is interrupted, and a new particle is selected. Otherwise, the next occupied cell is considered. If overlap tests with particles belonging to neighboring cells are false, the trial particle is then inserted onto the plane, as in the previous algorithm. Once inserted, the corresponding cell becomes occupied and the value of the two dimensional array is updated.

$$cell[i_0][j_0] = n_a. \tag{6.4}$$

By using this algorithm, test number is now bounded to 24 for a trial, regardless of the number of previously adsorbed particles. The computer time is now proportional to the particle number and not to the squared particle number. List methods are frequently used in Molecular Dynamics in order to restrict the particle number for computing forces.

6.2.4 Results

In one dimension, an equilibrium system is unable to display a phase transition at a finite temperature (we consider short-range interactions). Therefore, analytical results, which are obtained for equilibrium systems, are not generally useful for understanding the behavior in higher dimensional systems. Indeed, many systems exhibits phase transitions in higher dimensions, where exact results cannot be obtained. Conversely, for non equilibrium models, such as RSA, the one-dimensional solution is relevant for understanding the same model in higher dimensions.

Qualitatively, the adsorption kinetics can be described in several regimes: first, most of trial particles are adsorbed and the coverage increases rapidly with time. As the plane fills, rejection of trial particles increases. Finally, when the trial number becomes several times the number of adsorbed particles, the coverage becomes comparable to the saturation coverage (less than 10%) and the filling efficiency becomes low, because available regions for inserting new particles correspond to isolated targets where only one particle can be inserted. The available surface is a small fraction of the simulation cell.

The one dimensional model, also called the parking lot model, can be solved exactly (see Appendix C). We exploit these results for inferring generic behaviors in higher dimensions.

In one dimension, if we set the hard rod length to unity, the time evolution of the density (assuming that the line is empty initially) is:

$$\rho(t) = \int_0^t du \exp\left(-2 \int_0^u dv \frac{1 - e^{-v}}{v}\right). \tag{6.5}$$

When $t \to \infty$, the density goes to $0.7476\ldots$. In a RSA process, particle rearrangement are forbidden, contrary to equilibrium. At saturation, all intervals on the line are smaller than a hard rod length. Note that the maximum density strongly depends on the initial configuration, which is a significant difference with a kinetics evolving to equilibrium. Indeed, equilibrium is independent of initial configurations.

One obtains an apparently paradoxical situation: a process with a stochastic Markovian dynamics (namely, in which memory is limited to short range configurations), keeps memory of the initial configuration indefinitely.

Close to saturation, the asymptotic expansion of the density ($t \to \infty$), equation (6.5), gives

$$\rho(\infty) - \rho(t) \simeq \left(\frac{e^{-2\gamma}}{t}\right), \tag{6.6}$$

where γ is the Euler's constant. The saturated state is approached slowly and is given by a scaling algebraic law. In higher dimension, one can show that, for spherical particles, in the asymptotic regime, the saturation coverage evolves as $\rho(\infty) - \rho(t) \simeq 1/t^{1/d}$ where d is the space dimension. This gives an exponent equal to $1/2$ for $d = 2$.

Among the differences between the non equilibrium and equilibrium versions of the model, fluctuations of a finite system are not identical for the same density. At equilibrium, fluctuations can be calculated from a Monte Carlo simulation by monitoring moments of the particle distribution, $\langle N \rangle$ and $\langle N^2 \rangle$ in the grand-canonical ensemble. In a RSA simulation, these fluctuations are available as follows: performing a series of runs for a given system size, and starting from an identical initial configuration, one obtains a density histogram at a given time by averaging over all runs. One then calculates the mean values of $\langle N \rangle$ and $\langle N^2 \rangle$. Brackets correspond to an average over different realizations of the process.

These quantities can be defined in the absence of a Gibbs measure of the system. For a thermodynamic system, these averages can be calculated in a similar way, but because of the unicity of the equilibrium, a statistical average over different realizations is equivalent of an average over a single simulation at equilibrium. That is why at equilibrium, the second method is always selected, because less computation is required for calculating averages.

As mentioned above, fluctuations associated with a finite system are different in equilibrium than in a RSA process. In one dimension, these fluctuations can be obtained analytically in both cases and their are less pronounced in a RSA process. This behavior is similar in higher dimensions, where only numerical results can be obtained. The analysis of fluctuations of adsorbed configurations allows one to distinguish equilibrium and irreversible kinetics.

As seen in Chapter 4, the correlation function $g(r)$ can be defined from geometrical considerations (for hard particles) and not necessarily by using a Gibbs measure. Consequently, it is possible to calculate in a RSA process, pair correlations. By using the statistical average defined above (for fluctuation computation), one obtains $g(r)$ at a given time by using several realizations.

A significant result of the structure is that at saturation, the pair distribution diverges logarithmically at contact:

$$g(r, \rho_\infty) \sim \ln\left(\frac{(r-1)}{\sigma}\right). \tag{6.7}$$

This feature is specific to an RSA kinetics. At equilibrium, at the same density, the pair distribution function $g(r)$ is always finite at contact, in particular at density corresponding to the saturation density of the RSA process.

6.3   Inelastic hard sphere model

6.3.1   Introduction

Granular matter (powders, sands, ...) is characterized by the following properties: particle size is much larger than the atomic scales (at least several hundreds micrometers); the range of interaction between particles is less than the typical particle size; when particles collide, a fraction of the kinetic energy is lost and transformed in local heating; the particle mass being much larger than atoms, the thermal energy is negligible compared to gravitational energy and power supply (generally, provided by vibrations).

In the absence of a continuous power supply, a granular system looses rapidly this initial kinetic energy, which is transformed in heat. At a macroscopic level (which corresponds to the observation), the system appears as dissipative. Taking account of the time scale separation, one can considers that the collision time is negligible compared to the characteristic time of free steaming. Because the interactions are short ranged and particle shape is not modified with collisions (we consider "gentle" collisions), one can assume that the interaction potential is hard core potential.

The total momentum of the two particles involved in a collision is conserved:

$$\mathbf{v}_1 + \mathbf{v}_2 = \mathbf{v}'_1 + \mathbf{v}'_2. \tag{6.8}$$

During the collision, the relative velocity of the point of impact is changed as follows: Assuming that the tangential component of the velocity is conserved (which corresponds to a tangential coefficient of restitution equal to 1) one has the following relation

$$(\mathbf{v}'_1 - \mathbf{v}'_2).\mathbf{n} = -e(\mathbf{v}_1 - \mathbf{v}_2).\mathbf{n} \tag{6.9}$$

where e is the normal coefficient of restitution and $\mathbf{n}$ is a normal unit vector, whose direction is given by the straight line joining the two centers of colliding particles. The value of this coefficient is between 0 and 1; the latter corresponding to a system of elastic hard spheres .

6.3.2 Definition

The inelastic hard sphere model is defined as a system interacting by a hard core potential and loosing kinetic energy in collisions. Combining the conservation of the total impulse and the collision rules, one obtains the postcollisional velocities:

$$\mathbf{v}'_{i,j} = \mathbf{v}_{i,j} \pm \frac{1+e}{2}[(\mathbf{v}_j - \mathbf{v}_i).\hat{\mathbf{n}}]\hat{\mathbf{n}} \tag{6.10}$$

with

$$\hat{\mathbf{n}} = \frac{\mathbf{r}_1 - \mathbf{r}_2}{|\mathbf{r}_1 - \mathbf{r}_2|}. \tag{6.11}$$

This model is suitable for Molecular Dynamic simulations. We saw in Chapter 3 the algorithm of Molecular Dynamics of (elastic) hard spheres; it is easy to adapt this algorithm for inelastic hard spheres. The difference between the two systems, concerns the equations for updating velocities, which implies that the inelastic hard spheres looses continuously a fraction of its kinetic energy.

6.3.3 Results

The dissipative nature of collisions has some consequences: when one studies a granular system in a steady state, it is necessary to inject energy in the system. Moreover, when the density of the system is moderate or large, particles rapidly form aggregates. This last phenomenon always exists even at low density where even one starts with a uniform distribution of particles, the system evolves towards a state composed of clusters. The local density of clusters is then much larger than the initial uniform density and there are large regions of low density.

When the particle density increases sufficiently, the phenomenon od inelastic collapse will stop the simulation. Since the system loses kinetic energy, one has configurations in which three particles or more can trap one particle. Time evolution of the simulation is then dominated by a sequence of collisions between the central particle and its neighbors with a collision time which rapidly decreases to zero. Asymptotically, one obtains a glued set of particles.[1].

This effect, which occurs in a simulation for a small group of particles, can be understood by considering the simple phenomenon of a single particle bouncing on a plane under the influence of gravity. Let h denotes the height at which the ball is dropped. At the first collision between the particle and the plane, the elapsed time is $t_1 = \sqrt{2h/g}$ and the precollisional velocity is $\sqrt{2gh}$. After the first collision, the velocity becomes $e\sqrt{2gh}$. When the second collision occures, the elapsed time is,

$$t_2 = t_1 + 2et_1 \tag{6.12}$$

and for the n collision, one has

$$t_n = t_1\left(1 + 2\sum_{i=1}^{n-1} e^i\right). \tag{6.13}$$

Therefore, for an infinite number of collisions, one has

$$t_\infty = t_1\left(1 + \frac{2e}{1-e}\right) \tag{6.14}$$

$$= t_1\frac{1+e}{1-e} \tag{6.15}$$

---

[1]Particles are not strictly glued but the simulation is practically stopped, because this corresponds to an infinite sequence of collisions which occurs in a finite time.

A finite time of duration is elapsed until the bead comes to rest on the plan, whereas an infinite number of collisions was performed.

Because computation of a collision is proportional to the number of collisions, when an inelastic collapse occurs, the simulation does not evolve longer in time. For real systems, when the relative velocity at the point of impact becomes very small, collision does not remain inelastic, and the coefficient of restitution goes to one when the relative velocity goes to zero. Indeed, the assumption of the coefficient of restitution is constant is valid for collision velocities comparable to the thermal velocities. For very large velocities, plastic deformation of hard particles are significant and the coefficient of restitution decreases for large velocities. Conversely, when velocities go to zero, the coeffficient of restitution goes to 1, and particle collisions become quasi elastic.

Even though, one expects the total kinetic energy to decrease to zero with time (unless there is a power supply that compensates the dissipation due to collisions), simulation of inelastic hard spheres cannot reach this state, because simulation is stopped by the phenomenon of inelastic collapse.

If one wants to have a realistic model, it is necessary to consider how to supply power for a system studied in a steady state. In three dimensions, there is generally a vibrating wall whose collisions with particles supply energy to the system. In a steady state, collisions between particles, which dissipate energy, are compensated by collisions between particles and the vibrating wall.

In summary, the inelastic hard sphere model is a basic model for modeling granular gases.

6.3.4 Some properties

In the absence of a power supply, the system decreases continuously the temperature, there is a scaling regime before cluster formation in which the system remains homogeneous and whose velocity distribution is expressed as a scaling function. To understand this regime, one considers the loss of kinetic energy resulting from a collision between two particles. By using equation (6.10), one obtains

$$\Delta E = -\frac{1-\alpha^2}{4} m((\mathbf{v}_j - \mathbf{v}_i).\hat{\mathbf{n}})^2 \tag{6.16}$$

One obviously notes that if $\alpha = 1$ (elastic spheres), the kinetic energy is conserved, as seen in chapter 3. Conversely, the energy loss is maximum when the coefficient of restitution is equal to 0.

With the assumption of a homogeneous system, the mean collision frequency is proportional to $l/\Delta v$. The mean energy loss is given by $\Delta E = -\epsilon(\Delta v)^2$ where $\epsilon = 1 - \alpha^2$, which gives the evolution

$$\frac{dT}{dt} = -\epsilon T^{3/2} \tag{6.17}$$

and then the cooling law is

$$T(t) \simeq \frac{1}{(1 + A\epsilon t)^2} \tag{6.18}$$

This is known as the Haff's law (1983).

When the granular system has an external source of energy, it reaches a steady state where the properties are different from equilibrium. In particular, the velocity distribution is never Gaussian. This implies that the granular temperature defined as the mean square velocity is different from of the temperature associated with the width of the velocity distribution. One can show that the tails of the velocity distribution do not decay as a Gaussian generally, and that the shape is closely related to the details of the power supply.

Among the specific properties, note that in a mixture de two species of granular particles (for instance, different sizes of particles), the granular temperatures of each specie are differnt: there is no equipartition contrary to equilibrium.

6.4 Exclusion models

6.4.1 Introduction

Whereas the Gibbs-Botzmann distribution is central to equilibrium statistical mechanics owns, there is no general method for obtaining the configuration distribution for a steady state of a system. Exclusion models are toy models that they have beeen extensively studied by theory and simulations. These models can be used for describing vehicular traffic, in particular, for phenomena as traffic jams as well as fluctuation currents which spontaneously appear when the car density increases.

Many variants of the original model exist and we restrict our attention to basic examples in order to exhibit the most significant properties. In theoretical treatments, the one dimensional version of these models are most studied.

Consider a one dimensional lattice of N sites where n particles are placed. Each particle has a hopping probability p on the right si the nearest site is empty and a hopping probability $1 - p$ on the left if the nearest site is empty.

For non equilibrium systems, the details of the stochastic dynamics can be relevant for properties of the system. For these models, one can choose among at least three different methods for the dynamics.

- Parallel update: at the same time, all rules are applied to particles. This dynamics is sometimes called synchronous update. This kind of dynamics leads to significant particle correlations. The corresponding master equation is a finite difference equation in time.[2]

- Asynchronous update. This corresponds to the most used algorithm by choosing randomly and uniformly a particle at time t and to apply the update rules of the model. The corresponding master equation is a differential equation.

- When the update is sequential and ordered, one considers successive sites of the lattice. Ordering can be chosen from the left to the right or conversely. The corresponding equation is also finite difference equation in time.

6.4.2 Random walk on a ring

Stationary state and detailed balance

When the systems has periodic boundary conditions, the walker which reached the site N has a probability p of hopping on the site 1. It is easy to find out that such a system has a stationary state where the the probability of being on a site is independent of the site and is equal to $P_{st}(i) = 1/N$. Therefore, one has

$$\Pi(i \to i + 1)P_{st}(i) = \frac{p}{N} \tag{6.19}$$

$$\Pi(i + 1 \to i)P_{st}(i + 1) = \frac{1 - p}{N} \tag{6.20}$$

Except for the case where the hopping probability is the same to the right and to the right, namely $p = 1/2$, detailed balance is not satisfied although the state is stationary. This is not surprising, but illustrates that the stationary condition is less restrictive than the detailed balance condition. Only the later correspond to equilibrium situation.

---

[2]For the ASEP model, for avoiding overlap between particle hopping from the left or from the right at the same time, the algorithm considers alternatively a parallel update on a sub-lattice, which prevents the overlap configuration of two particles coming from the left and from the right at the same time. Therefore, one performs the parallel update on the first sub-lattice of even sites and a parallel update on the sublattice of odd sites.

Totally asymmetric exclusion process

In order to go further in the analytical treatment and to illustrate the phenomenology of this model, one can choose to prevent left hopping. For this case, on has $p = 1$: Using a continuous algorithm, a particle at site i has a probability dt of hopping to the right if the site is empty, otherwise it stays on the site. Consider P particles in a lattice of N sites, with the condition $P < N$. One introduces variables $\tau_i(t)$ which denote the occupation rate at time t of the site i. This variable is equal to 1 if a particle is on the site i at time t and 0 if the site is empty.

One can write an evolution equation of the system for the variable $\tau_i(t)$. If the site i is occupied, it can be free if the particle located on site i at time t can hop on the site $i + 1$, which must be empty. If the site i is empty, it can be filled if there is a particle on the site $i - 1$ at time t. Therefore, the variable $\tau_i(t + dt)$ is equal to $\tau_i(t)$ if no site on the left or the right of the site i is changed

$$
\tau_i(t+dt) \begin{cases} \tau_i(t) & \text{Probability of no hop 1-2dt} \\ \tau_i(t) + \tau_{i-1}(t)(1-\tau_i(t)) & \text{Probabilty of a left hop dt} \\ \tau_i(t) - \tau_i(t)(1-\tau_{i+1}(t)) = \tau_i(t)\tau_{i+1}(t) & \text{Probabilty of a right hop dt} \end{cases} \tag{6.21}
$$

Taking the average over the dynamic history, namely from time 0 to t, one obtains the evolution equation:

$$
\frac{d\langle \tau_i(t) \rangle}{dt} = -\langle \tau_i(t)(1-\tau_{i+1}(t)) \rangle + \langle \tau_{i-1}(t)(1-\tau_i(t)) \rangle \tag{6.22}
$$

The time evolution of a site i depends on the neighboring sites. Using a similar reasoning for the variable $\tau_i(t)$, one obtains the time evolution of an adjacent pair site which depends on the state of the sites to the right and right of the pair. Therefore,

$$
\frac{d(\langle \tau_i(t)\tau_{i+1}(t) \rangle)}{dt} = -\langle \tau_i(t)\tau_{i+1}(t)(1-\tau_{i+2}(t)) \rangle + \langle \tau_{i-1}(t)\tau_{i+1}(t)(1-\tau_i(t)) \rangle \tag{6.23}
$$

Finally, one obtains a infinite hierarchy of equations involving clusters of increasing sizes. One has a simple solution of the stationary state, because one can show that all configurations have an equal weight given by the equation

$$
P_{st} = \frac{P!(N-P)!}{N!} \tag{6.24}
$$

which corresponds to the inverse of the number of possibilities of dropping P particles on N sites.

Averaging in the stationary state gives

$$
\langle \tau_i \rangle = \frac{P}{N} \tag{6.25}
$$

$$
\langle \tau_i \tau_j \rangle = \frac{P(P-1)}{N(N-1)} \tag{6.26}
$$

$$
\langle \tau_i \tau_j \tau_k \rangle = \frac{P(P-1)(P-2)}{N(N-1)(N-2)} \tag{6.27}
$$

6.4.3 Model with open boundaries

By using open boundaries, the system can exchange particles with "reservoirs". If the site 1 is empty at time t, there is a probability (or a probability density for a continuous dynamics) α of injecting a particle at site 1, and if the site is occupied, there is a probability γ of removing the particle from the left site of the lattice. Similarly, if the site N is occupied, there is a probability β of removing the particle from the right side of the lattice and if the site N is empty, there is a probability δ of inserting a particle on site N.[3, 17]
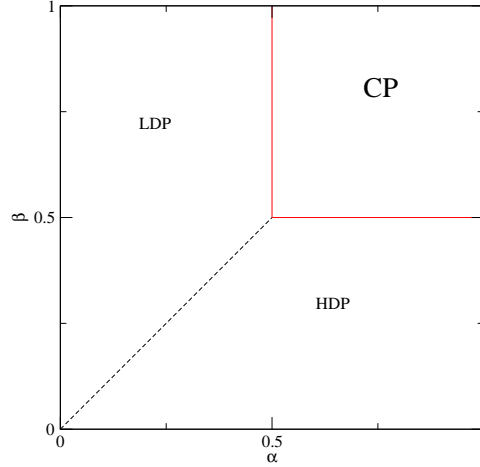
Figure 6.2: Phase diagram of ASEP model. The dashed line is a first-order line transition and the two full curves correspond to continuous transition lines.

On can write equations of time evolution in general, but analytical solutions cannot be obtained. For the sake of simplicity, we restrict ourselves to the totally asymmetric case. The evolution equations obtained for the system with periodic boundary conditions are the same for sites 2 to $N-1$, and for the sites 1 and N they are modified as follows: the site 1, if empty, can accept a particle from the reservoir with a probability α and, if occupied, lose its particle, either because the particle hops into the reservoir with the probability γ, or it hops on the right site. One then obtains

$$\frac{d\langle\tau_1(t)\rangle}{dt} = \alpha(1 - \langle\tau_1(t)\rangle) - \gamma\langle\tau_1(t)\rangle - \langle\tau_1(t)(1 - \tau_2(t))\rangle \tag{6.28}$$

In a similar manner for the site N, one has

$$\frac{d\langle\tau_N(t)\rangle}{dt} = \langle\tau_{N-1}(t)(1 - \tau_N(t))\rangle + \delta\langle(1 - \tau_N(t))\rangle - \beta\langle\tau_N(t)\rangle \tag{6.29}$$

It is possible to derive a solution in the stationary state. We only summarize basic features of the model by drawing the phase diagram, in the case where $\delta = \gamma = 0$, see figure 6.2.

The LDP (low density phase) region corresponds to a stationary density (in bulk) equal to α if $\alpha < 1/2$ and $\alpha < \beta$. The HDP (high density phase) region corresponds to a stationary density $1 - \beta$ and occurs for values of $\beta < 0.5$ and $\alpha > \beta$. The last region of the phase diagram is called maximal current phase and corresponds to values of α and β strictly larger than 1/2. The dashed line denotes the boundary between the LCP et HDP phase and corresponds to a first-order transition line. Indeed, in the thermodynamic limit, crossing the transition line leads to a density discontinuity

$$\Delta\rho = \rho_{HCP} - \rho_{LCP}$$
$$= 1 - \beta - \alpha \tag{6.30}$$
$$= 1 - 2\alpha \tag{6.31}$$

which is nonzero for $\alpha < 0.5$. For a simulation where one has a finite system, one obtains a rapidly variation with a increasing slope when the system size increases.

$\mathcal{A}$

RECAP ON ENSEMBLES

We first review the main ensembles used in Statistical Mechanics. We assume that the thermodynamic limit leads to the same quantities, a property for systems where interaction between particles are not long ranged or systems without quenched disorder.

A.1 Microcanonical ensemble

The system is characterized by the set of macroscopic variables: volume V, total energy E and the number of particles N. This ensemble is not appropriate for experimental studies, where one generally has

- a fixed number of particles, but a fixed pressure P and temperature T. This corresponds to a set of variables (N, P, T) and is the isothermal-isobaric ensemble,

- a fixed chemical potential μ, volume V and temperature T, ensemble (μ, V, T) or grand canonical ensemble,

- a fixed number of particles, a given volume V and temperature T, ensemble (N, V, T) or canonical ensemble.

The partition function $Z(E, V, N)$ is

$$Z(E, V, N) = \sum_\alpha \delta(E - E_\alpha) \tag{A.1}$$

where δ is a Kronecker symbol (equal to 1 when $(E - E_\alpha) = 0$ and 0 when $(E - E_\alpha) \neq 0$. Note that all microstates have the same weight for computing the partition function. The associated thermodynamic potential is the entropy given by

$$S(E, V, N) = k_B \ln(Z(E, V, N)) \tag{A.2}$$

where k_B is the Boltzmann constant.

The variables conjugated to the global quantities defining the ensemble fluctuate in time. For the micro-canonical ensemble, this corresponds to the pressure P conjugate to the volume V, to the temperature T conjugate to the energy E and to the chemical potential μ conjugate to the total number of particles N.

A.2 Canonical ensemble

The system is characterized by the following set of variables: the volume V; the temperature T and the total number of particles N. If we denote the Hamiltonian of the system $\mathcal{H}$, the partition function reads

$$Q(V, \beta, N) = \sum_\alpha \exp(-\beta \mathcal{H}(\alpha)) \tag{A.3}$$

where $\beta = 1/k_B T$ (k_B is the Boltzmann constant). The sum runs over all configurations of the system. If this number is continuous, the sum is replaced with an integral. α denotes the index of these configurations. The free energy $F(V, \beta, N)$ of the system is equal to

$$\beta F(V, \beta, N) = -\ln(Q(V, \beta, N)).$$ (A.4)

One defines the probability of having a configuration α as

$$p(V, \beta, N; \alpha) = \frac{\exp(-\beta \mathcal{H}(\alpha))}{Q(V, \beta, N)}.$$ (A.5)

where $\mathcal{H}(\alpha)$ denotes the energy of the configuration α. One easily checks that the basic properties of a probability are satisfied, i.e. $\sum_\alpha p(V, \beta, N; \alpha) = 1$ and $p(V, \beta, N; \alpha) > 0$.

The derivatives of the free energy are related to the moments of this probability distribution, which gives a microscopic interpretation of the macroscopic thermodynamic quantities. The mean energy and the specific heat are then given by

- Mean energy

$$U(V, \beta, N) = \langle \mathcal{H}(\alpha) \rangle = \frac{\partial(\beta F(V, \beta, N))}{\partial \beta}$$

$$U = \sum_\alpha \mathcal{H}(\alpha) p(V, \beta, N; \alpha)$$ (A.6)

- Specific heat

$$C_v(V, \beta, N) = -k_B \beta^2 \frac{\partial U(V, \beta, N)}{\partial \beta} = k_B \beta^2 \left(\langle \mathcal{H}(\alpha)^2 \rangle - \langle \mathcal{H}(\alpha) \rangle^2 \right)$$

$$C_v = k_B \beta^2 \left(\sum_\alpha \mathcal{H}^2(\alpha) p(V, \beta, N; \alpha) - \left(\sum_\alpha \mathcal{H}(\alpha) p(V, \beta, N; \alpha) \right)^2 \right)$$ (A.7)

A.3   Grand canonical ensemble

The system is then characterized by the following set of variables: the volume V, the temperature T and the chemical potential μ. Let us denote the Hamiltonian $\mathcal{H}_N$ the Hamiltonian of N particles, the grand partition function $\Xi(V, \beta, \mu)$ reads:

$$\Xi(V, \beta, \mu) = \sum_{N=0}^{\infty} \sum_{\alpha_N} \exp(-\beta(\mathcal{H}_N(\alpha_N) - \mu N))$$ (A.8)

where $\beta = 1/k_B T$ (k_B is the Boltzmann constant) and the sum run over all configurations of N particles and over all configurations for systems having a number of particles going from 0 to ∞. The grand potential is equal to

$$\beta \Omega(V, \beta, \mu) = -\ln(\Xi(V, \beta, \mu))$$ (A.9)

In a similar way, one defines the probability (distribution) $P(V, \beta, \mu; \alpha_N)$ of having a configuration α_N (with N particles) by the relation

$$p(V, \beta, \mu; \alpha_N) = \frac{\exp(-\beta(\mathcal{H}_N(\alpha_N) - \mu N))}{\Xi(V, \beta, \mu)} \tag{A.10}$$

The derivatives of the grand potential can be expressed as moments of the probability distribution

- Mean number

$$\langle N(V, \beta, \mu) \rangle = -\frac{\partial(\beta\Omega(V, \beta, \mu))}{\partial(\beta\mu)} = \sum_N \sum_{\alpha_N} p(V, \beta, \mu; \alpha_N) \tag{A.11}$$

- Susceptibility

$$\chi(V, \beta, \mu) = \frac{\beta}{\langle N(V, \beta, \mu) \rangle \rho} \frac{\partial \langle N(V, \beta, \mu) \rangle}{\partial \beta\mu} = \frac{\beta}{\langle N(V, \beta, \mu) \rangle \rho} \left(\langle N^2(V, \beta, \mu) \rangle - \langle N(V, \beta, \mu) \rangle^2 \right) \tag{A.12}$$

$$\chi(V, \beta, \mu) = \frac{\beta}{\langle N(V, \beta, \mu) \rangle \rho} \left[\sum_N \sum_{\alpha_N} N^2 p(V, \beta, \mu; \alpha_N) - \left(\sum_N \sum_{\alpha_N} N p(V, \beta, \mu; \alpha_N) \right)^2 \right] \tag{A.13}$$

A.4 Isothermal-isobaric ensemble

The system is characterized by the following set of variables: the pressure P, the temperature T and the total number of particles N. Because this ensemble is generally devoted to molecular systems and not used for lattice models, one only considers continuous systems. The partition function reads:

$$Q(P, \beta, N) = \frac{\beta P}{\Lambda^{3N} N!} \int_0^\infty dV \exp(-\beta PV) \int_0^V d\mathbf{r}^N \exp(-\beta U(\mathbf{r}^N)) \tag{A.14}$$

where $\beta = 1/k_B T$ (k_B is the Boltzmann constant).

The Gibbs potential is equal to

$$\beta G(P, \beta, N) = -\ln(Q(P, \beta, N)). \tag{A.15}$$

One defines the probability $p(P, \beta, \mu; \alpha_V)$ of having a configuration $\alpha_V \equiv \mathbf{r}^N$ (particle positions $\mathbf{r}^N$), with a temperature T and a pressure P).

$$p(P, \beta, \mu; \alpha_V) = \frac{\exp(-\beta V) \exp(-\beta(U(\mathbf{r}^N)))}{Q(P, \beta, N)}. \tag{A.16}$$

The derivatives of the Gibbs potential are expressed as moments of this probability distribution. Therefore, the mean volume

$$\langle V(P, \beta, N) \rangle = \frac{\partial(\beta G(P, \beta, N))}{\partial \beta P} \tag{A.17}$$

$$\langle V(P,\beta,N)\rangle = \int_0^\infty dV\, V \int_0^V d\mathbf{r}^N \Pi(P,\beta,\mu;\alpha_V). \tag{A.18}$$

This ensemble is appropriate for simulations which aim to determine the
equation of state of a system. Let us recall that a statistical ensemble can not be defined from a set of intensives variables only. However, we will see later that a technique so called Gibbs ensemble method is close in spirit of such an ensemble (with the difference we always consider in simulation finite systems).

A.5   Model systems

We restrict the lecture notes to classical statistical mechanics, which means that the quantum systems are not considered here. In order to provide many illustrations of successive methods, we introduce several basic models that we consider several times in the following

A.5.1   Simple liquids and Lennard-Jones potential

A *simple liquid* is a system of N point particles labeled from 1 to N, of identical mass m, interacting with an external potential $U_1(\mathbf{r}_i)$ and among themselves by a pairwise potential $U_2(\mathbf{r}_i,\mathbf{r}_j)$ (i.e. a potential where the particles only interact by pairs). The Hamiltonian of this system reads:

$$\mathcal{H} = \sum_{i=1}^N \left[\frac{\mathbf{p}_i^2}{2m} + U_1(\mathbf{r}_i) \right] + \frac{1}{2}\sum_{i\neq j} U_2(\mathbf{r}_i,\mathbf{r}_j), \tag{A.19}$$

where $\mathbf{p}_i$ is the momentum of the particle i. For instance, in the grand canonical ensemble, the partition function $\Xi(\mu,\beta,V)$ is given by

$$\Xi(\mu,\beta,V) = \sum_{N=0}^\infty \frac{1}{N!} \int \prod_{i=1}^N \frac{(d^d\mathbf{p}_i)(d^d\mathbf{r}_i)}{h^{dN}} \exp(-\beta(\mathcal{H}-\mu N)) \tag{A.20}$$

where h is the Planck constant and d the space dimension. The integral over the momentum can be obtained analytically, because there is factorization of the multidimensional integral on the variables $\mathbf{p}_i$. The one-dimensional integral of each component of the momentum is a Gaussian integral. Using the thermal de Broglie length

$$\Lambda_T = \frac{h}{\sqrt{2\pi m k_B T}}, \tag{A.21}$$

one has

$$\int_{-\infty}^{+\infty} \frac{d^d p}{h^d} \exp(-\beta p^2/(2m)) = \frac{1}{\Lambda_T^d}. \tag{A.22}$$

The partition function can be reexpressed as

$$\Xi(\mu,\beta,V) = \sum_{N=0}^\infty \frac{1}{N!} \left(\frac{e^{\beta\mu}}{\Lambda_T^d} \right)^N Z_N(\beta,N,V) \tag{A.23}$$

where $Z_N(\beta,N,V)$ is called the configuration integral.

$$Z_N(\beta,N,V) = \int d\mathbf{r}^N \exp(-\beta U(\mathbf{r}^N)) \tag{A.24}$$

92

One defines $z = e^{\beta \mu}$ as the fugacity. The thermodynamic potential associated with the partition function, $\Omega(\mu, \beta, V)$, is

$$\Omega(\mu, \beta, V) = -\frac{1}{\beta} \ln(\Xi(\mu, \beta, V)) = -PV \tag{A.25}$$

where P is the pressure. Note that, for classical systems, only the part of the partition function with the potential energy is non-trivial. Moreover, there is decoupling between the kinetic part and potential part, contrary to the quantum statistical mechanics.

To determine the phase diagram composed of different regions (liquid phase, gas and solid phases), the interaction potential between particles must contain a repulsive short-range interaction and an attractive long-range interaction. The physical interpretation of these contributions is the following: at short distance, quantum mechanics prevent atom overlap which explains the repulsive part of the potential. At long distance, even for neutral atoms, the London forces (whose origin is also quantum mechanical) are attractive. A potential satisfying these two criteria, is the Lennard-Jones potential

$$u(r) = 4\epsilon \left[\left(\frac{\sigma}{r} \right)^{12} - \left(\frac{\sigma}{r} \right)^{6} \right] \tag{A.26}$$

where ϵ defines a microscopic energy scale and σ denotes the atom diameter (see Fig.A.1).
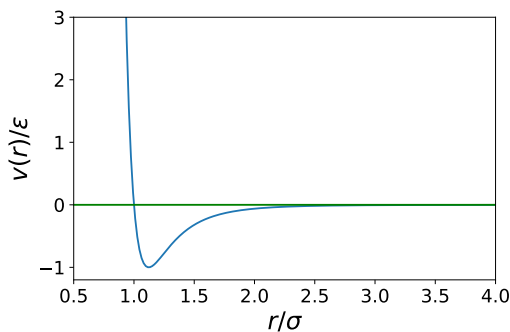

```python
import numpy as np
import matplotlib.pylab as plt
def lj(x):
        return 4*(x**(-12)-x**(-6))
x= np.linspace(0.5,4.0,200)
plt.ylim(-1.2,3.)
plt.xlim(0.5,4)
plt.plot(x,lj(x))
plt.xlabel(r'$r/\sigma$',fontsize=20)
plt.ylabel(r'$v(r)/\epsilon$',fontsize=20)
plt.plot([0.5,4.],[0,0],color='green')
plt.tick_params(labelsize=15)
plt.tight_layout()
plt.show()
```

Figure A.1: Reduced Lennard-Jones potential $u(r)/\epsilon$ versus r/σ. $u(r)/\epsilon$ versus r/σ.

All quantities are expressed in dimensionless units, as expected in simulation: temperature is then $T^* = k_B T/\epsilon$ where k_B is the Boltzmann constant, the distance is $r^* = r/\sigma$ and the energy is $u^* = u/\epsilon$. The three-dimensional Lennard-Jones model has a critical point at $T_c^* = 1.3$ and $\rho_c^* = 0.3$, and a triple point $T_t^* = 0.6$ and $\rho_t^* = 0.8$

A.5.2 Ising model and lattice gas. Equivalence

The Ising model is a lattice model where sites are occupied by particles with very limited degrees of freedom. Indeed, the particle is characterized by a spin which is a two-state variable $(-1,+1)$. Each spin interacts with its nearest neighbors and with a external field H, if it exists. The Ising model, initially introduced for describing the behavior of para-ferromagnetic systems, can be used in many physical situations The Hamiltonian is given by

$$\mathcal{H} = -J \sum_{<i,j>} S_i S_j - H \sum_{i=1}^{N} S_i \tag{A.27}$$

D	Lattice	T_c/J (exact)	$T_{c,MF}/J$
1		0	2
2	square	2.269185314	4
2	triangular	3.6410	6
2	honeycomb	1.5187	3
3	cubic	4.515	6
3	bcc	6.32	8
3	diamond	2.7040	4
4	hypercube	6.68	8

Table A.1: Critical Temperatures of the Ising model for different lattices in 1 to 4 dimensions

where the summation $< i, j >$ means that the interaction is restricted to distinct pairs of nearest neighbors and H denotes an external uniform field. If $J > 0$, interaction is ferromagnetic and if $J < 0$, interaction is antiferromagnetic.

In one dimension, this model can be solved analytically and one shows that the critical temperature is the zero temperature.

In two dimensions, Onsager (1944) solved this model in the absence of an external field and showed that there exists a para-ferromagnetic transition at a finite temperature. For the square lattice, this critical temperature is given by

$$T_c = J \frac{2}{\ln(1 + \sqrt{2})} \tag{A.28}$$

and a numerical value equal to $T_c \simeq 2.269185314...J$.

In three dimensions, the model can not be solved analytically, but numerical simulations have been performed with different algorithms and the values of the critical temperature obtained for various lattices and from different theoretical methods are very accurate (see Table A.1).

A useful, but crude, estimate of the critical temperature is given by the mean-field theory

$$T_c = cJ \tag{A.29}$$

where c is the coordination number.

Table A.1 illustrates that the critical temperatures predicted by the mean-field theory are always an upper bound of the exact values and that the quality of the approximation becomes better when the spatial dimension of the system is large and/or the coordination number is large.

The lattice gas model was introduced by Lee and Yang. The basic idea, greatly extended later, consists of assuming that the macroscopic properties of a system with a large number of particles do not crucially depend on the microscopic details of the interaction. By performing a coarse-graining of the microscopic system, one builds an effective model with a smaller number of degrees of freedom. This idea is often used in statistical physics, because it is often necessary to reduce the complexity of the original system for several reasons: 1) practical: In a simpler model, theoretical treatments are more tractable and simulations can be performed with larger system sizes. 2) theoretical: macroscopic properties are almost independent of some microscopic degrees of freedom and a local average is efficient method for obtaining an effective model for the physical properties of the system. This method underlies the existence of a certain universality, which is appealing to many physicists.

From a Hamiltonian of a simple liquid to a lattice gas model, we proceed in three steps. The first consists of rewriting the Hamiltonian by introducing a microscopic variable: this step is exact. The second step consists of performing a local average to define the lattice Hamiltonian; several approximations are performed in this step and it is essential to determine their validity. In the third step, several

changes of variables are performed in order to transform the lattice gas Hamiltonian into a spin model Hamiltonian: this last step is exact again.

Rewriting of the Hamiltonian

First, let us reexpress the Hamiltonian of the simple liquid as a function of the microscopic[1] density

$$\rho(\mathbf{r}) = \sum_{i=1}^{N} \delta(\mathbf{r} - \mathbf{r}_i). \tag{A.30}$$

By using the property of the Dirac distribution

$$\int f(x)\delta(x-a)dx = f(a) \tag{A.31}$$

one obtains

$$\sum_{i=1}^{N} U_1(\mathbf{r}_i) = \sum_{i=1}^{N} \int_V U_1(\mathbf{r})\delta(\mathbf{r} - \mathbf{r}_i)d^d\mathbf{r} = \int_V U_1(\mathbf{r})\rho(r)d^d\mathbf{r} \tag{A.32}$$

in a similar way

$$\sum_{i \neq j} U_2(\mathbf{r}_i, \mathbf{r}_j) = \sum_{i \neq j} \int_V U_2(\mathbf{r}, \mathbf{r}_j)\delta(\mathbf{r} - \mathbf{r}_i)d^d\mathbf{r}$$

$$= \sum_{i \neq j} \int_V \int_V U_2(\mathbf{r}, \mathbf{r}')\delta(\mathbf{r} - \mathbf{r}_i)\delta(\mathbf{r}' - \mathbf{r}_j)d^d\mathbf{r}d^d\mathbf{r}'$$

$$\sum_{i \neq j} U_2(\mathbf{r}_i, \mathbf{r}_j) = \int_V \int_V U_2(\mathbf{r}', \mathbf{r})\rho(\mathbf{r})\rho('\mathbf{r})d^d\mathbf{r}d^d\mathbf{r}' \tag{A.33}$$

Local average

The area ("volume") V of the simple liquid is divided into N_c cells such that the probability of finding more than one particle center per cell is negligible[2] (typically, this means that the diagonal of each cell is slightly smaller than the particle diameter, see Fig. A.2). Let us denote by a the linear length of the cell, then one has

$$\int_V \prod_{i=1}^{N} d^d\mathbf{r}_i = a^d \sum_{\alpha=1}^{N_c} \tag{A.34}$$

which gives $N_c = V/a^d$. The lattice Hamiltonian is

$$\mathcal{H} = \sum_{\alpha=1}^{N_c} U_1(\alpha)n_\alpha + 1/2 \sum_{\alpha,\beta}^{N_c} U_2(\alpha,\beta)n_\alpha n_\beta \tag{A.35}$$

---

[1] The local density is obtained by performing a local average that leads to a smooth function

[2] The particle is an atom or a molecule with its own characteristic length scale.
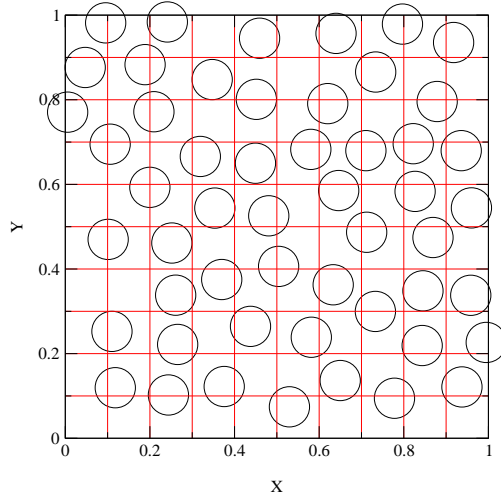
Figure A.2: Particle configuration of a two-dimensional simple liquid. The grid represents the cells used for the local average. Each cell can accommodate zero or one particle center.

where n_α is a Boolean variable, namely $n_\alpha = 1$ when a particle center is within a cell α, and 0 otherwise. Note that the index α of this new Hamiltonian is associated with cells whereas the index of the original Hamiltonian is associated with the particles. One obviously has $U(\alpha, \alpha) = 0$, no self-energy, because there is no particle overlap. Since the interaction between particles is short range, $U_2(r)$ is also short range, and is replaced with an interaction between nearest neighbor cells:

$$\mathcal{H} = \sum_{\alpha=1}^{N_c} U_1(\alpha)n(\alpha) + U_2 \sum_{<\alpha\beta>} n_\alpha n_\beta \tag{A.36}$$

The factor 1/2 does not appear because the bracket $< \alpha\beta >$ only considers distinct pairs.

Equivalence with the Ising model

We consider the previous lattice gas model in a grand canonical ensemble. The relevant quantity is then

$$\mathcal{H} - \mu N = \sum_{\alpha} (U_1(\alpha) - \mu)n_\alpha + U_2 \sum_{<\alpha,\beta>} n_\alpha n_\beta. \tag{A.37}$$

Let us introduce the following variables

$$S_i = 2n_i - 1. \tag{A.38}$$

As expected, the spin variable is equal to +1 when a site is occupied by a particle ($n_i = 1$) and −1 when the site in unoccupied ($n_i = 0$). One then obtains

$$\sum_{\alpha} (U_1(\alpha) - \mu)n_\alpha = \frac{1}{2} \sum_{\alpha} (U_1(\alpha) - \mu)S_\alpha + \frac{1}{2} \sum_{\alpha} (U_1(\alpha) - \mu) \tag{A.39}$$

and

$$U_2 \sum_{<\alpha,\beta>} n_\alpha n_\beta = \frac{U_2}{4} \sum_{<\alpha,\beta>} (1 + S_\alpha)(1 + S_\beta)$$

$$= \frac{U_2}{4} \left(\frac{N_c c}{2} + c \sum_\alpha S_\alpha + \sum_{<\alpha,\beta>} S_\alpha S_\beta \right) \tag{A.40}$$

where c is the coordination number (number of nearest neighbors) of the lattice. Therefore, this gives

$$\mathcal{H} - \mu N = E_0 - \sum_\alpha H_\alpha S_\alpha - J \sum_{<\alpha,\beta>} S_\alpha S_\beta \tag{A.41}$$

with

$$E_0 = N_c \left(\langle U_1(\alpha) \rangle - \frac{\mu}{2} + \frac{U_2 c}{8} \right) \tag{A.42}$$

where $\langle U_1(\alpha) \rangle$ corresponds to the average of U_1 over the sites.

$$H_\alpha = \frac{\mu - U(\alpha)}{2} - \frac{c U_2}{4} \tag{A.43}$$

and

$$J = -\frac{U_2}{4} \tag{A.44}$$

where J is the interaction strength. Finally, one gets

$$\Xi_{gas}(N, V, \beta, U(r)) = e^{-\beta E_0} Q_{Ising}(H, \beta, J, N_c). \tag{A.45}$$

This analysis confirms that the partition function of the Ising model in the canonical ensemble has a one-to-one map with the partition function of the lattice gas in the grand canonical ensemble. One can easily show that the partition function of the Ising model with the constraint of a constant total magnetization corresponds to the partition function in the canonical ensemble of the lattice gas model.

Some comments on these results: first, one checks that if the interaction is attractive, $U_2 < 0$, one has $J > 0$, which corresponds to a ferromagnetic interaction. Because the interaction is divided by 4, The critical temperature of the Ising model is four times higher than of the lattice gas model. Note also that the equivalence concerns the configuration integral and not the initial partition function. This means that, like for the Ising model, the lattice gas does not own a microscopic dynamics, unlike to the original liquid model. By performing a coarse-graining, one has added a symmetry between particles and holes, which does not exist in the liquid model. This leads for the lattice gas model a symmetrical coexistence curve and a critical density equal to 1/2. A comparison with the Lennard-Jones liquid gives a critical packing fraction equal to 0.3 in three dimensions. In addition, the coexistence curves of liquids are not symmetric between the liquid phase and the gas phase, whereas the lattice gas due to its additional symmetry $\rho_{liq} = 1 - \rho_{gas}$, leads to a symmetric coexistence curve.

Before starting a simulation, it is useful to have an estimate of the phase diagram in order to correctly choose the simulation parameters. The mean-field theory gives a first approximation, for instance, of the critical temperature. For the Ising model (lattice gas), one obtains

$$T_c = cJ = \frac{c U_2}{4} \tag{A.46}$$

As expected, the mean-field approximation overestimates the value of the critical temperature because the fluctuations are neglected. This allows order to persist to a temperature higher than the exact critical temperature of the system. Unlike to the critical exponents which do not depend on the lattice, the critical temperature depends on the details of the system. However, larger the coordination number, the closer the mean-field value to the exact critical temperature.

A.6   Conclusion

In this appendix, we have drawn the preliminary scheme before the simulation: 1) Select the appropriate ensemble for studying a model 2) When the microscopic model is very complicated, perform a coarse-graining procedure which leads to an effective model that is more amenable for theoretical treatments and/or more efficient for simulation. As we will see in the following chapters, refined Monte Carlo methods consists of including more and more knowledge of the Statistical Mechanics, which finally leads to a more efficient simulation. Therefore, I recommend reading of several textbooks on the Statistical Physics[10, 2, 9, 28]. In addition to these lecture notes, several textbooks or reviews are available on simulations[8, 15, 16, 1].

[1] K Binder. Applications of monte carlo methods to statistical physics. *Reports on Progress in Physics*, 60(5):487–559, 1997.

[2] D. Chandler. *Introduction to Modern Statistical Mechanics*. Oxford University Press, New York, USA, 1987.

[3] B Derrida, M R Evans, V Hakim, and V Pasquier. Exact solution of a 1d asymmetric exclusion model using a matrix formulation. *J. Phys. A: Math. Gen.*, 26(7):1493, 1993.

[4] C. Dress and W. Krauth. Cluster algorithm for hard spheres and related systems. *Journal Of Physics A-Mathematical And General*, 28(23):L597–L601, December 1995.

[5] Alan M. Ferrenberg, D. P. Landau, and Robert H. Swendsen. Statistical errors in histogram reweighting. *Phys. Rev. E*, 51(5):5092–5100, 1995.

[6] Alan M. Ferrenberg and Robert H. Swendsen. New monte carlo technique for studying phase transitions. *Phys. Rev. Lett.*, 61:2635–2638, Dec 1988.

[7] Alan M. Ferrenberg and Robert H. Swendsen. Optimized monte carlo data analysis. *Phys. Rev. Lett.*, 63(12):1195–1198, 1989.

[8] D. Frenkel and B. Smit. *Understanding Molecular Simulation: from algorithms to applications*. Academic Press, London, UK, 1996.

[9] Nigel Goldenfeld. *Lectures on Phase Transitions and the Renormalization Group*. Addison-Wesley, New-York, USA, 1992.

[10] J. P. Hansen and I. R. Mc Donald. *Theory of simple liquids*. Academic Press, London, UK, 1986.

[11] J. R. Heringa and H. W. J. Blote. Geometric cluster monte carlo simulation. *Phys. Rev. E*, 57(5):4976–4978, May 1998.

[12] J. R. Heringa and H. W. J. Blote. Geometric symmetries and cluster simulations. *Physica A*, 254(1-2):156–163, May 1998.

[13] Haye Hinrichsen. Non-equilibrium critical phenomena and phase transitions into absorbing states. *Adv. Phys.*, 49(7):815–958, 2000.

[14] William G. Hoover. Canonical dynamics: Equilibrium phase-space distributions. *Phys. Rev. A*, 31(3):1695–1697, Mar 1985.

[15] Werner Krauth. *Statistical Mechanics: Algorithms and Computations*. Oxford University Press, London, UK, 2006.

[16] David P. Landau and Kurt Binder. *A Guide to Monte Carlo Simulations in Statistical Physics*. Cambridge University Press, New York, USA, 2000.

[17] Kirone Mallick. Some exact results for the exclusion process. *Journal of Statistical Mechanics: Theory and Experiment*, 2011(01):P01024, 2011.

[18] Shuichi Nose. A unified formulation of the constant temperature molecular dynamics methods. *J. Chem. Phys.*, 81(1):511–519, 1984.

[19] P. Poulain, F. Calvo, R. Antoine, M. Broyer, and Ph. Dugourd. Performances of wang-landau algorithms for continuous systems. *Phys. Rev. E*, 73(5):056704, 2006.

[20] Udo Seifert. Stochastic thermodynamics, fluctuation theorems and molecular machines. *Reports on Progress in Physics*, 75(12):126001, 2012.

[21] Ken Sekimoto. *Stochastic Energetics*. Springer Berlin / Heidelberg, 2010.

[22] Robert H. Swendsen and Jian-Sheng Wang. Nonuniversal critical dynamics in monte carlo simulations. *Phys. Rev. Lett.*, 58(2):86–88, 1987.

[23] J. Talbot, G. Tarjus, P. R. Van Tassel, and P. Viot. From car parking to protein adsorption: an overview of sequential adsorption processes. *Colloids and Surfaces A: Physicochemical and Engineering Aspects*, 165(1-3):287–324, May 2000.

[24] S. H. Tsai, H. K. Lee, and D. P. Landau. Molecular and spin dynamics simulations using modern integration methods. *American Journal Of Physics*, 73(7):615–624, July 2005.

[25] Donald L Turcotte. Self-organized criticality. *Reports on Progress in Physics*, 62(10):1377–1429, 1999.

[26] Fugao Wang and D. P. Landau. Determining the density of states for classical statistical models: A random walk algorithm to produce a flat histogram. *Phys. Rev. E*, 64(5):056101, 2001.

[27] Fugao Wang and D. P. Landau. Efficient, multiple-range random walk algorithm to calculate the density of states. *Phys. Rev. Lett.*, 86(10):2050–2053, 2001.

[28] A. P. Young. *Spin glasses and random fields*. World Scientific, Singapore, 1998.

[29] Chenggang Zhou and R. N. Bhatt. Understanding and improving the wang-landau algorithm. *Phys. Rev. E*, 72(2):025701, 2005.

Contents